Application of Segmented Flow Technique in

Catalytic Organic Syntheses

CARDIFF
UNIVERSITY

PRIFYSGOL
CAERDYⱮ

School of Chemistry & School of Engineering

University of Cardiff

Submitted for the Degree of Doctor of Philosophy

by

Batoul Ahmed Omer

February 2008

UMI Number: U585109

Abstract

Microflow technology has become an innovative and fashionable tool in synthetic organic chemistry, opening the way to novel challenging interactions between chemistry and other scientific disciplines. The system properties and reaction conditions in microflow chemistry are different to those in flask as a result of higher surface-to-volume ratios and shorter diffusion distances bringing significant advantages over conventional flask method such as improved heat transfer and reduced mixing times. More and more multiphase microflow systems have begun to emerge over the last few years, offering a variety of methodologies. The attention to the various emerging microflow techniques represented the starting point for the development of the present work. The study presented in this thesis focuses on the application of microflow systems using segmented flow technique to various organic transformations by development of a practical and economical system setup in order to provide a basic methodology for synthetic chemists. First, we carried a comparison study between microflow and flask reaction using a simple biphasic hydrolysis under segmented flow. The study was then extended to investigate the effect of parallel *vs.* segmented flow, in addition to the variation of reaction parameters in the microflow system, such as heating, sonication, and microchannel size. We selected for our study two classes of catalytic organic reactions of particular synthetic relevance, namely palladium-catalysed Heck coupling and ruthenium-catalysed ring-closing metathesis. We carried out biphasic Heck catalysis then moved onto the study of segmented flow application to monophasic reactions both in single step and multistep syntheses. Overall the use of microflow technique, applied to a number of reactions of various types and carried out with many chemical and engineering variables, allowed us to observe overall reaction performances enhancement compared to conventional flask chemistry, on the whole rather agreeably, reproducibly, and displaying very regular trends.

Acknowledgements

List of Abbreviations

bp	boiling point
Cy	cyclohexyl
DCM	dichloromethane
DMF	dimethylformamide
FEP	fluoroethylenepropylene
ID	inner diameter
IR	infrared spectroscopy
Mes	mesityl
mp	melting point
MPLC	medium-performance liquid chromatography
NMR	nuclear magnetic resonance spectroscopy
OD	outer diameter
PDMS	polydimethylsiloxane
PEEK	polyetheretherketone
PFA	perfluoroalkoxyethylene
PFD	perfluorodecalin
Ph	phenyl
PMMA	polymethylmethacrylate
PTC	phase transfer catalyst
PTFE	polytetrafluoroethylene
RCM	ring closing metathesis
TBAB	tetrabutylammonium bromide
TBAHS	tetrabutylammonium hydrogen sulphate
Teflon-FEP	fluorinated ethylenepropylene
T_g	glass transition temperature
TLC	thin layer chromatography
TPPTS	Triphenyl phosphine trisulfonate sodium salt
UV	ultra violet

Table of Contents

Preface

Carrying out chemical reactions in microflow system can display significant advantages over conventional flask methods. The system properties and reaction conditions applied in microflow system are different to those in flask as a result of higher surface-to-volume ratios and shorter diffusion distances provided by the small size of the microsystem (a few micrometres wide). In addition, the small flow volumes, combined with the high surface-to-volume ratios, significantly improve the heat transfer, *i.e.* the movement of heat current between the channel surface and the flow as well as within the flow. On the other hand, the short diffusion distances result in reduced mixing times. Consequently microflow technology has become one of the most revolutionary and fashionable branches in chemistry bringing enormous improvement and potential especially in synthetic organic chemistry, and has opened wide possibilities to create novel interactions between chemistry and other science disciplines. A basic microflow system consists of a microchannel connected to the reagents' reservoir at one end and the product collection container at the other. The typical microflow reaction takes place once the reagents are continually delivered into the microchannel, allowing the resulting reaction mixture to flow in a continuous fashion through the channel at a fixed flow rate (volume/time) for a definite time known as the residence time which corresponds to the reaction time. After flowing at a definite residence time, the product is then collected from the systems output continuously. The continuous nature of the system combined with the small flow volume brings additional advantages to the microflow reactions, such as more control over reaction times, consumption of small amount of reagents, reproducibility, and controlled mixing of reagents. Hence microflow technique can be an ideal tool for reaction optimisation compared to conventional batch method.

Furthermore, the ability to couple the microflow system with continuous on-line purification, analysis and additional automotive systems makes the microflow process more efficient in terms of time and cost, making the technique more appealing to chemical and pharmaceutical industry. In addition, scale up of microflow reactions can be carried out easily by increasing the reactor volume or by setting up several microflow systems in parallel. This is especially appealing for scaling up of potentially hazardous reactions. In spite of the many literature examples of reactions been studied using microtechnology, most of the work carried in this area focused on the development of systems using single phase flow chemistry. More and more multiphase microflow systems have begun to emerge over the last few years. In a microchannel, the multiphase flow generates different flow patterns such as parallel flow, where the multiple phases flow side-by-side in parallel manner, while in segmented flow, the phases segregate each other in an alternating fashion. Once these segments are formed, an internal vortices or turbulences are generated within each segment which resulting in enhanced mixing compared to parallel flow. Hence segmented flow is believed to add extra advantage to multiphase microflow system over other flow patterns. The study presented in this thesis focuses on the application of microflow system using segmented flow technique to various organic transformations using a practical and economical system setup in order to develop a basic methodology for synthetic chemists. We initially aimed to look into biphasic organic systems using segmented flow, but later on our ideas developed into applying segmented flow to monophasic reactions using an inert immiscible phase. First, we demonstrate a comparison study between microflow and flask reaction using a simple biphasic hydrolysis under segmented flow. Then study was extended to investigate the effect of parallel *vs.* segmented flow, in addition to the variation of reaction parameters in the microflow system, such as heating, sonication,

and microchannel size. The following chapter focuses on more complex organic transformations that we carried aiming to achieve reaction enhancement. We studied a number of organic reactions of particular synthetic relevance, and selected two as the most successful ones, namely palladium-catalysed Heck coupling and ruthenium-catalysed ring-closing metathesis. We carried out biphasic Heck catalysis then moved onto the study of segmented flow application to monophasic reactions both in single step and multistep syntheses. Overall the use of microflow technique, applied to such a large number of reactions of various types and carried out with many chemical and engineering variables, allowed us to observe overall reaction performances enhancement compared to conventional flask chemistry, on the whole rather agreeably, reproducibly, and displaying very regular trends.
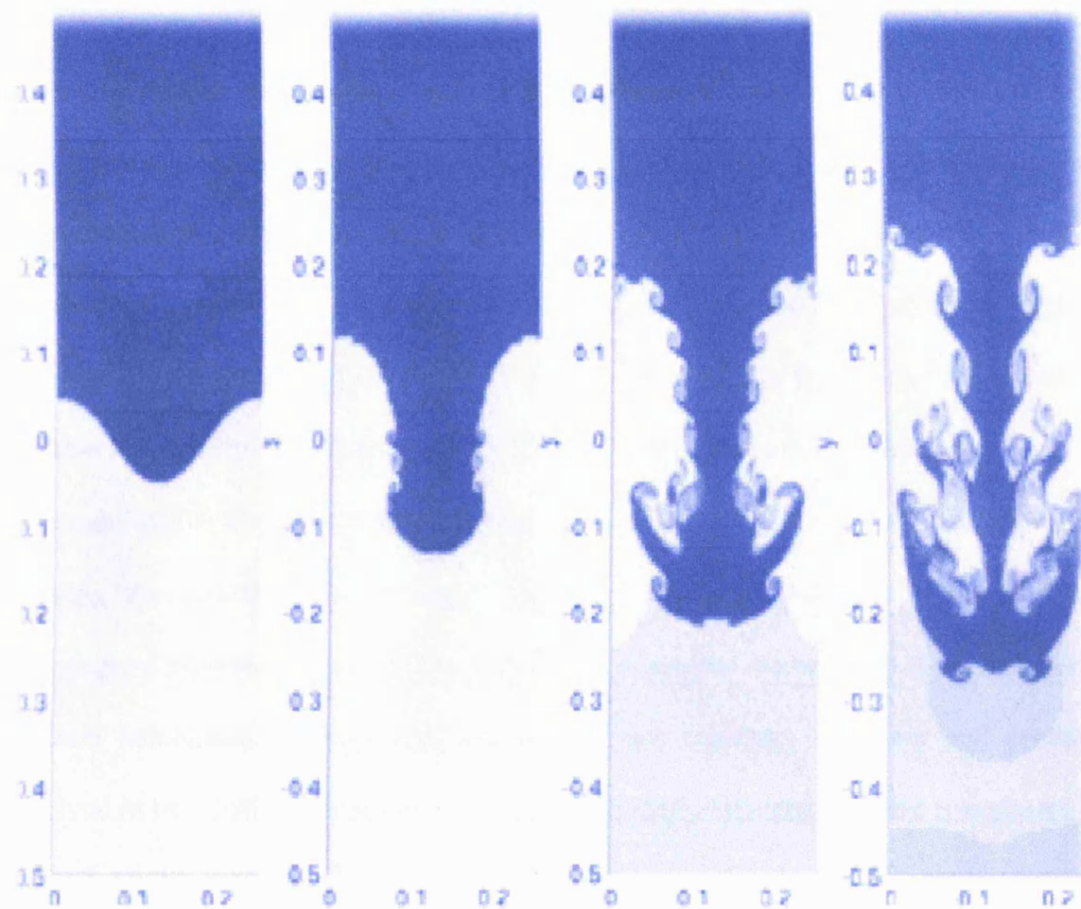
Chapter 1

Introduction to liquid-liquid

microflow systems

1.1. Background

The use of organic solvents involved in a large number of chemical processes inevitably causes solvent loss into the environment due to their volatility, with consequences on the environment and adverse health effects. Therefore, the search for cleaner chemical processes to reduce the release of harmful chemicals into the environment is highly desirable and constitutes an interesting challenge in chemistry nowadays. One possible solution is to use the *biphasic* or *liquid-liquid* system approach, by introducing a more environmentally friendly immiscible non-organic medium to an organic medium, allowing the consumption of lower amounts of organic solvents. An additional advantage of biphasic systems is the ease of recycling the reactants by exploiting their different solubilities between the two media. For example, reactants and product dissolved in two distinct phases can be separated simply by separating the two phases at the end of the reaction. As a consequence of such advantages, the application of biphasic systems is gaining a great deal of interest in different areas of chemistry especially in catalysis.[1-4] The typical choice of solvent combination in a biphasic system consists of an organic solvent combined with water as the non-organic immiscible solvent. However, there is a limited amount of catalysts or reagents that are water-soluble and water-stable, bringing limitations to a number of applications. Immiscible solvents other than water are recently becoming more and more favourable to apply in biphasic reactions, due to the solubility and stability of a wide variety of catalysts and reagents in such solvents. For example, ionic liquids and fluorinated solvents have many successful applications in biphasic synthesis such as Heck coupling and hydroformylation using ionic liquid media, while organic: fluorinated biphasic system is used in the Baeyer-Villiger oxidation reaction (Scheme 1.1) in the presence of

Lewis acid catalyst scandium bis-(perfluorooctanesulfonyl)amide Sc[N(SO$_2$C$_8$F$_{17}$)$_2$]$_3$.[5-8]

Ionic liquid ([bmim][BF$_4$])

Fluorinated solvent (Perflurohexane)

1 mol %

Sc[N(SO$_2$C$_8$F$_{17}$)$_2$]$_3$

H$_2$O$_2$ aq.

CF$_3$C$_6$F$_{11}$: Dioxane
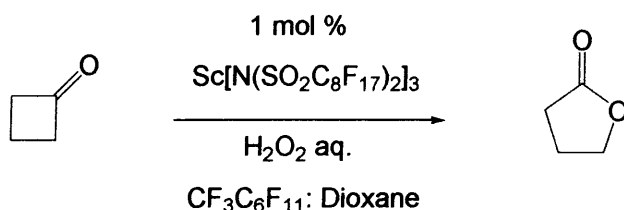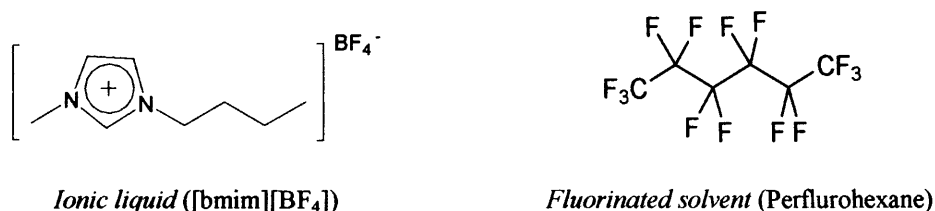
Scheme 1.1. Sc-catalysed Baeyer-Villiger oxidation of cyclobutanone in organic - fluorinated media using dioxane and perfluoro(methylcyclohexane) (1st catalyst recycling (96% yield): 2nd catalyst recycling (97% yield): 3rd catalyst recycling (94% yield).[8]

In biphasic systems, molecules at the region of contact between the two phases have a different molecular environment than those in the bulk of both phases. While there are equal cohesive forces in all directions between molecules inside the phase bulk, those at the region of contact have unbalanced cohesive forces as they are not entirely surrounded by the same molecules. Consequently, they are strongly attracted towards the direction of the bulk phase. As a result, a boundary between the two phases is formed, known as the interface or surface area, making it more difficult for one phase to mix with the other. An example of a boundary formation in nature is that between the liquid–air surface in which the unbalanced attractive forces result in a contraction of the

liquid surface towards the liquid bulk by pulling the liquid molecules at the surface into the bulk. Such phase contraction is the reason for formation of spherical shaped liquid droplets in nature.
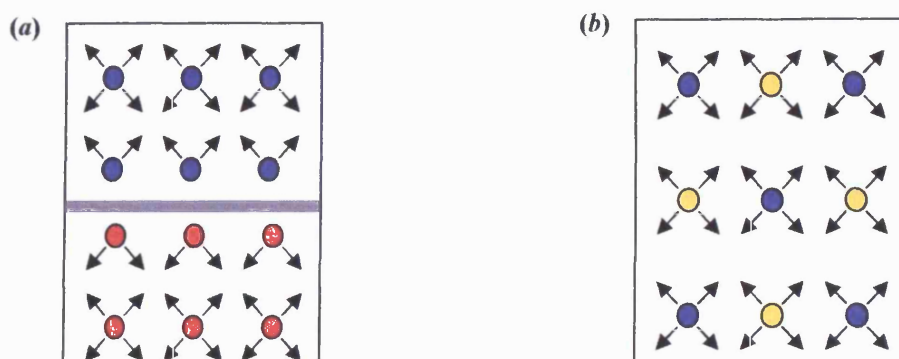
Figure 1.1. (*a*) Formation of an interface between two immiscible liquids (red and blue circles) as a result of unbalanced forces at the boundary in contrast to (*b*) a single phase system of two miscible solvents (yellow and blue circles).

The force at the surface or interface is defined as the *surface tension* or *interfacial tension* (γ). The term 'interfacial' is used to accompany the concept of tension when both phases are liquids whereas 'surface' is usually used for gas-liquid, gas-solid or solid-liquid systems. The stronger the cohesive forces in a phase, the higher the interfacial or surface tension. Hence, any decrease in the strength of the interaction will lead to a weaker tension which consequently increases the miscibility of the system. There are many ways of achieving this, for example, the addition of surfactants, mechanical stirring or applying high temperatures. In addition, each phase is subject to forces from the other, especially in liquid-liquid system compared to gas-liquid, making

the interfacial tension weaker in liquid-liquid system. The formation of a boundary in some liquid-liquid system does not depend only on the differences in the molecular environment between the two phases, but also on the degree of phase saturation in certain solvent systems. This is especially the case for partially miscible liquid-liquid systems. For example, in a biphasic system consisting of phase α and phase β, by addition of a small amount of phase α to a large amount of phase β a miscible system is formed. When phase α is continuously added to the system, a single phase is retained until phase β becomes fully saturated with phase α, thus causing phase separation. If addition of phase α continues until phase β become the minor phase, a miscible system will form again.[1, 9, 10]

Reactions in liquid-liquid systems can take place either at the interface or in the bulk of a phase. The occurrence of a reaction taking place at the interface depends on the reactants meeting at the interface, meaning that the interface area as well as the diffusion rate through the bulk plays an important role. On the other hand, if a reaction takes place in one of the phases, the reactants has to transfer first from one phase to the phase where the reaction is occurring, by diffusing through the interface before the reaction takes place. In this case, the rate of diffusion through the interface is an important factor. However, diffusion is more complicated through the interface than across the bulk as the mass transfer of the reactant through the interface must be taken into an account, as well as the solubility of the reactants in each phase has to also be considered. In a system where the solubility of a reactant is equal in both phases (α and β), the reactant would diffuse through the interface from the most concentrated phase to the less concentrated phase. Hence, the diffusion rate J (mol m^{-2} s^{-1}) in such system is expressed as a function of the diffusion coefficient D (m^2 s^{-1}), the diffusion distance x

5

(m), and the concentrations of both phases α and β (mol m^{-3}), as shown in Equation 1.1 (differential form).[1]

$$J = -D\frac{d([\alpha]-[\beta])}{dx}$$

(Eq. 1.1)

On the other hand, a reactant with different solubility in both phases will diffuse in the direction of the phase in which the reactant is more soluble, regardless of the concentration, until saturation conditions are reached. Consequently, in this case the diffusion rate is affected by the concentration relative to the saturation. The ratio of distribution of solute between the two phases is known as partition coefficient P which is determined by the relative solubility of the solute S in each phase of the system under identical physical conditions, as shown in Equation 1.2.[1, 9, 11, 12]

$$P = \frac{[S]\text{phase }\alpha}{[S]\text{phase }\beta}$$

(Eq. 1.2)

1.2. Liquid-liquid flow in microchannel

For an immiscible liquid-liquid system in a flask, the liquid phase with greater density is found at the bottom while the lighter liquid is on top forming an undisturbed flat interface. When the system is agitated, drops of various sizes of one phase form and disperses within the other phase. In a microchannel, the two immiscible liquids found to create various flow patterns, from segregated plugs (*i.e.* droplets or segments) of

6

alternating phases to parallel flow in which both phases flow side by side.[13] These flow

patterns are characterised by a number of dimensionless parameters, influenced by

factors such as the microchannel properties, flow velocity, and the liquid properties.[14]

Variation of these parameters affects the stability of the flow pattern and can lead to

transition from one flow pattern to another. The characteristics of liquid flow in a

channel were first studied by Osborne Reynolds in 1883, by pumping a liquid

continuously into a glass tube while introducing a fine strand of coloured liquid to the

flow (Figure 1.2). Reynolds observed that, at low flow rate, laminar flow was the

dominating behaviour, in which the coloured strand flowed in straight parallel streams

along the flow direction (Figure 1.3). As the flow rate was increased, the coloured

strands were broken into vortices until a point where turbulent flow behaviour was

dominant across the tube (Figure 1.3).[15, 16] This transformation from laminar to

turbulent flow is characterised by the dimensionless quantity known as the *Reynolds*

number (Re).[15]

$$Reynolds\ number\ (Re) = \frac{\rho v d}{\mu} = \frac{Inertia\ forces}{Viscous\ forces} \qquad (Eq.\ 1.3)$$

Reynolds number relates inertia and viscous forces as shown in Equation 1.3, where ρ is

the density (Kg m^{-3}), v represents the velocity (m s^{-1}), d is the characteristic length (m),

and μ is the viscosity (Kg m^{-1} s^{-1}). At low values of the *Reynolds number (Re < 2000)*,

laminar flow behaviour dominate, while at high *Reynolds number (Re > 3000)* turbulent

flow behaviour is the dominant mode. Within the intermediate range of *Reynolds*

number (2000 $\leq$ *Re* $\leq$ 3000) the flow is neither entirely laminar nor turbulent since the

transformation take place over a range of *Re* values. The viscous and inertia forces are related to the channel surface tension by the dimensionless *Capillary* (*Ca*) and *Weber* (*We*) *numbers*.
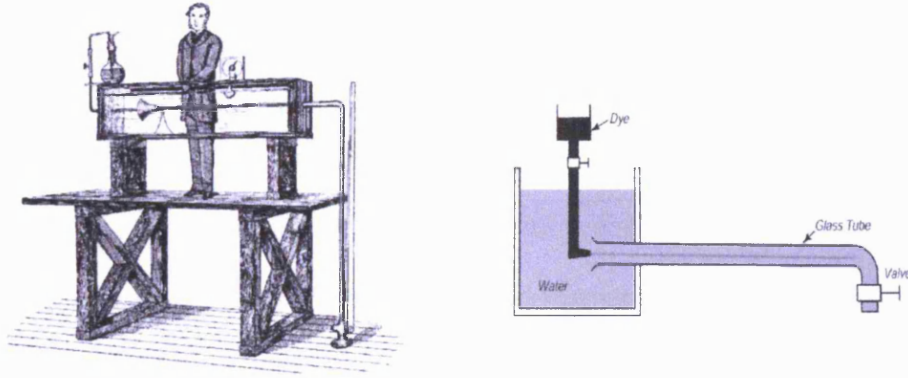
Figure 1.2. Reynolds apparatus for flow pattern study.[17]
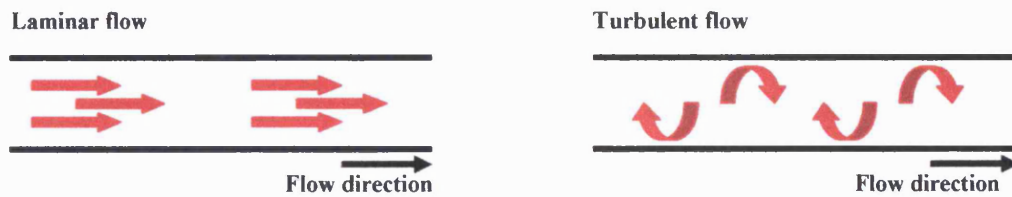
Figure 1.3. Schematic illustration of the liquid flow in a channel shown by red arrows: *(left)* laminar flow at low *Re* and *(right)* turbulent flow at high *Re*.

Capillary number (*Ca*)[18] relates viscosity and surface tension as presented in Equation 1.4, where μ is the liquid viscosity, v is the flow velocity and γ is the surface tension. On the other hand, the *Weber number* (*We*)[18] relates the inertia forces to the surface tension, as shown in Equation 1.5, where ρ is the liquid density, d is the characteristic length, v is the flow velocity and γ is the surface tension.

$$Capillary\ number\ (Ca) = \frac{\mu\, v}{\gamma} \qquad\qquad \text{(Eq. 1.4)}$$

$$Weber\ number\ (We) = \frac{\rho\, v^2 d}{\gamma} \qquad\qquad \text{(Eq. 1.5)}$$

The relatively small size of the microchannel cross section causes the viscous forces to dominate over the inertia, resulting in a low Reynolds number. Hence, laminar flow behaviour is dominant and mixing occurs *via* diffusion rather than turbulences. Laminar flow systems are preferable to uncontrolled turbulent flow on account of a much better reproducibility, while on the other hand the formation of turbulences leads to unpredictable patterns. In theory, a liquid-liquid system should flow in microchannel under laminar conditions, however, the presence of a liquid-liquid interface boundary will create a complex interplay between the inertial and viscous forces balance within each single phase on one hand, and the interfacial tension on the other hand, resulting in a variety of interfacial boundary shapes leading to various flow patterns. Günther *et al.* [14] illustrated the relationship between these influential forces in different types of liquid-liquid systems by means of a diagram as a function of the channel cross section area and velocity as shown in Figure 1.4. [14, 18] In a macroscale channel, gravity has an effect on the flow pattern of a biphasic system; consequently the flow pattern varies between vertical and horizontal channels. However, in a microchannel, the gravity effect is dominated by the viscosity forces which is expressed by the *Bond number* (*Bo*) as a ratio of gravity force to surface tension [18] (Equation 1.6) where $\Delta\rho$ is the density difference, g is body force due to gravity, *d* is the characteristic length and γ the interfacial tension.

$$Bond\ number\ (Bo) = \frac{(\Delta\rho)g\,d^2}{\gamma} \hspace{3cm} (Eq.\,1.6)$$
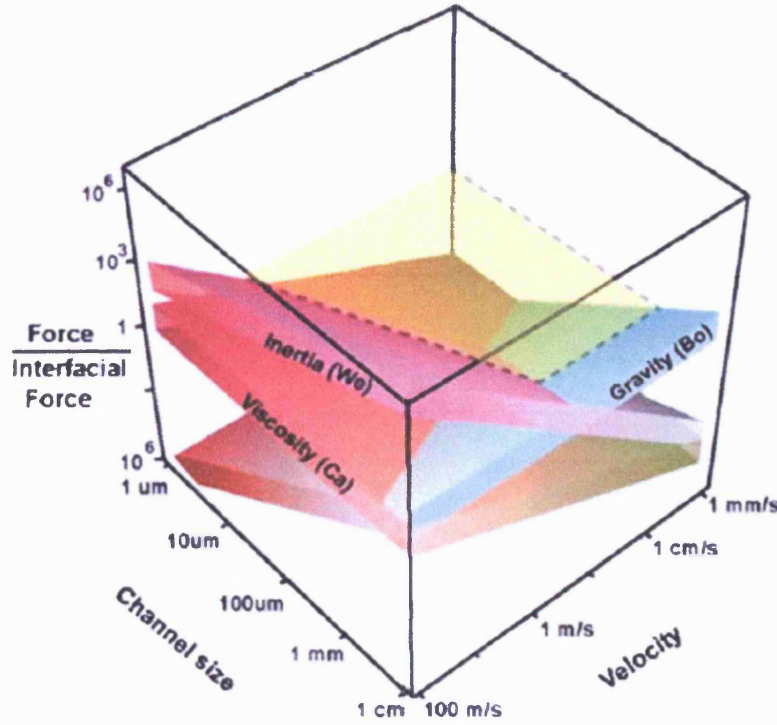
Figure 1.4. Effect of interfacial forces on inertia, viscous, gravity forces with respect to velocity and channel cross section area: inertia forces represented by the pink plane; viscosity forces represented by the orange plane; gravity forces represented by the blue plane.[14]

1.2.1. Channel surface and liquid-liquid interaction

When the cohesive forces of a liquid phase exceed the attractive forces between the liquid and the surface (adhesive forces), high surface tension is attained, resulting in formation of droplets of liquid on the surface. On the other hand, low surface tension

is achieved when adhesive forces dominate the cohesive forces hence the liquid spreads over and wets the surface. The extent of contraction or spreading of the liquid on a surface depends on the degree of surface tension or, in other words, the wetting property of the surface. The degree of wetting can be expressed with the contact angle (θ) between the surface and the liquid. For example, a drop of water on a hydrophobic (non-wetting) surface would have a large contact angle going toward 180°, as illustrated in Figure 1.5 (a), whereas a small contact angle, approaching zero, means that the water spreads on a hydrophilic surface (wetting) as illustrated in Figure 1.5 (b).[18]
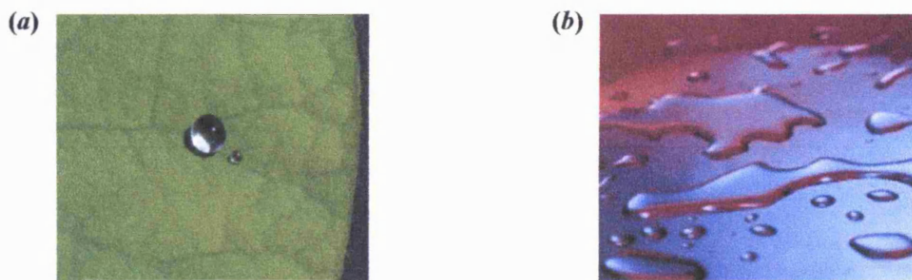
Figure 1.5. Water drop on (*a*) non-wetting surface *vs.* (*b*) wetting surface.[19, 20]

In a binary system, when a drop of oil and a drop of water are placed on top of each other on a hydrophilic surface, the water spreads and forms a barrier between the oil layer and the surface as shown in Figure 1.6(*a*). On the other hand, when a hydrophobic surface is used instead, both the oil and water layers will have direct contact with the surface, as shown in Figure 1.6(*b*).[21] Similarly, the behaviour of a liquid-liquid system inside a microchannel will depend on the nature of the channel

11

surface in addition to other parameters such as viscosity and velocity. In the case of a hydrophobic channel, the water phase will tend to form droplets within the oil phase as illustrated in Figure 1.6 (c). On the other hand, when oil and water flow in a channel with a hydrophilic surface, the water phase tend to spread over the surface forming a film separating the mono-disperse oil droplets from the wall, as illustrated in Figure 1.6 (d).
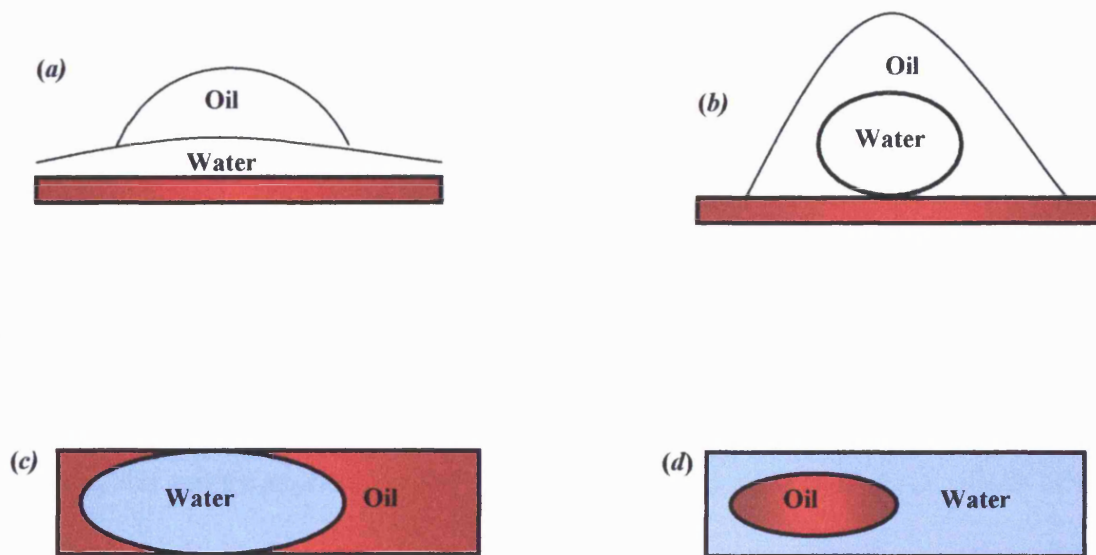
Figure 1.6. (*a*) Water layer spreading on a hydrophilic surface forming a barrier between the oil layer and the surface; (*b*) water droplet forms on a hydrophobic surface forming a contact point between both the oil and the water layer in addition to the oil-water interface area; (*c*) water segments flowing in oil phase in a channel with hydrophobic surface; (*d*) oil droplet flowing in water flow in a channel with hydrophilic surface.

This phenomenon is quantitatively described by Young's Equation (Equation 1.7), which relates the surface tension to the liquid-liquid interfacial tension, where γ (oil-

water) represents the interface tension between oil and water, θ represents the surface-liquid contact angle, and γ (oil-surface) and γ (water-surface) represent the surface tension between the channel and the liquid.[14]

$$\gamma \text{ (oil} - \text{water) cos } \theta \ = \ \gamma \text{ (oil} - \text{surface)} - \gamma \text{ (water} - \text{surface)} \qquad \text{(Eq. 1.7)}$$

As illustrated in Figure 1.6 and expressed in Equation 1.7, by changing the property of the surface it is possible to change the type of interface area between two immiscible liquids. Hence, in a microchannel, the flow pattern can be manipulated by having a control over the wetting characteristics of the microchannel either by treating the surface channel or by varying the liquids properties. For example, hydrophobic polymer surfaces can be irradiated by UV to break the polymeric chain hence changing the surface tension, on the other hand surfaces such as glass or silicon can be turned into hydrophobic surfaces through silanization, *i.e.* a process in which the hydroxyl groups are coupled with silane to deactivate it leading to a non-wetting surface.[18, 22-26] An alternative way of gaining control over the wetting properties of glass or silicone surfaces is through the use of surfactants to alter properties of the liquids. Dreyfus *et al.*[27] investigated the effect of surfactants on the flow pattern of a water-tetradecane immiscible system using a cross inlet junction as depicted in Figure 1.7. The addition of surfactants to the tetradecane phase helps to improve the wetting property towards the tetradecane. Initially, the experiment was conducted by injecting the water and tetradecane into a microchannel through the three inlet port. The water

was pumped through the two side inlets while the tetradecane through the central inlet using a range of flow rates.
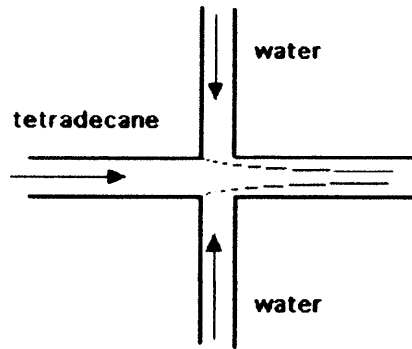
Figure 1.7. Cross inlet junction used by Dreyfus *et al.* to investigate the liquid-liquid flow pattern behaviour. [27]

When the tetradecane was pumped at a high flow rate and water at low flow rate, a well defined and separated aqueous droplet flow carried through the wetting tetradecane flow was obtained (Figure 1.8(*a*)). As the flow rate of tetradecane decreased, the aqueous droplets began to expand in length forming a pearl necklace-like flow. Increasing the flow rate of water resulted in either a pear-like droplet flow at low flow rate of tetradecane or a stratified stream at high flow rate of tetradecane. When the same experiment was repeated without the use of a surfactant, an irregular flow pattern formed (Figure 1.8(*b*)), as the tetradecane had a weak wetting property towards the channel surface. In conclusion, all the above mentioned examples demonstrated that the interplay between factors like the channel surface and interfacial forces as well as the flow rate has a crucial role on the manipulation of the flow pattern of a liquid-liquid system in a microchannel.

14
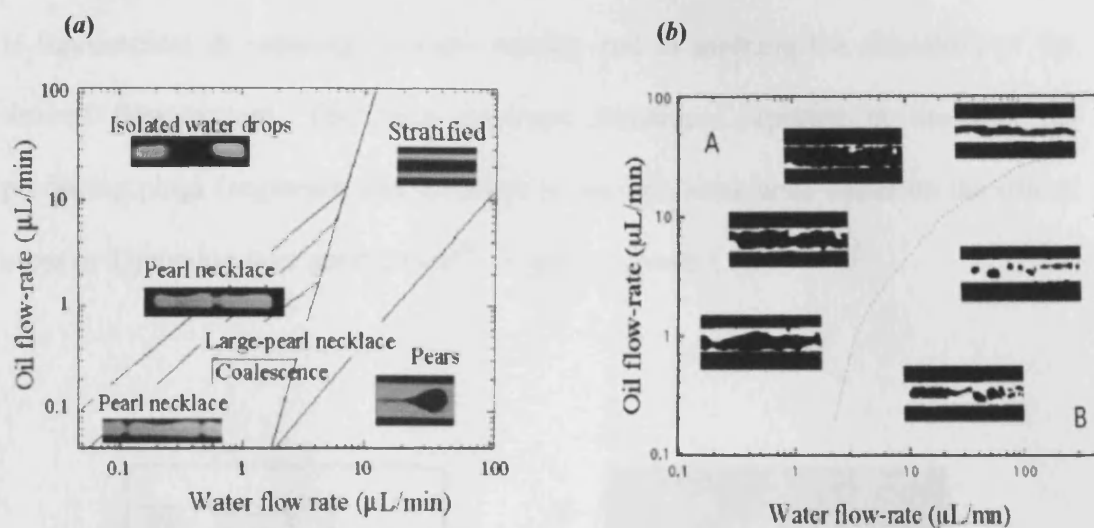
Figure 1.8. Various possible water-tetradecane flow patterns using a cross inlet junction; (*a*) flow patterns under wetting conditions with respect to tetradecane: (*b*) flow patterns under non wetting conditions with respect to tetradecane.[27]

1.2.2. Flow pattern formation of liquid-liquid systems in microchannel

1.2.2.1. Plug flow: segmented and droplet flow

So far we have briefly defined the relationship between a group of dimensionless numbers (*Re, Ca, We, Bo*, Equations 1.3 to 1.6) which influence the flow patterns of a biphasic liquid system in the microchannel, by taking into account all the physical properties of the flow in the channel such as viscosity, density, velocity and surface tension. We have also seen how the flow pattern stabilisation is affected by the manipulation of both the liquid and the surface properties, either by modification of the surface wettability or by addition of surfactants to the liquid. In addition to the above mentioned factors, the formation of specific flow patterns can also be affected

by the design of the microchannel inlet system. The general importance of inlet design is fundamental in ensuring efficient mixing and in assisting the formation of the desired flow pattern. The most common techniques reported in literature for producing plugs (segments and droplets) in various sizes were based on the use of cross or T-junction inlet geometries[28] (Figures 1.7 and 1.9).
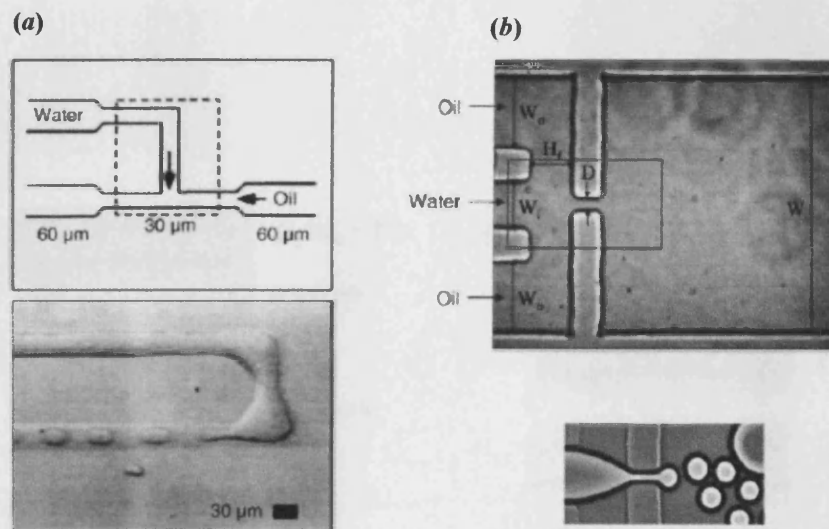
Figure 1.9. Formation of plug flow using (a) a side T-inlet junction and (b) a flow focused junction. [29,30]

In such geometries the immiscible to-be-dispersed phase is fed into the main channel that carries the other continuous phase. If the continuous phase wets the walls of the channels preferentially to the other phase, the non-wetting phase enters the main duct then breaks into plugs, as depicted in Figure 1.9(a). A less common method for small plug formation involves the so-called *flow focusing* technique [29, 30] in which the droplet flow is created through a central channel into a focused narrow cavity while being surrounded by the second phase, as depicted in Figure 1.9(b). Formation of plug flow at the inlet is affected by the interplay between interfacial tension, shear force

16

and pressure gradient between the two phases.[31, 32] The pressure variation is a result of increased interfacial resistance of the flow emerging from the inlet against the other flow. This leads to an interfacial instability aiming to minimize the interface area of the emerging flow creating a segment or droplet *via* a mechanism of expulsion.[30] The plug length is largely influenced by the volumetric flow ratio of both phases rather than flow velocity or viscosity, as illustrated by the micrograph of Luo *et al* in Figure 1.10.[14, 18, 21]
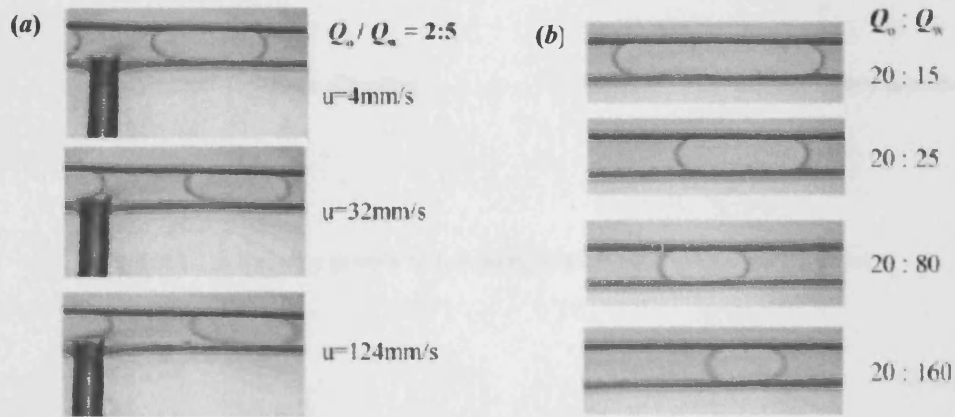
Figure 1.10. (*a*) Micrograph illustrating the effect of velocity variation (mm·s^{-1}) of oil and water flow system on the segment size. (*b*) Micrograph illustrating the effect of volumetric flow ratio variation of oil and water flow (Q_o:Q_w) on the segment size.[18]

The interaction between the segment and the microchannel wall causes a shear stress due to the adhesive forces (*i.e.* viscosity). This shear stress results in velocity streams travelling straight in the direction of the flow from the back to the front of the segment. As the flow stream approaches the interface boundary, diversion of the stream occurs causing internal circulating vortices inside the segment (Figure

1.11(*a*)). Symmetrical circulating vortices form as a result, mainly localized in the top half and the other on the bottom half of the segment. One complete cycle of recirculation occurs when the segment has travelled its length.[33, 34]
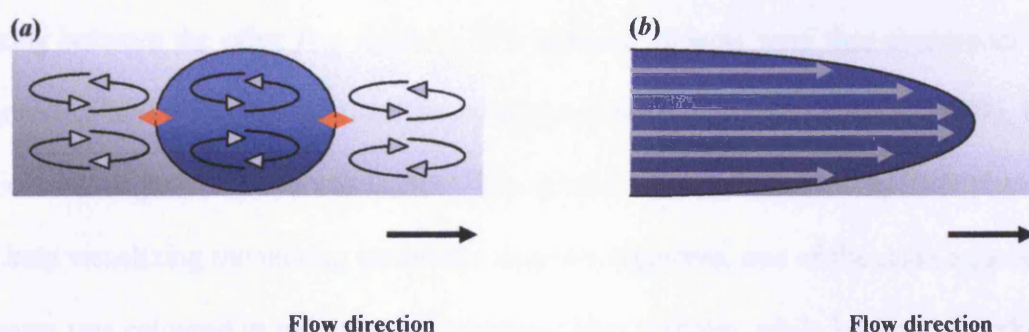
Figure 1.11. Velocity profile in (*a*) segmented flow and (*b*) laminar flow.

At low values of Reynolds number, the velocity profile of a monophasic flow in a microchannel is parabolic and varies across the diameter of the channel, having a minimum value near the channel walls, and a maximum value at the centre of the flow (Figure 1.11(*b*)). This velocity gradient arises from the adhesive forces between the channel walls and the liquid, causing the liquid layers nearest to the walls to be slower than that in the centre.[16, 35] Hence, as the front of the liquid phase advances, a gradient of concentration generates along the channel length, affecting the reactivity thus creating a limitation to the use of laminar flow, in spite of the advantages given by its fast diffusion. An additional limitation arises from the initial distance that reactants have to run through before they completely mix. In this case, one way to

improve the rate of mixing and overcome the velocity gradient problem is to generate a controlled and reproducible turbulence *via* segmentation at low *Re* values.[36] Ismagilov *et al.* studied the influence of the segment length on the rate of mixing as illustrated on the microphotographs in Figure 1.12(*a*).[21] Three aqueous streams were combined in a poly(dimethylsiloxane) (PDMS) hydrophobic microchannel, two of them containing reagents and the third being injected in between in order to delay the mixing between the other two streams. The aqueous streams were then continuously segmented into a flow of immiscible fluorinated perfluorodecalin solvent (PFD), in which the reagents were mixed inside the segments while transported by PFD phase. To help visualizing the mixing inside the aqueous segments, one of the main aqueous streams was coloured in red using an inorganic iron complex while keeping the other streams colourless. The length of the segment was varied with the volumetric flow ratio of the aqueous phase to the PFD phase. According to the microphotographs, shorter segments achieved faster mixing as the red colour distributed rapidly around the segment compared to longer segment. The same authors then conducted the experiment without the presence of the carrier flow to obtain laminar flow behaviour resulting in slower colour distribution than that in segmented flow as a result of laminar flow behaviour. Even though the mixing inside a segment is more effective than in a laminar flow, there are some disadvantages nonetheless. For instance, Ismagilov argued that while symmetrical vortices form on the top and the bottom halves of a segment, there might be little or no mixing in the central region of the segment. Hence, the author developed a way to enhance the mixing inside segments using *chaotic advection* in which additional vortices are generated by stretching and folding the segment (Figure 1.12(*b*) and (*c*)). This was achieved using a microchannel with asymmetrical zigzag edges geometry instead of a straight microchannel.[32, 37]
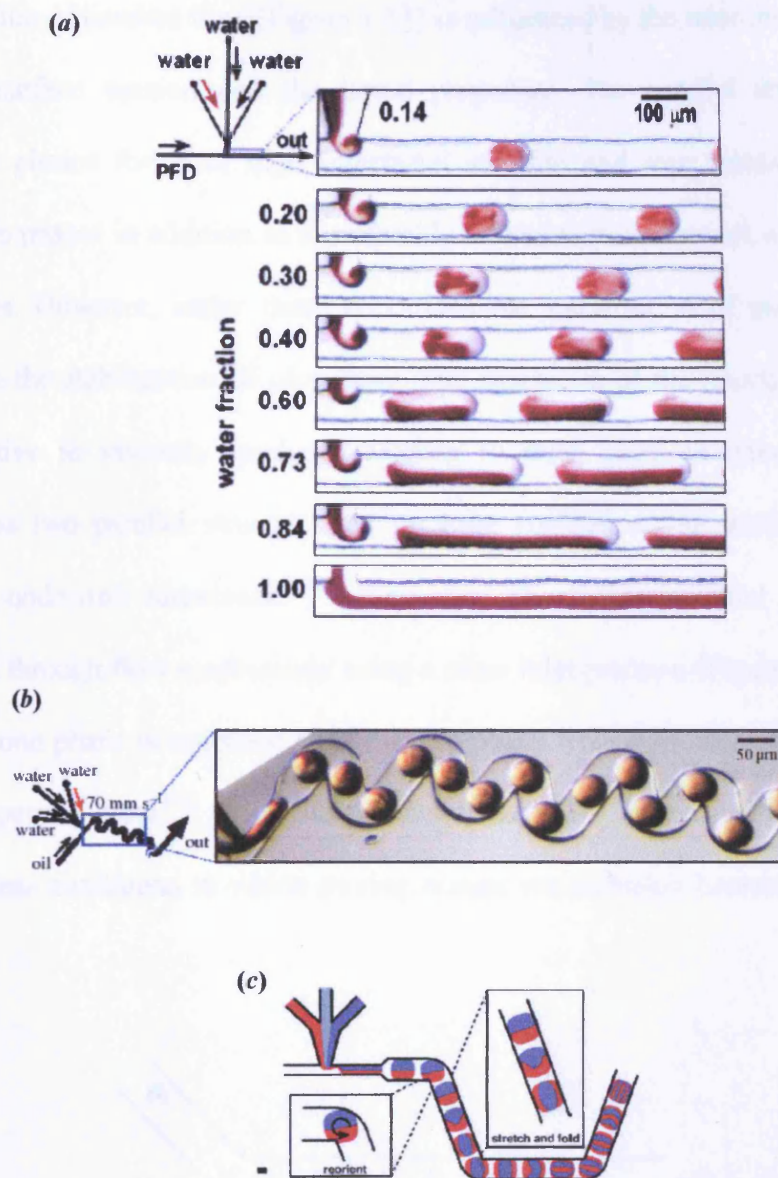
19

Figure 1.12. (*a*) Microphotograph demonstrating the effect of segment length on the internal circulation by varying the amount of aqueous stream while travelling at the same velocity (50 mm·s⁻¹) into the microchannel.[21] (*b*) Microphotograph demonstrating of a microchannel zigzag design. (*c*) Illustration of mixing mechanism in a zigzag microchannel.[32, 37]

1.2.2.2. Parallel flow

The formation of parallel flow (Figure 1.13) is influenced by the relationship between interfacial-surface tension and the liquid properties. The parallel stream of two immiscible phases forms at high interfacial stability and low viscosity gradients between the phases in addition to a preferably wetted surface channel with respect to both phases. However, under these conditions the stabilization of parallel flow is harder than the stabilization of plug flow. The steadiness of the interface, in fact, is very sensitive to viscosity gradients leading in most cases to uneven velocities between the two parallel streams, thus creating vortices at the interface giving a degree of undesired turbulence[14,18] One way of creating parallel flow can be established through flow *confinement* using a cross inlet junction (Figure 1.7 and 1.8), *i.e.* where one phase is squeezed by the other phase from both sides to form a thin stream of parallel flow.[38] Once the parallel streams are formed, each phase flows under laminar conditions in which mixing occurs *via* diffusion between the phases.
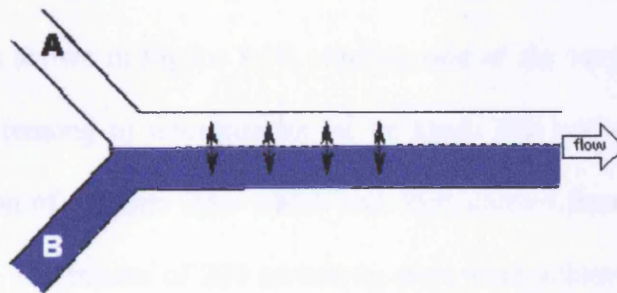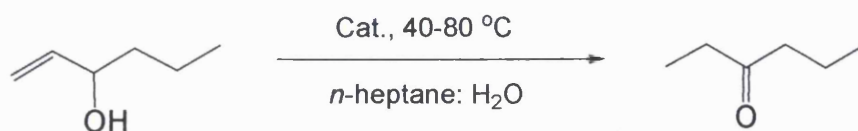

Figure 1.13. Schematic illustration of mixing by diffusion in parallel flow.

21

1.3. Liquid-liquid microflow systems in organic synthesis

Miniaturisation of chemical processes using microflow systems can exhibit significant advantages over existing flask methods, such as high surface-to-volume ratio, short diffusion distances, fast and efficient heat dissipation and mass transfer. These properties have been advantageously used in liquid-liquid organic synthesis. In liquid-liquid reactions, segmented and droplet flow systems seemed to win the interest over reactions carried in parallel flow systems. The reason for that is perhaps due to the easy formation and control of the plug flow regime over parallel flow, in addition to an increase in interfacial area, and efficient mixing inside segments. De Bellefon et al.[39] showed one of the earliest examples of biphasic reaction optimisation performed in a microreactor under segmented flow conditions. Isomerization of allylic alcohol into carbonyl compounds was carried out using a microchannel tube combined with a micromixer (Figure 1.14). In order to achieve this, various transition metal complexes with a library of water-soluble ligands were screened for the isomerization of 1-hexene-3-ol to ethyl propyl ketone using aqueous-hydrocarbon solvent system. The catalysts and substrates were introduced simultaneously in pulsed injection fashion as shown in Figure 1.14, creating one of the very first examples of high throughput screening in microreactor of its kind. The use of the micromixer helped the formation of droplets flow which was then carried through the integrated microchannel tube. The results of 224 screening tests were achieved in shorter time than using conventional methods, clearly demonstrating the efficiency of microsystems for optimising reaction conditions and finding efficient catalysts while operating at a fast rate with small loading.

Scheme 1.2. Isomerization reaction of 1-hexene-3-ol to ethyl-propyl ketone in microreactor.
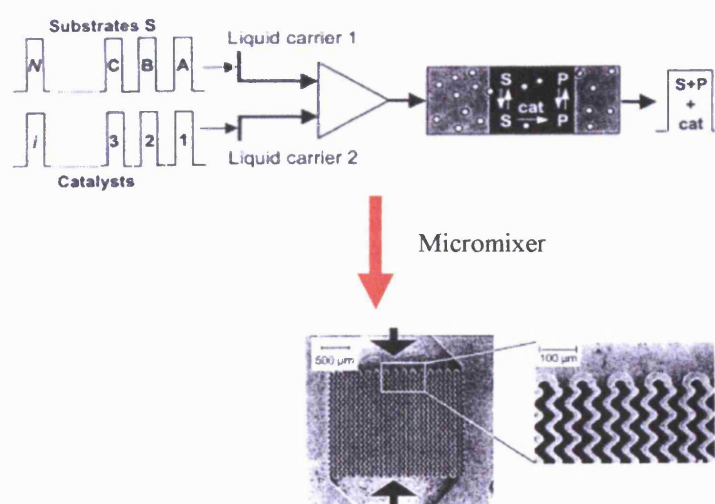
Figure 1.14. Schematic illustration of the flow setup with micromixer used in the high throughput screening of the isomerization of allyl alcohol.[39]

Meanwhile, Mikami *et al.*[40] exploited the fruitful advantages of liquid-liquid microflow system to carry out a Mukaiyama aldol biphasic catalysis between an aldehyde and silyl enol ether using a fluorinated:organic solvent system in the presence of lanthanide complex scandium bis-(perfluorooctanesulfonyl)amide Sc[N(SO$_2$C$_8$F$_{17}$)$_2$]$_3$ as a Lewis acid catalyst. Using *Direct Nanoflow System* apparatus (DiNas), supplied by KYA TECH Corp, the reagents were delivered into the

23

microflow system resulting in a parallel flow regime between the fluorinated and organic medium (Figure 1.15). At the end of the reaction, the product was easily separated from the organic phase while the catalyst remained in the fluorinated phase. Using the same approach, Mikami et al.[41] were also able to increase the reaction rate of the Baeyer–Villiger reaction catalyzed by $Sc[N(SO_2C_8F_{17})_2]_3$, where the lactone product was obtained in high regioselectivity even at low catalyst concentration.
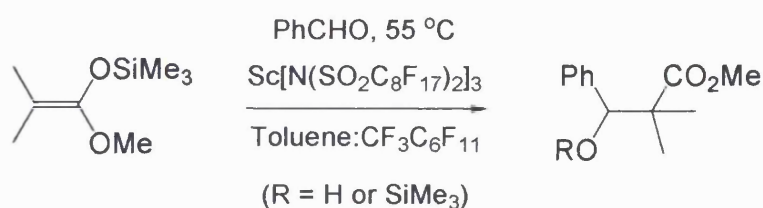
Scheme 1.3 Mukaiyama aldol reaction.
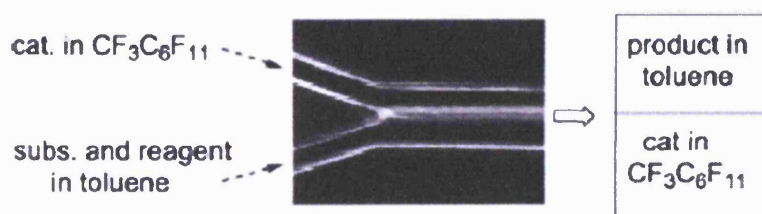
Figure 1.15. Mukaiyama aldol reaction in a borosilicate microreactor under parallel flow in organic - fluorinated media using toluene and perfluoro(methylcyclohexane). [40]

24
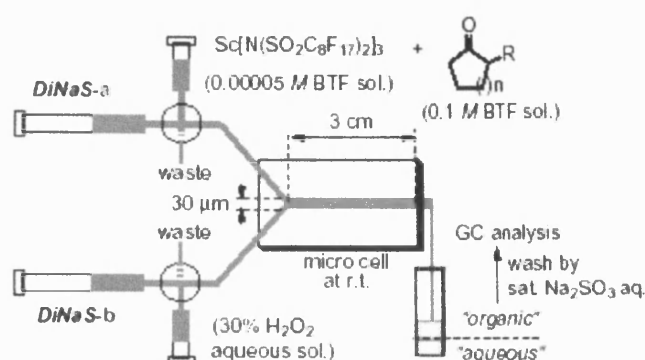
Figure 1.16. Baeyer–Villiger reaction in microreactor using DiNas system (n=1,2; R=alkyl, aryl).[41]

Liquid-liquid microflow systems using parallel flow were also used by Kitamori *et al.*[42] to further improve the phase transfer reaction between *p*-nitrobenzene diazonium tetrafluoroborate and 5-methylresorcinol in water:ethyl acetate solvent system using a glass microdevice (Scheme 1.4). The microsystem offered a rapid phase transfer of starting material and product across the interface, thus speeding up the chemical reaction and improving the product isolation. Reaction took place as the organic and aqueous layer came in contact, while the product passed in the organic phase as it formed. Compared to the conventional method, the microreactor study proved successful in giving higher reaction conversion, close to 100%. In addition, while the conventional flask conditions favoured the formation of a bis-azo side-product as a result of an undesirable side reaction, in the microreactor system, on the other hand, the fast removal of the product into the organic phase allowed the side reaction to be avoided.
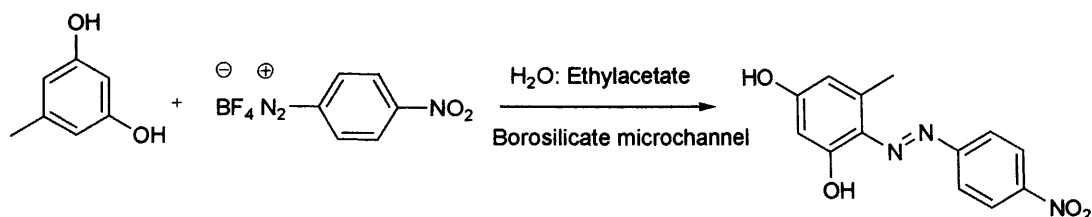
Scheme 1.4. Phase transfer catalysis reaction of p-nitrobenzene diazonium tetrafluoroborate with 5-methylresorcinol.

At a later stage, the same authors achieved another successful phase transfer catalysis under segmented flow conditions.[43] The benzylation of ethyl-2-oxocyclopentanecarboxylate was carried out in an organic:aqueous solvent system in the presence of tetrabutylammonium bromide (TBAB) using a glass microchannel (Scheme 1.5). Further studies demonstrated that the smaller the glass microchannel cross section area the higher the reaction rate.
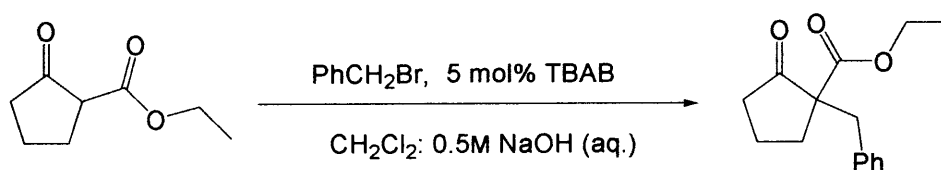
Scheme 1.5. Phase transfer alkylation of ethyl 2-oxocyclopentane carboxylate with benzyl bromide in presence of TBAB.

Another literature example of phase transfer catalysis in biphasic microreactor under segmented flow was reported by Okamoto et al. working at the Organic Synthesis Laboratory of Sumitomo Chemical Co. Ltd.[44] Segmentation was generated using

26

alternating pumping mechanism (Figure 1.17) to increase the rate of the biphasic

alkylation reaction of malonic ester with iodoethane (Scheme 1.6) in the presence of

phase transfer catalyst tetrabutylammonium hydrogen sulphate (TBAHS).[45-47]
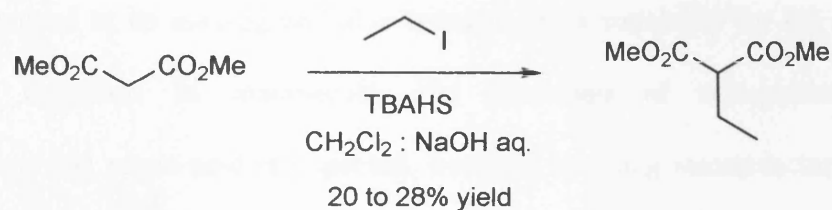
Scheme 1.6. Alkylation of malonic ester with iodoethane in presence of phase transfer catalysis using

TBAHS.
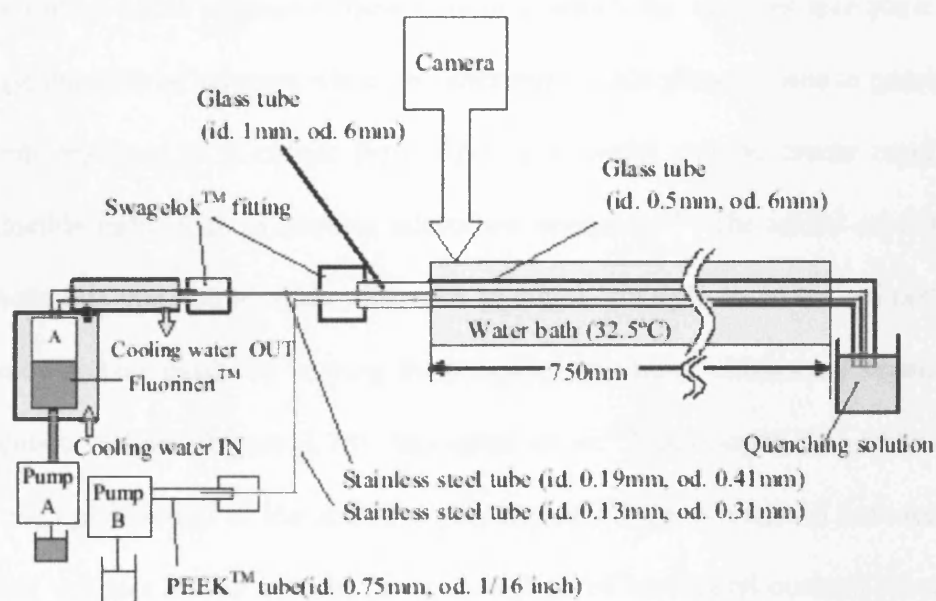
Figure 1.17. Experimental set-up for alternating pumping of solution A, containing iodoethane and

malonic acid dimethyl ester in dichloromethane, and solution B containing TBAHS in a solution of

NaOH aq.[44]

The industrially important nitration reaction of aromatic rings in a liquid-liquid microflow system was investigated by few authors using either parallel[48] or segmented flow.[49] In all studies a polytetrafluoroethylene (PTFE) capillary microchannel, connected to an inlet junction, was used to form either segmented or parallel flow. The use of PTFE was desirable because of the easy microfabrication methods involved in its making and also because of its suitability for the study of exothermic reactions. In macroscale, the formation of side-products like dinitrobenzene and picric acid is expected, however by using microreactor systems the formation of side products was reduced as well as obtaining an increase in the reaction rate.

The additional benefit of liquid-liquid flow system is that monophasic reactions can also be carried out in segmented flow fashion in which the reactions take place within a compartmentalized segment while the other immiscible phase is used to generate the segments and acts as a carrier flow. This is a useful way to create regular and reproducible turbulence in laminar microflow reactions.[30] The added advantage of this method is that optimisation processes in which multiple reactions are performed can be carried out easily by varying the reaction conditions within each segment in a consecutive fashion (Figure 1.18). Ismagilov et al.[50] developed this technique to study the optimization of the selective protodeacetylation of ouabain hexaacetate in nanoliter volumes and as a result the consumption of hexaacetyl ouabain substrate is decreased to less than 1 mg per condition. In order to accomplish this, the segments containing the ouabain hexaacetate substrate were introduced in a consecutive sequence into an immiscible fluorinated flow, in which each segment was injected with a different protodeacetylation reagent including a selection of Lewis acids,

inorganic bases and Lipases enzymes. For further efficiency, each segment was analysed at the end of the reaction using a continuous on-line Matrix-Assisted Laser Ionization Mass-Spectrometry (MALDI-MS) detection. The best conditions were found under basic conditions as illustrated in Figure 1.18. [51, 52]
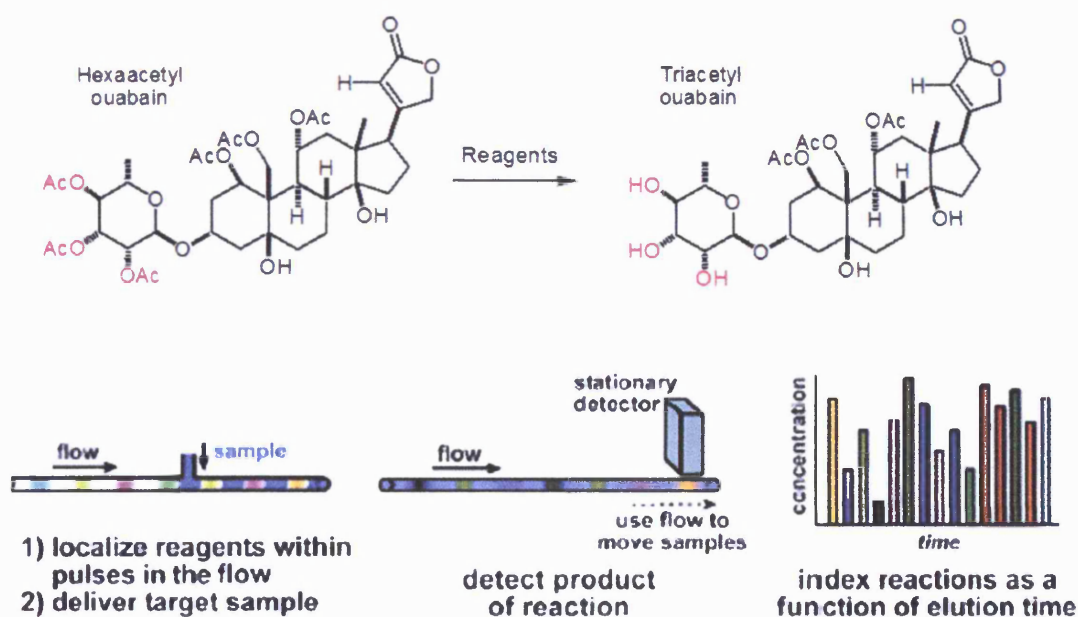
Figure 1.18. Optimisation microflow system used for the deacetylation reaction of ouabain hexaacetate equipped with MALDI- MS for online analysis.[50, 52]

1.4.   References

[1]   D. J. Adams,; P. J. Dyson,; S. J. Tavener, Chemistry in Alternative Reaction Media; Wiley, 2004.

[2]   T. Ohkouchi, T. Kakutani, M. Senda, *Bioelectrochem. Bioenerg.* **1991**, *25*, 81-89.

[3]   R. Lahtinen, D. J. Fermin, K. Kontturi, H. H. Girault, *J. Electroanal. Chemistry* **2000**, *483*, 81-87.

[4]   T. J. Davies, A. C. Garner, S. G. Davies, R. G. Compton, *Chem. Phys. Chem.* **2005**, *6*, 2633-2639.

[5]   M. J. Earle, K. R. Seddon, *Pure Appl. Chem.* **2000**, *72*, 1391-1398.

[6]   H. Zhao, S. V. Malhotra, *Aldrichimica Acta.* **2002**, *35*, 75-83.

[7]   S. J. Tavener, J. H. Clark, *J. Fluorine Chem.* **2003**, *123*, 31-36.

[8]   X. Hao, O. Yamazaki, A. Yoshida, J. Nishikido, *Green Chem.* **2003**, *5*, 524-528.

[9]   I. N. Levine, Physical chemistry, McGraw-Hill Science Engineering, 2001.

[10]   H. N. V. Temperley, D. H. Trevena, *Liquids and their properties*, Ellis Horwood Limited, **1978**.

[11]   W. Nitsch, *Faraday Discuss. Chem. Soc.* **1984**, *77*, 85-96.

[12]   G. J. Hanna, R. D. Noble, *Chem. Rev.* **1985**, *85*, 583-598.

[13]   G. N. Doku, W. Verboom, D. N. Reinhoudt, A. van den Berg, *Tetrahedron* **2005**, *61*, 2733-2742.

[14] A. Gunther, K. F. Jensen, *Lab Chip* **2006**, *6*, 1487-1503.

[15] F. A. Holland, R. Bragg, Fluid Flow for Chemical Engineering, 2nd Ed., Butter Worth- Heinemann, 1995.

[16] J. M. Coulson, J. F. Richardson, J. R. Backhurst, J. H .Harker, Chemical Engineering, Vol. 1, 4th Ed., Pergamon Press, 1990.

[17] www.physics.utoronto.ca

[18] C. N. Baroud, H. Willaime, *C. R. Physique* **2004**, *5*, 547-555; J. H. Xu, G. S. Luo, S. W. Li, G. G. Chen. *Lab Chip* **2006**, *6*, 131-136.

[19] B. S. Ghill, www. victoria-adventure.org

[20] INMAGINE, www.gb.inmagine.com.

[21] J. D. Tice, H. Song, A. D. Lyon, R. F. Ismagilov, *Langmuir* **2003**, *19*, 9127-9133.

[22] K. Efimenko, W. Wallace, J. Genzer, *J. Colloid Interface Sci.* **2002**, *254*, 306-315.

[23] J. Brzoska, J. Ben Azouz, F. Rondelez, *Langmuir* **1994**, *10*, 4367-4373.

[24] B. Zhao, N. O. L. Viernes, J. S. Moore, D. J. Beebe, *J. Am. Chem. Soc.* **2002**, *124*, 5284-5285.

[25] H. Ren, R. B. Fair, M. G. Pollack, E. J. Shaughnessy, *Sens. Actuators B* **2002**, *87*, 201-206.

[26] P. G. Wapner, W. P. Hoffmann, *Sens. Actuators B* **2000**, *71*, 60-67.

[27] R. Dreyfus, P. Tabeling, H. Willaime, *Phys. Rev. Lett.* **2003**, *90*, 144505(1-4).

[28] T. Henkel, T. Bermig, M. Kielpinski, A. Grodrian, J. Metze, J. M. Köhler, *Chem. Eng. J.* **2004**, *101*, 439-445.

[29] S. L. Anna, N. Bontoux, H. A. Stone, *Appl. Phys. Lett.* **2003**, *82*, 364-366.

[30] H. Song, D. L. Chen, R. F. Ismagilov, *Angew. Chem. Int. Ed.* **2006**, *45*, 7336-7356.

[31] A. D. Lyon, J. D. Tice, R. F. Ismagilov, *Anal. Chim. Acta* **2004**, *507*, 73-78.

[32] M. R. Bringer, H. Song, J. D. Tice, C. J. Gerdts, R. F. Ismagilov, *Appl. Phys. Lett.* **2003**, *83*, 4664-4666.

[33] M. N. Kashid, I. Gerlach, S. Goetz, J. Franzke, J. F. Acker, F. Platte, D. W. Agar, S. Turek, *Ind. Eng. Chem. Res.* **2005**, *44*, 5003-5010.

[34] N. Harries, J. R. Burns, D. A. Barrow, C. Ramshaw, *Int. J. Heat Mass Transfer* **2003**, *46*, 3313-3322.

[35] W. S. Janna, Introduction to fluid mechanics, Brooks, **1983**.

[36] J. D. Tice, H. Song, R. F. Ismagilov, *Angew. Chem. Int. Ed.* **2003**, *42*, 767-772.

[37] C. J. Gerdts, M. R. Bringer, H. Song, J. D. Tice, R. F. Ismagilov, *Phil. Trans. R. Soc. Lond. A* **2004**, *362*, 1087-1104.

[38] A. Hibara, M. Tokeshi, K. Uchiyama, H. Hisamoto, T. Kitamori, *Anal. Sci.* **2001**, *17*, 89-93.

[39] C. de Bellefon, N. Tanchoux, S. Caravieihes, P. Grenouillet, V. Hessel, *Angew. Chem. Int. Ed.* **2000**, *39*, 3442-3445.

[40] K. Mikami, M. Yamanaka, M. N. Islam, K. Kudo, N. Seino, M.Shinoda, *Tetrahedron* **2003**, *59*, 10593-10597.

[41] K. Mikami, M. N. Islam, M. Yamanaka, Y. Itoh, M.Shinoda, K. Kudo, *Tetrahedron. Lett.* **2004**, *45*, 3681-3683.

[42] H. Hisamoto, T. Kitamori, T. Saito, M. Tokeshi, A. Hibara, *Chem. Commun.* **2001**, 2662-2663.

[43] M. Ueno, H. Hisamoto, T. Kitamori, S. Kobayashi, *Chem. Commun.* **2003**, 936-937.

[44] H. Okamoto, *Chem. Eng. Technol.* **2006**, *29*, 504-506.

[45] I. Glasgow, N. Aubry, *Lab Chip* **2003**, *3*, 114-120.

[46] J. M. MacInnes, Z. Chen, R. W. K. Allen, *Chem. Eng. Sci.* **2005**, *60*, 3453-3467.

[47] A. D. Stroock, S. K. W. Dertinger, A. Ajdari, I. Mezic, H. A. Stone, G. M. Whitesides, *Science*, **2002**, 295, 647-651.

[48] J. R. Burns, C. Ramshaw, *Trans I. Chem. Eng.* **1999**, *77*, 206-211.

[49] G. Dummann, U. Quittmann, L. Groschel, D. W. Agar, O. Worz, K. Morgenschweis, *Catal. Today* **2003**, *79-80*, 433-439.

[50] T. Hatakeyama, D. L. Chen, R. F. Ismagilov, *J. Am. Chem. Soc.* **2006**, *128*, 2518-2519.

[51] D. L. Chen, L. Li, S. Reyes, D. N. Adamson, R. F. Ismagilov, *Langmuir* **2007**, *23*, 2255-2260.

[52] D. L. Chen, R. F. Ismagilov, *Curr. Opin. Chem. Biol.* **2006**, *10*, 226-231.

OAc   NaOH (aq.)   ONa

O_2N O_2N
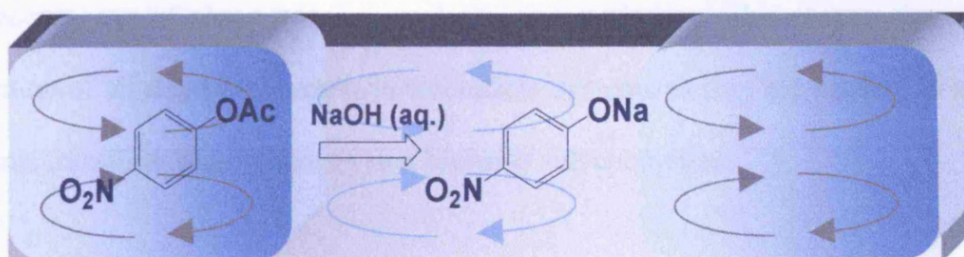
Chapter 2

Biphasic hydrolysis in microflow system

This chapter presents the study of the effect of applying multiphase microflow systems to a simple organic transformation. Our main aim was to highlight the two main benefits provided by microflow systems, compared to conventional flask, to biphasic systems, namely (i) the reduced dimensions and improved geometry leading to an increased reaction interface and (ii) the ability to produce different flow patterns, as outlined in Chapter 1. These advantages add new optimization parameters to biphasic systems other than the more common set of conventional parameters such as temperature, heating techniques, use of phase transfer catalysts, and sonication. This chapter discusses the variation of all these parameters in microflow systems as they are applied to a simple organic transformation occurring in a biphasic solvent system.

2.1. Microflow *vs.* conventional flask

We started our study by initially investigating the effect of microflow systems, compared to conventional methods, on the reactivity of the biphasic hydrolysis of *p*-nitrophenyl acetate to *p*-nitrophenolate[1] under basic conditions using aqueous sodium hydroxide (Scheme 2.1). Under these conditions, the hydrolysis of *p*-nitrophenyl acetate involves a bimolecular nucleophilic attack by the hydroxyl ion on the unsaturated carbonyl moiety leading to elimination of the acetate and formation of the *p*-nitrophenolate sodium salt.
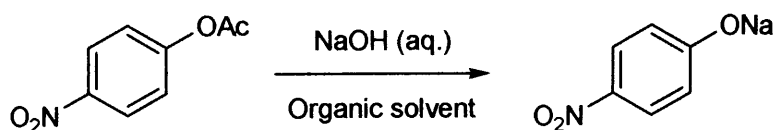
Scheme 2.1. Hydrolysis of *p*-nitrophenyl acetate under biphasic conditions using NaOH (aq.).

Once the aryl acetate is hydrolysed, the product is transferred into the aqueous phase resulting in a colour change in the aqueous layer from colourless to yellow. We could easily follow the reaction by monitoring the UV absorption of the aqueous phase (p-nitrophenolate product $\lambda_{max} = 400$ nm), either manually at intervals, or in a continuous manner using a UV flow cell. Due to mainly the nature of the biphasic system studied, and in part due to the design of the microflow apparatus, segmentation was the most favoured flow pattern formed, hence we initially used segmented flow conditions (Figure 2.2, top) to carry the microflow *vs.* conventional comparison. The microreactor setup (Figure 2.1), microfabricated in-house using polymethylmethacrylate (PMMA) and containing a T-junction inlet was used to carry out the hydrolysis reaction under segmented flow conditions (refer to Section 4.1 for details of microfabrication).

Figure 2.1. Microreactor setup include (A) *KD Scientific* syringe pump connected to (B) PMMA microreactor device fitted in a stainless steel housing and after the reaction the solution is collected in a suitable container (C) or the microreactor is connected to a continuous UV analysis.

Regular segmentation took place as a 0.05M solution of *p*-nitrophenyl acetate in toluene

and a 0.5M aqueous solution of sodium hydroxide were introduced simultaneously into

the microchannel in a 1:1 flow rate ratio for different residence times. The hydrolysis

reaction of *p*-nitrophenyl acetate was carried out simultaneously in microchannel and in

a standard flask using mechanical stirring in order to carry out a comparison between

microflow system and flask method. The colouration of the aqueous segments

intensified as segments travel down the microchannel, due to the increasing amount of

p-nitrophenolate product, exactly the same colour changes observed in the flask

reaction. We also noticed that the segmentation pattern consisted of round-shaped

aqueous segments while the organic phase spread along the channel in between aqueous

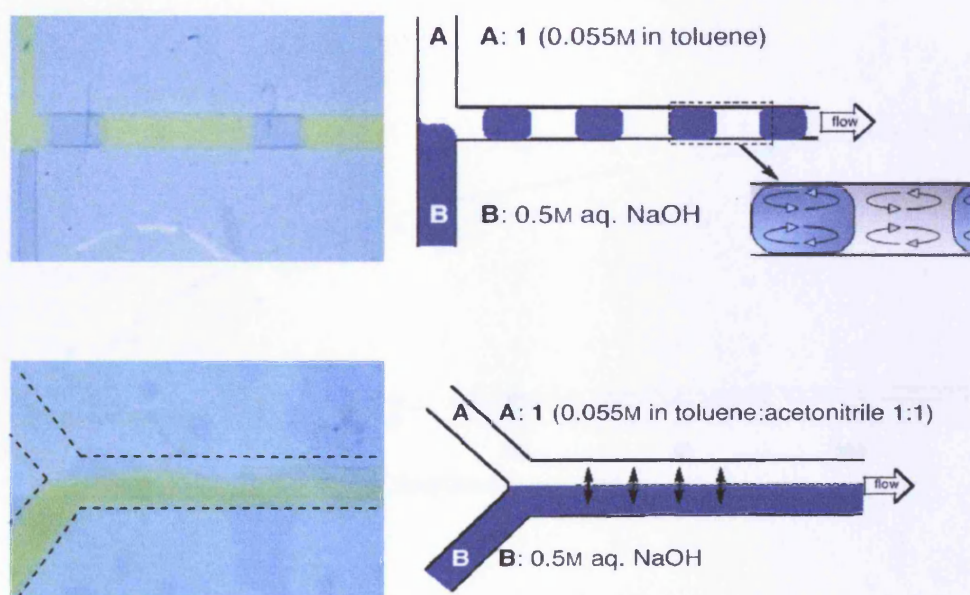segments, as a result of the hydrophobicity of the channel surface.

Figure 2.2 Organic: aqueous segmented flow in T-inlet junction *(top)*, and parallel flow with V-inlet junction *(bottom)*.

33

Furthermore, we observed by microscope that a very thin film of the organic phase formed between the aqueous segments and the channel surface, which in theory could have undesirable effects on the segments internal vortices, due to the weaker liquid-liquid shear stress compared to the solid-liquid case. Ismagilov *et al.*, however, have shown that the presence of a thin film does not affect the circulation significantly.[2] The diagram in Figure 2.3 which compares the percentages of conversion between the reaction in microflow (a) and the reaction in conventional flask (c) at room temperature clearly shows that microsystem resulted in a significant enhancement in the reaction conversion, even when higher temperature (50 °C) applied to the flask reaction (b).
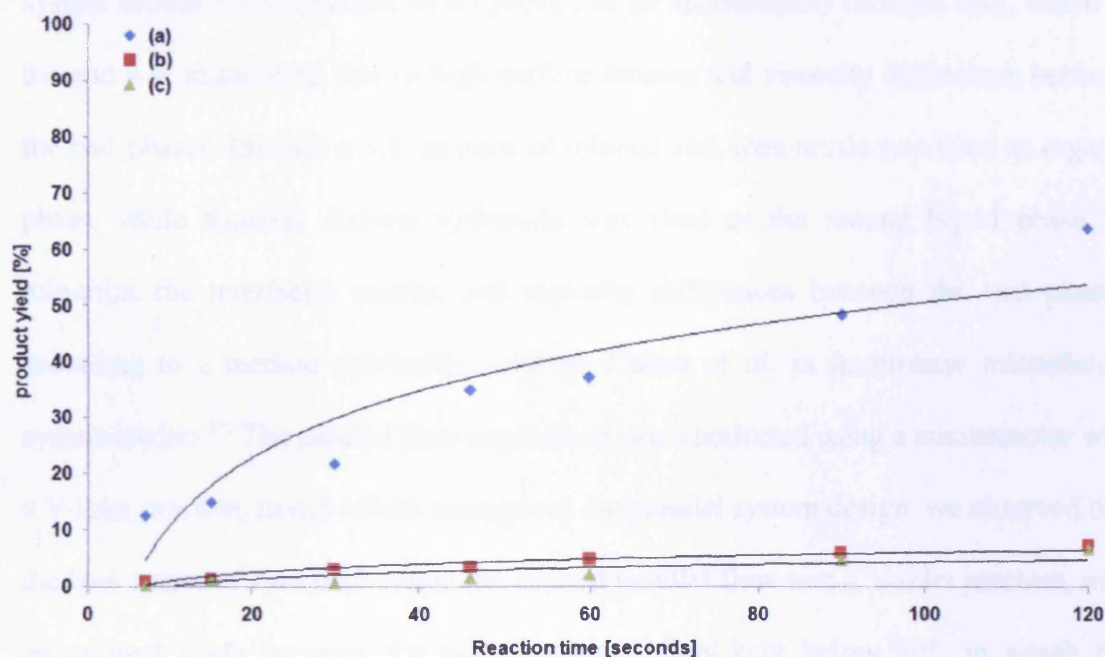
Figure 2.3. Hydrolysis of *p*-nitrophenyl acetate using NaOH (aq.): (a) Segmented flow at room temperature using PMMA microreactor (length 400 mm, cross section area 300 μm x 300 μm); (b) hydrolysis at 50 °C in flask with stirring; (c) hydrolysis at room temperature in flask with moderate stirring by use of a magnetic bar. Reaction time is the residence time that the reaction mixture spends in the flow channel (see Chapter 4, Eqs. 4.1a-c).

2.2. Parallel flow *vs.* segmented flow

Once we had shown that the use of segmentation in microflow system had a significant effect on the hydrolysis reaction conversion, we next aimed to investigate whether the observed effect was due to the internal vortices generated due to segmentation, or perhaps it was due to the general decrease in dimensions, independently from the flow pattern created. For this purpose we carried out a comparison study between segmented and parallel flow, in order to measure the effect respectively of the presence and of the absence of segment internal circulation on the hydrolysis. In parallel flow, *i.e.* in absence of internal circulation, the reaction can only occur through diffusion along the interface boundary. Creating parallel flow using toluene and water (the same solvent system chosen for segmented flow) proved to be an extremely difficult task, which in the end was abandoned, due to high surface tension and viscosity differences between the two phases. Instead, a 1:1 mixture of toluene and acetonitrile was used as organic phase, while aqueous sodium hydroxide was used as the second liquid phase, to minimize the interfacial tension and viscosity differences between the two phases, according to a method previously used by Kuban *et al.* in multiphase microfluidic system studies.[3] The parallel flow experiment was conducted using a microreactor with a V-inlet junction; in our efforts to improve the parallel system design, we observed that the best choice of system to create the desired parallel flow was a V-inlet junction, with an optimal angle between the two incoming inlets kept below 90°, in which the microchannel width doubles in size past the joining point of the two phases, as illustrated in Figure 2.2 (bottom).Comparison of the results shown in Figure 2.4 clearly demonstrate the difference between parallel and segmented flow pattern compared to reactions carried out in conventional flask. When carrying out the reaction in conventional flask, using toluene:acetonitrile (c) instead of toluene only (d), an increase

in the product conversion was observed. This is probably due to the decrease in the interfacial tension between the organic and aqueous phases leading to an improved miscibility between the phases.
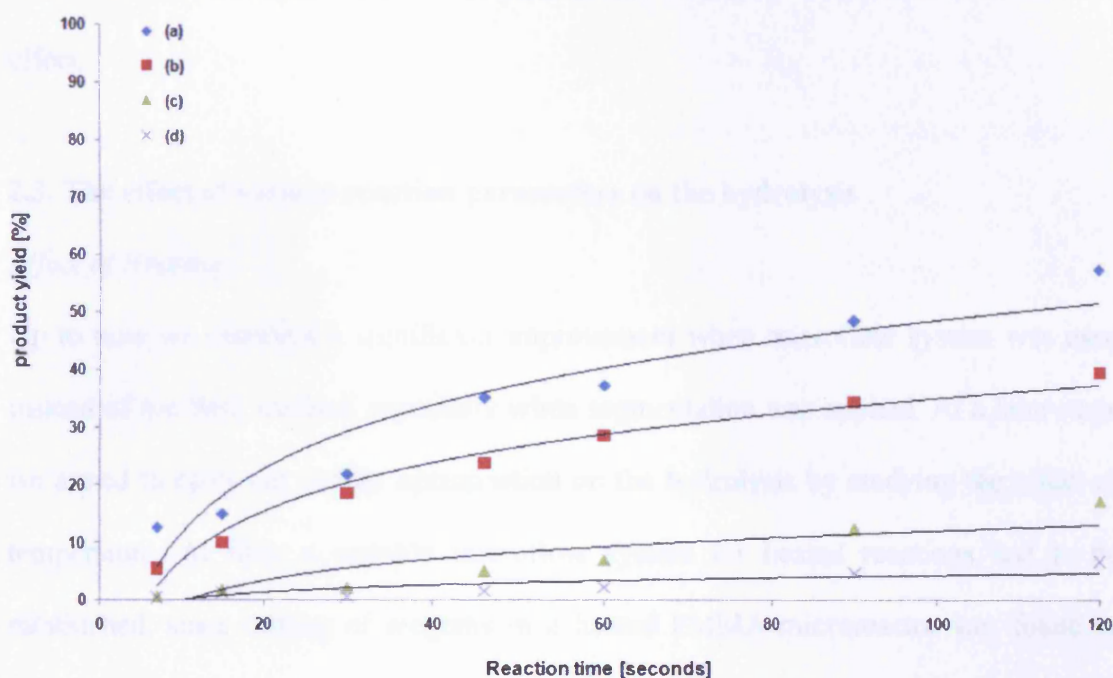
Figure 2.4. Hydrolysis of *p*-nitrophenyl acetate: using a PMMA microreactor (length 400 mm, cross section area 300 μm x 300 μm) at room temperature (a) under segmented flow using a T-inlet geometry (organic phase is toluene) and (b) parallel flow using a V-inlet geometry (organic phase is acetonitrile:toluene 1:1): (c) in a flask with moderate stirring by use of a magnetic bar (organic phase is acetonitrile:toluene 1:1); (d) in a flask with moderate stirring by use of a magnetic bar (organic phase is toluene). Reaction time is the residence time that the reaction mixture spends in the flow channel (see Chapter 4, Eqs. 4.1a-c).

However, when performing the reaction in a microreactor, the opposite trend was observed; the use of plain toluene as the organic phase (a), in fact, led to higher

conversions compared to toluene:acetonitrile (b). The better performance obtained in the microchannel by using water/toluene compared to water/toluene/acetonitrile, opposite to what observed in the flask reaction, is most probably due to the difference of flow regime (segmented *vs.* parallel) rather than to the choice of organic phase, showing that the benefits of segmentation over parallel flow overcome the benefits of the solvent effect.

2.3. The effect of various reaction parameters on the hydrolysis

Effect of Heating:

Up to now we observed a significant improvement when microflow system was used instead of the flask method, especially when segmentation was applied. At a later stage we aimed to carry out further optimization on the hydrolysis by studying the effect of temperature. At first, a suitable microflow system for heated reactions had to be established, since mixing of reagents in a heated PMMA microreactor was found to cause degradation of the PMMA material at temperatures above ambient. Hence, we considered to use alternative polymeric materials, mainly fluoropolymers such as polytetrafluoroethylene (PTFE) and perfluoroalkoxyethylene (PFA) which are more temperature and chemically resistant. However, the attempts to make a sealed reactor from other materials beside PMMA were not successful, due to the complex nature of the microfabrication process. This consists, in fact, of two main stages, namely the *milling,* to create an open microchannel in uniform depth, followed by the *bonding,* to create an enclosed microchannel (as described in Section 4.1). Both processes had proved really easy when PMMA was used, whereas when microfabrication was carried out on PTFE and PFA, both materials created difficulties although reacting differently. Specifically, when PTFE was used, the milling process was successful but the bonding

proved impossible by means of several techniques; then, when PFA was used, it was the milling process that proved hard, whereas the bonding did not create significant problems. Consequently, we decided to adopt a more practical solution by using commercially available microflow tubing made from various materials such as PFA, Polyetheretherketone (PEEK), stainless steel or more favourably PTFE with circular duct. PTFE, in fact, being amongst the best known and most widely used chemically inert and temperature resistant material, is commercially available in various channel duct sizes at low prices. In addition, the flexibility of the PTFE allowed us to easily arrange the tubing as required. It proved easy, in fact, to coil the PTFE microtubing around a test tube which could then be immersed in a heating or cooling bath, or inserted into a focused microwave cavity. The coiled PTFE setup is used with a combination of T-inlet or cross-inlet connector fitting (Experimental, Section 4.1). These connectors act like the T-inlet junction in the PMMA microreactor setup. PTFE microtube was initially tested for its effectiveness in conducting heat by measuring the tempreture using a digital thermoprobe of a water flow in a coiled setup (heated length 400 mm, with internal diameter of 300 μm) immersed in an oil bath. After setting the oil bath temperature to 80 °C then heating the tube for few a hours, the first temperature reading was carried out at the output of the tubing which was at a distance of *ca.* 6 cm from the heated part. As a result, the reading (60 °C) was much lower than the set temperature (80 °C), perhaps indicating very rapid cooling within the 6 cm distance. The second reading was carried out by connecting the probe into the heated portion of the coiled channel by inserting the probe into the channel using a T-connector. The temperature reading (76 °C) was just below the set temperature. By carrying out the hydrolysis reaction of *p*-nitrophenylacetate under segmented flow conditions using a coiled PTFE setup, slightly lower conversions compared to PMMA microreactor were

observed at room temperature as shown in Figure 2.5 ((d) *vs.* (e)). The better performance in the PMMA microreactor is probably due to the more uniformed segmented flow observed visually during the PMMA reaction, as a result of a better T-inlet setup in the PMMA microreactor compared to the T-connector in the PTFE setup (Experimental section 4.1).
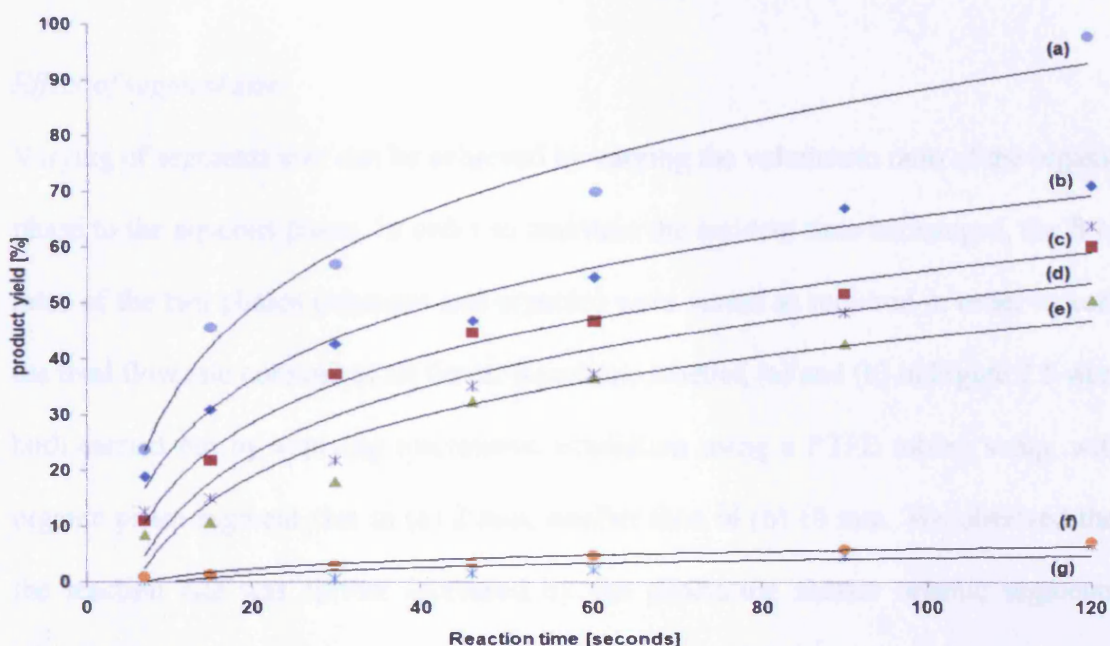

Figure 2.5. Hydrolysis of *p*-nitrophenyl acetate using different reaction conditions: (a) short organic segments (approx. 2 mm) generated in PTFE tubing while microwave irradiating at 50 °C; (b) long organic segments (approx. 10 mm) generated in PTFE tubing while microwave irradiating at 50 °C; (c) segmented flow in PTFE tubing heated in an oil bath at 50 °C (average segment size ~10 mm); (d) segmented flow at room temperature in PMMA microreactor (average segment size ~8 mm); (e) Segmented flow at room temperature in PTFE tubing (average segment size ~10 mm); (f) hydrolysis at 50 °C in flask with moderate stirring by use of a magnetic bar; (g) hydrolysis reaction at room temperature in flask with moderate stirring by use of a magnetic bar. Channel dimensions for experiment (a), (b), (c), and (e): channel length 400 mm, internal diameter 300 µm; channel dimensions for experiment (d): channel length 400 mm, channel cross section 300 µm x 300 µm. Reaction time is the residence time that the reaction mixture spends in the flow channel (see Chapter 4, Eqs. 4.1a-c).

Furthermore, when temperature was applied (50 °C) to the hydrolysis reaction carried out under segmented flow conditions using the PTFE microtube setup, a reaction improvement was achieved compared to the reaction at ambient temperature (Figure 2.5 ((e) *vs.* (c)). In addition, when we compared heating methods, we found that microwave irradiation using the PTFE microtube had a very positive effect on the hydrolysis reaction compared to oil bath heating (Figure 2.5, (b) *vs.* (c)).

Effect of segment size:

Varying of segments size can be achieved by varying the volumetric ratio of the organic phase to the aqueous phase. In order to maintain the resident time unchanged, the flow rates of the two phases (aqueous and organic) were varied as required in order to keep the total flow rate constant at all times. Reactions labelled (a) and (b) in Figure 2.5 were both carried out by applying microwave irradiation using a PTFE tubing setup, with organic phase segment size in (a) 2 mm, smaller than in (b) 10 mm. We observed that the reaction rate was further increased by the generating shorter organic segments. Circulation, in fact, is expected to improve in segments of smaller size due to the shorter mixing times obtained with shorter distances.[2]

Effect of channel size and shape:

Since the reduced dimensions in microchannel compared to flask have an effect on the diffusion rate, we studied the effect of reducing progressively the cross section area of the microchannel. When we conducted the hydrolysis under segmented flow conditions using different sizes of microchannel, higher conversions were obtained when progressively smaller microchannel cross section areas were employed as shown in Figure 2.6 ((a) to (d)). Such results were obtained with very regular trends and in

agreement with theory, since smaller channel dimensions mean higher interface-to-volume ratios. [4] We decided next to conduct a comparison study by using two distinct microchannel shapes, rectangular and square, while maintaining the same cross section area.
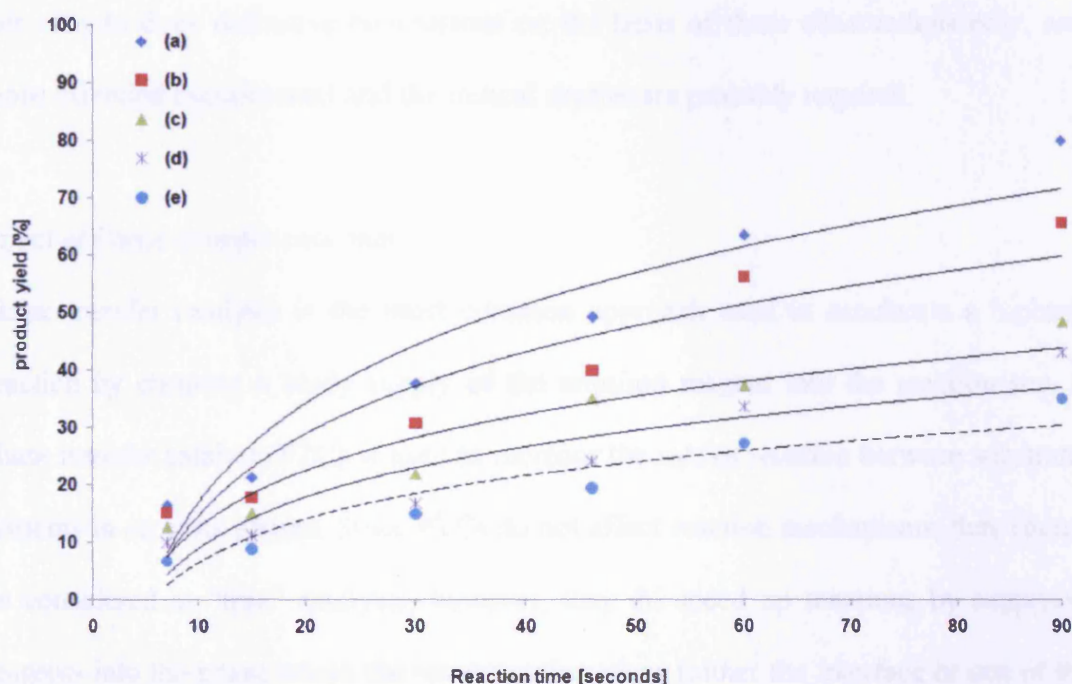

Figure 2.6. Effect of microchannel cross section area on hydrolysis of *p*-nitrophenyl acetate at room temperature under segmented flow conditions by pumping *p*-nitrophenyl acetate and NaOH (aq.) in a 1:1 flow rate ratio using a PMMA microreactor with fixed length 400 mm: (a) in a square-shaped channel with cross section area of 15,625 μm^2 (b) in a square-shaped channel with cross section area of 62,500 μm^2 (c) in a square-shaped channel with cross section area of 90,000 μm^2 (d) in a square-shaped channel with cross section area of 144,400 μm^2 (e) in a rectangular -shaped channel with cross section area of 144,500 μm^2. Reaction time is the residence time that the reaction mixture spends in the flow channel (see Chapter 4, Eqs. 4.1a-c).

41

In Figure 2.6, reactions (a) to (d) were conducted in a square-shaped channel of increasing cross section areas, whereas reaction (e) was carried in a rectangular channel. Reactions (d) and (e) were carried in microchannels having the same cross section area but different geometry, square and rectangular, in which the segments generated were all approximately equal in size. As demonstrated from the results in Figure 2.6, there is a slight preference for square-shaped channel over rectangular. However, it is hard in this case to draw definitive conclusions on the basis of these observations only, and more extended experimental and theoretical studies are probably required.

Effect of Phase transfer catalysis:

Phase transfer catalysis is the most common approach used to accelerate a biphasic reaction by ensuring a ready supply of the required reagent into the reaction site. A phase transfer catalyst (PTC) is used to increase the rate of reaction between substrates presents in separate phases. Since PTCs do not affect reaction mechanisms, they cannot be considered as "true" catalysts; however, they do speed up reactions by supplying reagents into the phase where the reaction takes place (either the interface or one of the phases). PTCs are classified into two main types, *i.e.* ionic compounds such as bulky ammonium or phosphonium salts (for anionic substrates) and polydentate complexes such as crown ethers, glycols and criptands (for cationic substrates). [7] In our studies in the microreactor system of the hydrolysis reaction in Scheme 2.1, we used a tetraalkylammonium salt as PTC because of the anionic nature of the hydroxyl substrate. When 10 mol% tetrabutylammonium hydrogen sulfate was used as phase transfer catalyst (PTC) at room temperature under segmented flow conditions (Figure 2.7) (d), an increase in the conversion rate was observed compared to when no PTC was used (e).

Effect of Sonication:

The other enhancement method used involved the use of ultrasound, in which the transmission of a sound wave through the reaction medium provides a form of chemical excitation, through the phenomenon of *cavitation*, where cavities formed in the liquid are compressed resulting in localized high temperatures and pressures.[8] For the application of the sonication technique, the microchannel tubing was immersed in the ultrasound bath during the reaction time, carried under segmented flow conditions.
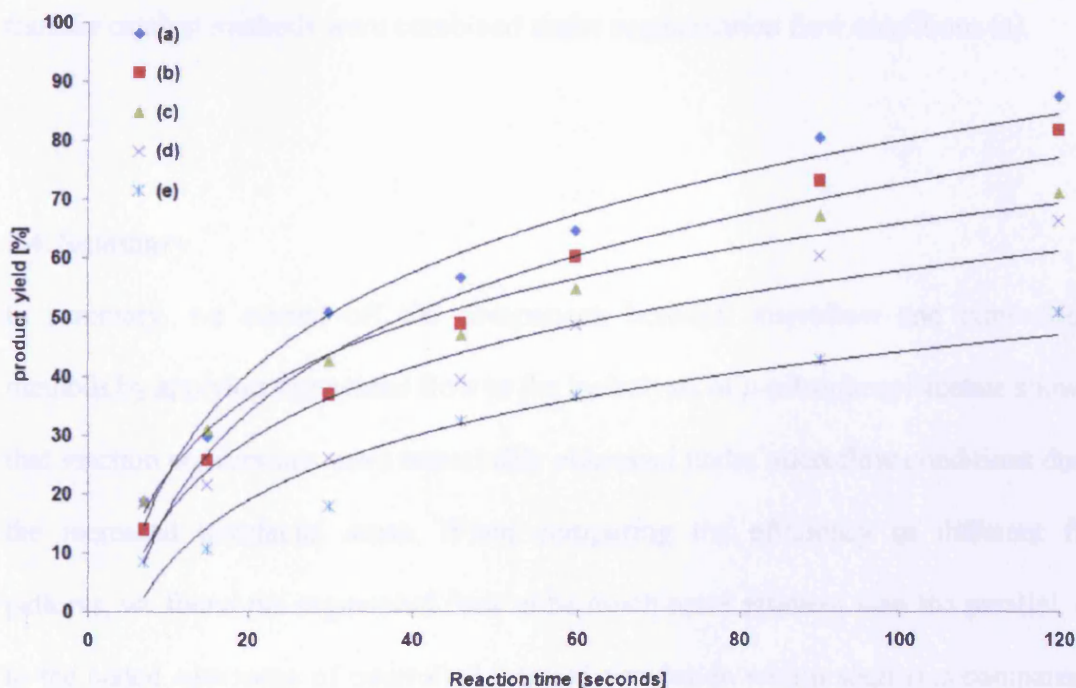

Figure 2.7. Hydrolysis of *p*-nitrophenyl acetate in PTFE microtube (length 400 mm, internal diameter 300 μm) under segmented flow conditions by pumping *p*-nitrophenyl acetate and NaOH (aq.) in a 1:1 flow rate ratio using: (a) 10 mol% of PTC and sonication; (b) sonication; (c) microwave irradiation at 50 °C; (d) 10 mol% of PTC at room temperature; or (e) room temperature. Reaction time is the residence time that the reaction mixture spends in the flow channel (see Chapter 4, Eqs. 4.1a-c).

As a reasonable amount of heat is generated during sonication, the temperature of the sonication bath was maintained constant at 25°C. We observed that a higher conversion rate was obtained in microchannel under sonication (Figure 2.7) (b) compared to the normal room temperature reaction (e), to the use of microwave irradiation (c), and to the addition of PTC (d). During sonication, irregular sized segments (approx. 1-10 mm length) formed with some organic emulsions inside the aqueous segments. The increased surface-to-volume ratio by the combined effect of the sonication and the segmentation regime is probably the cause of the increase in conversion rate. In a further experiment, the best enhancement was obtained when sonication and phase transfer catalyst methods were combined under segmentation flow conditions (a).

2.4. Summary

In summary, we started off the comparison between microflow and conventional methods by applying segmented flow to the hydrolysis of p-nitrophenyl acetate showing that reaction conversions were remarkably enhanced under microflow conditions due to the increased interfacial areas. When comparing the efficiency of different flow patterns, we found the segmented flow to be much more efficient than the parallel, due to the added advantage of controlled internal circulation within segments compared to the simple laminar diffusion-controlled parallel flow. Further optimization studies were then carried by looking not only at characteristic microflow parameters such as channel dimension/geometry and segment length, but also looking at 'traditional' parameters, namely temperature, heating methods, use of phase transfer catalysts and sonication. The use of high temperature highlighted some limitations of PMMA material and led to the successful utilization of PTFE microtube as a very valid alternative to

microfabricated devices. Microwave irradiation brought added improvement to reaction conversions compared to traditional heating methods. The combination of sonication and segmented flow was found to enhance the rate more than segmented flow and phase transfer catalyst combined. Finally, the maximum enhancement was obtained when segmented flow was used in combination with both traditional methods of sonication and phase transfer catalysis. Overall the monitoring of the hydrolysis reaction by varying such a number of parameters led to the observation of general improvements on the whole reproducibly and in agreement with expectations, and also displaying very regular trends.

2.5. References

[1] H. J. Goren, *Eur. J. Biochem.* **1974**, *41*, 263–272.

[2] J. D. Tice, H. Song, A. D. Lyon, R. F. Ismagilov, *Langmuir* **2003**, *19*, 9127–9133.

[3] P. Kuban, J. Berg, P. K. Dasgupta, *Anal. Chem.* **2003**, *75*, 3549–3566.

[4] W. Ehrfeld, V. Hessel, H. Löwe, Microreactors, New Technology for Modern Chemistry. Wiley, 2000; M. Matlosz, W. Ehrfeld, J. P. Baselt, *Microreaction Technology – IMRET 5: Proceedings of the Fifth International Conference on Microreaction Technology*, Springer, Berlin, **2001**.

[5] M. A. Kabir, M. M. K. Khan, M. A. Bhuiyan, *Fluid Dyn. Res.* **2004**, *35*, 391–408; M. T. Kreutzer, F. Kapteijn, J. A. Moulijn, J. J. Heiszwolf, *Chem. Eng. Sci.* **2005**, *60*, 5895–5916.

[6] T. J. Chung, Computational Fluid Dynamics, Cambridge University Press, 2002.

[7] B. Cornils, W. A. Hermann, Aqueous-phase Organometallic Catalysis: Concept and Applications, Wiley, 2004; J. A. B. Satrio, L. K. Doraiswamy, *Chem. Eng. Sci.*, **2002**, 57, 1355–1377; A. W. Herriott, D. Picker, *J. Am. Chem. Soc.*, **1975**, *97*, 2345–2349; M. Mieczyslaw, *Pure Appl. Chem.*, **2000**, *72*, 1399-1403; M. Ueno, H. Hisamoto, T. Kitamori, S. Kobayashi, *Chem. Commun.*, **2003**, 936–937.

[8] T. J. Mason, J. P. Lorimer, Sonochemistry: theory, applications and uses of ultrasound in chemistry. J. Wiley and son, 1988; J. L. Luche, *Ultrason. Sonochem.*, **1996**, *3*, S215–S221; A. Tuulmets, *Ultrason. Sonochem.* **1997**, *4*, 189–193; M. H. Entezari, A. Keshavarzi, *Ultrason. Sonochem.* **2001**, *8*, 213–216.
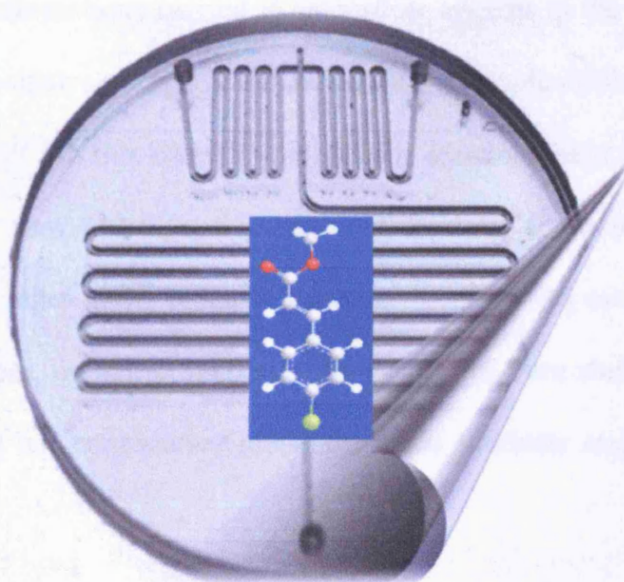
Chapter 3

Organic synthesis in microflow systems

Several metal-catalysed organic reactions have been studied in this project exploiting the advantages provided by microflow system. The present chapter reports two of the most successful studies we carried out using microflow technique, namely the palladium-catalysed Heck coupling, and the ruthenium-catalysed ring-closing metathesis. Both reactions were chosen amongst the rare examples in literature of metal-catalyzed transformations carried in microflow systems at the time. Since then, the number of metal-catalysed organic reactions subject to microflow studies has been increasing remarkably.[1] In this chapter, monophasic reactions were studied both under single phase laminar flow and biphasic segmented flow (by addition of an immiscible inert phase). On the other hand, biphasic reactions were carried out under segmented flow only. Furthermore, multistep synthesis flow reactions were studied to explore the potential of carrying out consecutive metal catalysed synthetic steps efficiently in a continuous manner.

3.1. Heck reaction

Heck coupling is one of the best-known methods used in organic synthesis for formation of substituted alkenes by the coupling of two sp^2 carbon centres (Scheme 3.1). Since reported by Heck in the late 1960s[2], the reaction has occupied a special place among metal-catalyzed transformations along Suzuki, Still and metathesis reactions due to its versatility and applicability to a wide range of substrates. As a result, Heck coupling has become a popular transformation used in the synthesis of many structurally diverse compounds, such as *Taxol*[3], *morphine*[4], *Alphacalcidiol*[5], *Vernolepin*[6], and other various macrocyclic compounds[7] (depicted below). The Heck
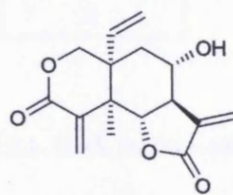
coupling normally takes place between an organohalide (aryl or vinyl) and an alkene (Scheme 3.1) typically in the presence of a zerovalent palladium catalyst.
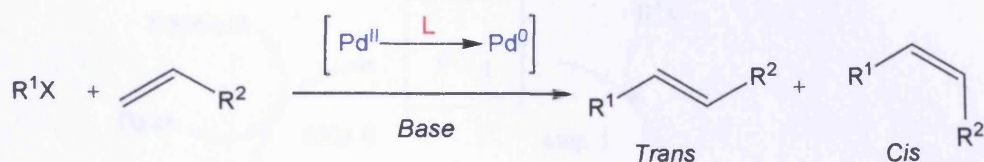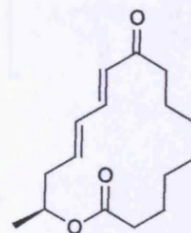

Scheme 3.1. Functionlisation of alkenes *via* Heck coupling of aryl/vinyl halide and alkene: (X = halide, triflate, or diazonium salt; L = ligand).
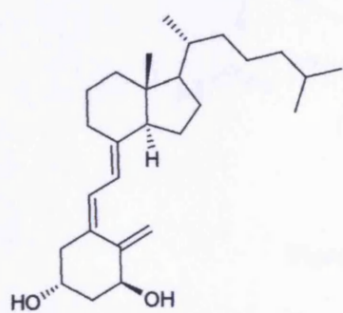
| *Alphacalcidiol* | *(+)-Vernolepin* | *Macrocyclisation product* |

The formation of the Pd^0 active species is accomplished typically *in situ* by the reduction of more stable Pd^{II} salts, using a neutral ligand **L** such as triphenylphosphine PPh_3.[2] Throughout the years, the choice of Heck substrates have widened from aryl halides to other equally or more reactive substrates such as aryl triflates or aryl diazonium salts, while new catalytic systems have also been developed to adapt Heck coupling to the use of poor reactive substrates such as aryl chlorides. The first step of the Heck coupling mechanistic cycle (Figure 3.1) involves an oxidative addition of the halide R^1X to the catalytically active species Pd^0L_2 resulting in formation of R^1PdXL_2

complex. Alkene insertion into the R^1PdXL_2 complex follows as second step, leading to the elimination of one ligand molecule **L** to form $(PdXL)R^2C-C\underline{H}R^1$.
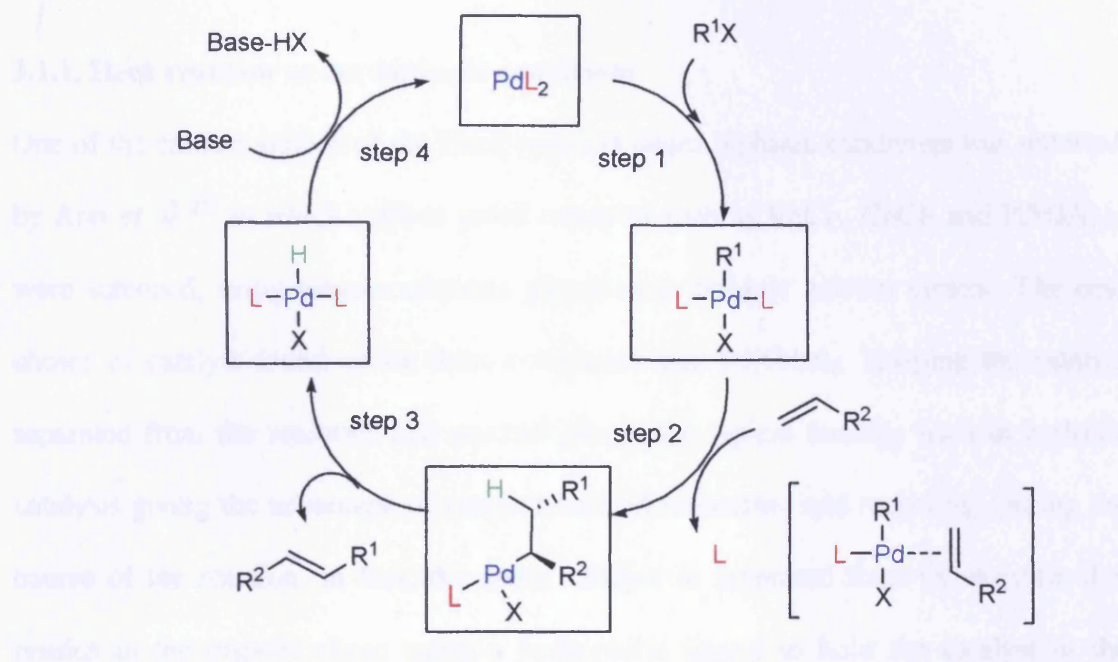

Figure 3.1. Heck reaction catalytic cycle.

The alkene insertion is subject to both electronic and steric effects of the substituents on the C=C bond, therefore the R^1 group usually occupies the less substituted carbon on the alkene, provided that R^2 has the favourable electronic effect. In the third step, β-hydride elimination on the $(PdXL)R^2C-C\underline{H}R^1$ complex takes place to form Pd hydride $\underline{H}PdXL_2$ and the desired coupled product $R^2HC=CHR^1$. The β-hydride elimination occurs in a *syn* fashion, therefore the **Pd-L** and C-$\underline{H}$ moieties must be co-planar for the elimination to take place. For steric reasons, R^1 and R^2 will tend to eclipse the smallest group on the adjacent carbon as β-hydride elimination take place, leading predominantly to the *trans* isomer. For the catalytic cycle to restart, the Pd^0 catalyst is

49

regenerated *via* reductive elimination of **HPdXL₂** to form **PdL₂** by using a base to eliminate **HX**. [7]

3.1.1. Heck reaction under biphasic conditions

One of the earliest studies of the Heck reaction under biphasic conditions was reported by Arai *et al.* [8] in which various metal catalysts such as $RhCl_3$, $CoCl_2$ and $Pd(OAc)_2$ were screened, using toluene:ethylene glycol as a biphasic solvent system. The best choice of catalyst found under these conditions was $Pd(OAc)_2$. Keeping the catalyst separated from the reactants and product phase is a typical strategy used in biphasic catalysis giving the advantage of product/catalyst separation and recycling. During the course of the reaction, in fact, the metal catalyst is separated from the reactant that resides in the organic phase using a hydrophilic ligand to hold the catalyst in the ethylene glycol phase. Hence, the ethylene glycol layer containing the catalyst can be recycled at the end of the reaction. Triphenyl phosphine trisulfonate sodium salt (TPPTS) is a hydrophilic ligand analogue to triphenyl phosphine (PPh_3) used widely in biphasic Heck systems to form a hydrophilic complex with Pd.[7] The TPPTS ligand is obtained from PPh_3 by introducing sulfonate salts as a polar functionality (Scheme 3.2).[9]
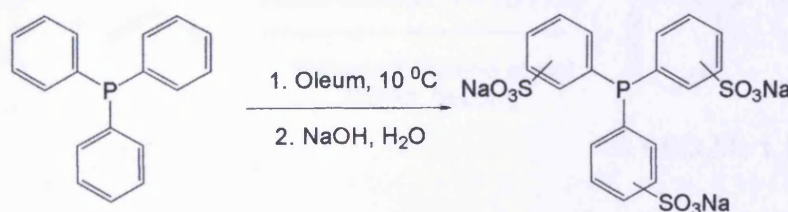
Scheme 3.2. Sulfonation of triphenylphosphine (PPh_3) ligand to triphenyl-phosphine trisulfonate sodium salt (TPPTS).
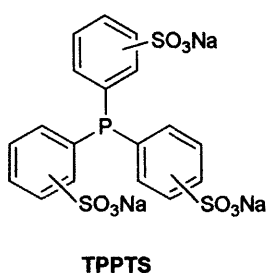
Figure 3.2. Triphenylphosphine trisulfonated ligand (TPPTS).

Our initial aim was to conduct a number of Heck reactions under biphasic conditions using a microflow system. The idea was to carry out comparison studies between the flask and microflow system methods for further optimisation, by exploiting the increased interfacial area and heat transfer provided by segmented flow. Using identical flask conditions to the study by Arai *et al.*, we carried out an arylation of methyl acrylate and styrene using a number of metal catalysts, first under flask conditions, and then repeated in the microreactor (Scheme 3.3). Table 3.1 reports the performance of the conventional screening of the metal catalysts used in the coupling of iodobenzene with styrene and methyl acrylate using the TPPTS ligand.

Metal catalyst:TPPTS (1:2)

Toluene:Ethylene glycol
KOAc, heating

R = CO₂Me **1**, Ph **2**
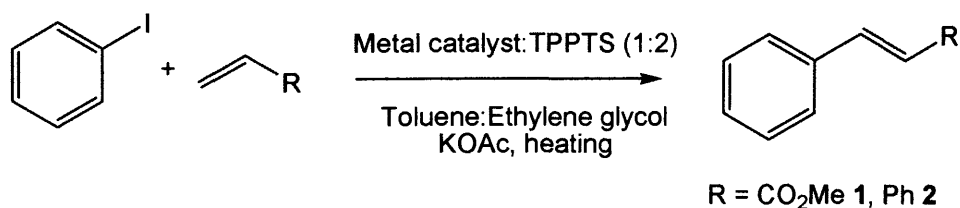
Scheme 3.3. Heck coupling of iodobenzene with methyl acrylate to form methyl cinnamate (**1**) or styrene to form stilbene (**2**) under biphasic conditions.

Table 3.1. Variation of metal catalyst in conventional flask at low and high temperature, in the Heck coupling of iodobenzene with methyl acrylate to form methyl cinnamate (**1**) or styrene to form stilbene (**2**) under biphasic conditions.

Metal Catalyst	*Yield* [%] *70 °C* [a]	*Yield* [%] *140 °C* [b]
PdCl$_2$	99 (1), 91 (2)	92 (1), 98 (2)
Pd(OAc)$_2$	98 (1), 99 (2)	94 (1), 89 (2)
Ni(OAc)$_2$	78 (1), 82 (2)	84 (1), 70 (2)
RuCl$_3$	62 (1), 51 (2)	66 (1), 71 (2)

Reaction conditions: Metal catalyst (1 mol%), TPPTS (2 mol%), iodobenzene (0.2 mmol), alkene (0.2 mmol), KOAc (0.2 mmol), in toluene: ethylene glycol (1:1). [a] Heating at 70°C, reaction time (9–11 hours). [b] Heating at 140 °C, reaction time (4.5–7 hours).

Both Pd(OAc)$_2$ and PdCl$_2$ catalysts were found to have a better performance than Ni(OAc)$_2$ and RuCl$_3$ catalysts. The optimised flask conditions in the presence of potassium acetate as an inorganic base resulted in total selectivity towards *trans*-methylcinnamate **1** and *trans*-stilbene **2** with good isolated yields within reaction times between 4.5 to 7 hours at 140 °C. Next we decided to screen the catalysts under the same reaction conditions but at a lower temperature of 70 °C, obtaining similar high yields as with that of higher temperature, however with longer reaction times. At higher temperatures (140 °C) the reaction is faster not only because of chemical reactivity but also as a result of weaker interfacial tension between the toluene and ethylene glycol layers, resulting in enhanced mixing. However, although an increase in temperature is

expected to enhance the catalysts activity, there is always the risk of catalyst decomposition. Therefore we next tested the effect of increasing the stirring speed from moderate to high in the flask reaction at 70 °C as an alternative method to weaken interfacial tension between the two phases. However, we observed no significant effect in reducing the reaction time. By exploiting the same idea in microflow systems, we were hoping to increase the interface-to-volume ratio between the two phases *via* segmentation. Applying the same conditions as that in the flask, the arylation of styrene and methyl acrylate using iodobenzene was carried out at 70 °C under segmented flow using a PTFE microflow setup coiled around a glass tube (Figure 3.3). The reaction was initiated by introducing three standard solutions into the microchannel: (i) a 1:1 mixture of iodobenzene and alkene (either styrene or methyl acrylate) in toluene; (ii) a metal catalyst-TPPTS complex solution in ethylene glycol; and (iii) a potassium acetate solution in ethylene glycol. The three solutions were delivered through the inlet individually using a standard T-inlet connection (Experimental, Section 4.1).
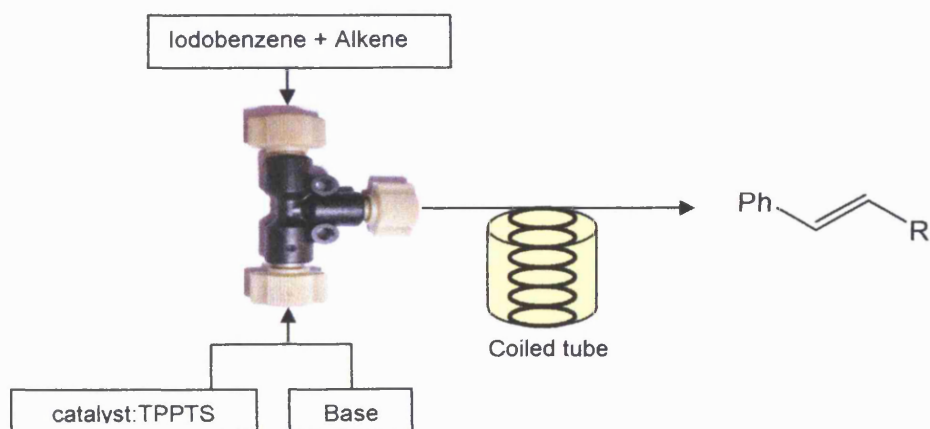

Figure 3.3. Microflow setup for biphasic conditions using coiled PTFE tubing immersed in a heating bath.

For the purpose of comparison, it was neither necessary nor practical to carry both flask and microflow reactions all the way to completion, but instead both reaction times were fixed. The advantage of using segmented microflow technique compared to flask method is evident by looking at the results at 70 °C in Table 3.2. However, as the microflow reaction was heated to 140 °C, the regularly shaped segments began to distort resulting in irregular flow velocity. In theory the problem could have been solved by extending the length of the microtube in order to compensate the lost residence time, however, in practice it is not possible to determine the exact residence time since the flow velocity is not under control.

Table 3.2. Heck coupling of iodobenzene with methyl acrylate to form methyl cinnamate (**1**) or styrene to form stilbene (**2**) under biphasic conditions: microflow vs. flask; and comparison low vs. high temperature in microflow.

Metal Catalyst	Flask 70 °C [a] Yield [%]	PTFE Microflow 70 °C [a] Yield [%]	PTFE Microflow 140 °C [b] Yield [%]
PdCl$_2$	12 (1), 8 (2)	48 (1), 33 (2)	67 (1), 56 (2)
Pd(OAc)$_2$	10 (1), 11(2)	37 (1), 42 (2)	71 (1), 58 (2)

Reaction conditions: Metal catalyst (1 mol%), TPPTS (2 mol%), iodobenzene (1.0 mmol), alkene (1.0 mmol), KOAc (1.0 mmol), residence time of 55 minutes. [a] heating at 70 °C in toluene: ethylene glycol (1:1). [b] heating at 140 °C in o-xylene: ethylene glycol (1:1).

In principle the use of back-pressure regulators could have helped preventing the irregular segmentation inside the microchannel, since at higher pressures the solvent boiling point increases. However, the use of back-pressure regulators in combination with syringe pumps is not suitable; syringe pumps, in fact, cannot hold high back-pressures, and in those conditions only HPLC pumps could be used. Instead, the microflow reaction was repeated by replacing toluene with a higher boiling solvent, o-xylene. Initially a conventional flask trial was carried out in order to make sure that exchanging solvents had no influence on the outcome of the reaction, and it was observed that using o-xylene instead of toluene had no effect on reaction rate and yield. As a result, the microflow reaction using o-xylene at 140 °C was carried out smoothly with little irregularity in the flow velocity. Data in Table 3.2 demonstrate that microflow reactions carried out at higher temperature (140 °C) require shorter residence times to drive the reaction almost to completion, compared to microflow and flask reaction at lower temperatures (70 °C).

Meanwhile, we also investigated the use of microwave irradiation as alternative to conventional heating using oil bath. Table 3.3 shows that the use of microflow reaction with microwave heating proved to be a desirable combination to further optimise the Heck coupling to obtain (E)-methylcinnamate 1 or (E)-Stilbene 2. In a typical microwave experiment, a PTFE microflow setup coiled around a glass tube was inserted into the Discovery CEM microwave cavity. An increase in isolated yields for the microflow Heck reaction was achieved when microwave irradiation was applied at 70 °C compared to conventional heating (Table 3.3). Comer and Organ[10] reported a series of microwave-assisted organic syntheses, most of which metal-catalysed, using a glass microflow system. The authors observed that during microwave irradiation of Suzuki-Miyaura coupling, the palladium catalyst blacked out along the glass microchannel,

resulting in a Pd-coated channel surface. This phenomenon was exploited favourably by the same authors, resulting in improvements of several other metal-catalysed syntheses including ring closing metathesis. The same phenomenon was observed in our study when we carried out the Heck coupling of iodobenzene with alkenes using a *Discovery CEM* microwave conventional glass flask. However, when the experiment was performed using a coiled PTFE microtube, precipitation of palladium particulate instead of surface blacking occurred, especially at higher temperatures combined with higher palladium loading.

Table 3.3. Heck coupling of iodobenzene with methyl acrylate to form methyl cinnamate (1) or styrene to form stilbene (2) under biphasic conditions; microwave heating *vs.* oil bath heating of microflow system.

Metal Catalyst	Catalyst load [mol%]	Oil Bath Yield [%]	Microwave Yield [%]
PdCl$_2$	1	48 (1), 33 (2)	54 (1), 50 (2)
PdCl$_2$	10	51 (1), 55 (2)	67 (1), 59 (2)
Pd(OAc)$_2$	1	37 (1), 42 (2)	51 (1), 49 (2)
Pd(OAc)$_2$	10	49 (1), 56 (2)	69 (1), 70 (2)

Reaction conditions: Metal catalyst (1 or 10 mol%), TPPTS (2 or 20 mol%), iodobenzene (1.0 mmol), alkene (1.0 mmol), KOAc (1.0 mmol), in toluene: ethylene glycol (1:1), heating at 70°C using either microwave irradiation at 150 Watt or oil bath heating, residence time of 55 minutes.

It is important to point out that the microwave assisted experiments shown in Table 3.3 were slightly problematic, as explained below, causing some small degree of irreproducibility. Therefore every experiment was repeated several times in order to confirm each yield result confidently. We observed, in fact, that the change of colour in the reaction mixture would sometimes be distributed inhomogeneously along the microtube, suggesting that the microwave irradiation was not absorbed uniformly by the reaction flow. We therefore tested the efficiency of the PTFE microflow setup by irradiating a continuous flow of water at 100 °C over a range of flow rates (10–300 µl/min). As a result we observed that the water was boiling at irregular intervals, suggesting that the microwave irradiation was absorbed in a discontinuous fashion. Since the irradiation generated in the *Discovery CEM* apparatus is unpulsed, we can only conclude that some miscommunication between temperature IR sensor and the control unit is responsible for the observed phenomenon. Most likely this could be due to the position of the IR sensor with respect to the channel, *i.e.* placed at the bottom of the apparatus and not directed at the microchannel as a result the microwave apparatus cannot read the actual temperature of the flow inside the channel.[11] At a later stage we considered a possible solution to the problem by filling the CEM glass tube cavity with water, while keeping the PTFE microtube coiled around, in order to retain the microwave heating and stabilize the IR sensor reading. Although such idea appeared sensible, however it would have been difficult to differentiate between the effect of the microwave irradiation and the conductive heating caused by the filling liquid. Improved microflow setups for microwave irradiation were developed by a few authors in the recent years. [10] Ley, for instance, carried out several microwave syntheses of heterocyclic compounds using a microflow setup similar to ours, consisting of a Teflon tube coiled around a rod, but equipped with a different kind of focused microwave

apparatus where the IR sensor is positioned in a more favourable way ensuring a better temperature control. Comer and Organ, on the other hand, in their above-mentioned study of metal-catalysed reactions used a straight glass capillary system in which the IR sensor probe was positioned directly at the channel. Meanwhile, Bagley and co-workers improved the performance of the flow system by developing instead a sand-filled flow cell in which the IR sensor is positioned directly underneath the reaction chamber containing the flowing mixture resulting in a better IR reading than using the coiled tube. A different type of improved setup was also developed by Haswell and co-workers in the study of heterogeneous metal-catalysed reactions using a glass microreactor placed in microwave cavity in which a thin gold film layer in the proximity of the catalyst bed was used to maximize the absorption of the microwave radiation. All the above mentioned studies by various groups show the importance of improved microflow setup required for a successful microwave flow synthesis, with particular attention paid to the accuracy of the temperature monitoring. In conclusion, although we observed an overall enhancement of reaction outcome by the use of microwave irradiation on the above-reported biphasic Heck reactions, however we were not able to improve our system further, and therefore were not fully convinced that the use of microwave in our systems could bring reliable improvement compared to oil bath heating. For these reactions, therefore, conventional heating was chosen at the time as more reliable method.

3.1.2. Heck Reaction under monophasic conditions

3.1.2.1. Laminar flow

The first microflow study we conducted on monophasic Heck coupling was carried out under laminar flow conditions, screening various metal catalysts on the arylation of methyl acrylate Heck reaction (Scheme 3.4). The monophasic reaction was conducted using a very similar microflow setup (Figure 3.4) to that used in biphasic Heck coupling, where two solutions were introduced into the system: (i) a solution of iodobenzene, methyl acrylate and triethylamine in dimethylformamide (DMF); and (ii) a standard solution of metal catalyst-PPh$_3$ complex in DMF.
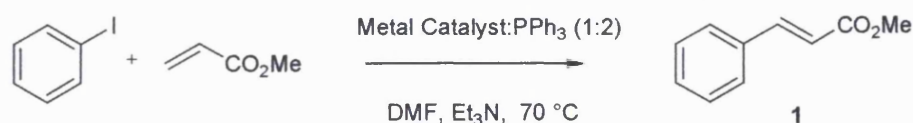
Scheme 3.4. Heck coupling of iodobenzene with methyl acrylate under monophasic conditions.
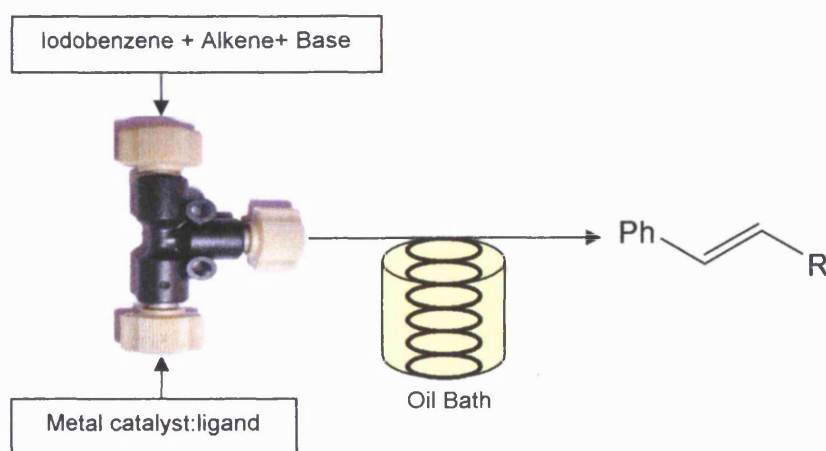
Figure 3.4. PTFE microtubing reaction set-up for laminar flow conditions.

Data in Table 3.4 demonstrate that the performance of the monophasic coupling using the microflow system is better than that carried in a flask, and $PdCl_2$ and $Pd(OAc)_2$ showed better performance than other screened catalysts, both in flask and microflow. However, on many occasions when using both Pd catalysts we observed the formation of a black particulate (Figure 3.5), similar to that observed in the biphasic reactions discussed in section 3.1.1, as a result of catalyst decomposition.

Although the amount of particulate formed in biphasic systems was not significant, however in monophasic systems this caused the microchannel to clog during the reaction. In order to bypass the problem, we initially tried to vary the catalyst-to-reagent ratio by changing the catalyst molar equivalents using different catalyst loading (5 mol%, and 1 mol%).

Figure 3.5. Microscope scan of Pd particulate formation inside PTFE microchannel (courtesy of Chemical Engineering Department of University of Bath, microscope model Nikon Diaphot 300).

Table 3.4. Monophasic Heck coupling of iodobenzene with methyl acrylate: flask *vs.* laminar flow.

Metal Catalyst	Flask Yield of 1 [%]	PTFE microflow Yield of 1 [%]
PdCl$_2$	30	47
Pd(OAc)$_2$	26	53
RuCl$_3$	12	45
Ni(OAc)$_2$	20	34
Pt(COD)Cl$_2$	8	21
CoCl$_2$	17	28

Reaction conditions: In microflow system –metal catalyst (10 mol%), PPh$_3$ (20 mol%), iodobenzene (1.0 mmol), methyl acrylate (1.0 mmol), Et$_3$N (1.0 mmol), in DMF, heating at 70 °C in an oil bath, residence time of 35 minutes under laminar flow. *Reaction conditions*: In flask – metal catalyst (10 mol%), PPh$_3$ (20 mol%), iodobenzene (0.2 mmol), methyl acrylate (0.2 mmol), Et$_3$N (0.2 mmol), in DMF, heating at 70 °C in an oil bath, reaction time of 35 minutes.

We observed that reducing the catalyst loading decreased the amount of particulate formed inside the microchannel, but at the same time lowered the reaction yields significantly (Table 3.5). Alternatively, we tried to use dilution by creating system diluted ten-fold while maintaining the catalyst-to-reagent ratio, which was found to reduce the formation of particulate considerably even at high catalyst load (10 mol%). However, as the dilution increased, longer residence times were needed.

Table 3.5. Monophasic Heck coupling of iodobenzene with methyl acrylate: variation of catalyst loading in microchannel.

Metal Catalyst	Catalyst load [mol%]	Yield of 1[%]
PdCl₂	1	19
PdCl₂	5	33
PdCl₂	10	47
Pd(OAc)₂	1	21
Pd(OAc)₂	5	22
Pd(OAc)₂	10	53

Reaction conditions: Metal catalyst: ligand (1:2), iodobenzene (1.0 mmol), methyl acrylate (1.0 mmol), Et₃N (1.0 mmol), in DMF, heating at 70°C in an oil bath, residence time of 35 minutes under laminar flow conditions.

In pursue for a Heck system with less particulate formation combined with better yields using microflow, we investigated the effect of ligand type on the catalyst stability. First, diphosphine *rac*-BINAP (Figure 3.6) was selected in the attempt to stabilise the Pd centre further due to chelate effect, followed by *N,N'*-bis-mesityl-imidazolium chloride to create a Pd-carbene complex. Pd-carbene complexes, in fact, are known to form very active catalysts for Heck coupling with Pd because of their electronic similarity with phosphines[7], and are therefore capable of stabilizing the metal centre without the steric bulk. Finally we also chose *N,N*-dimethyl-*β*-alanine, since recent studies showed that the use of amino acids as additives to Pd(OAc)₂ forms systems with enhanced reactivity in Heck coupling[12].
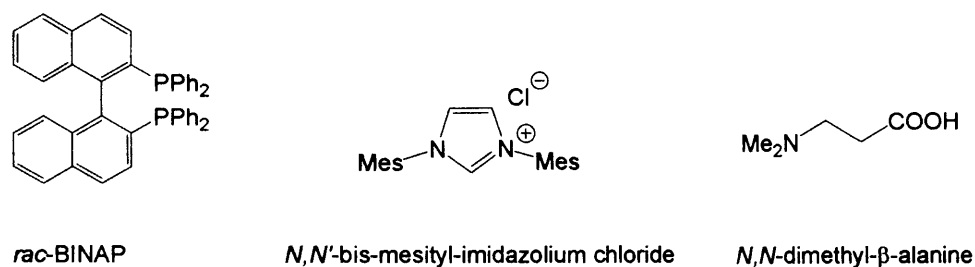
Figure 3.6. Variation of ligand type in Heck coupling.

We prepared catalyst–ligand complexes in 1:2 ratios then tested them by using identical Heck conditions. By screening different ligands, we observed that the type of ligand influences the degree of particulate formation significantly (Table 3.6); the occurrence of high clogging was inevitable when either N,N-dimethyl-β-alanine or the imidazolium salt were used, thus not allowing to complete the reaction. This was not the case for both phosphine ligands; when BINAP was used, a moderately low product yield was obtained, although palladium particulate formation was delayed. Overall, however, the addition of mono-dentate phosphine PPh_3 was found to be the best option in giving relatively lower clogging and better yield compared to the other ligands. Further attempts to increase the stability of the Pd catalyst led to the use of tetra-kis(triphenylphosphine) palladium $Pd(PPh_3)_4$. We found that the use of commercially available $Pd(PPh_3)_4$, rather than its *in situ* preparation, created a more stable and more active Heck system, with much lower particulate formation and the highest yield in the set.

Table 3.6. Monophasic Heck coupling of iodobenzene with methyl acrylate: variation of ligand type in the microchannel Heck reaction.

Metal Catalyst	Added Ligand	Degree of clogging	Yield of 1[%]
Pd(OAc)$_2$	PPh$_3$	low	53
Pd(OAc)$_2$	rac-BINAP	low	39
Pd(OAc)$_2$	N,N'-bis-mesityl imidazolium chloride	high	-
Pd(OAc)$_2$	N,N-dimethyl-β-alanine	high	-
Pd(PPh$_3$)$_4$	-	very low	62

Reaction conditions: Metal catalyst (10 mol%), ligand (20 mol%), iodobenzene (1.0 mmol), methyl acrylate (1.0 mmol), Et$_3$N (1.0 mmol), in DMF, heating at 70°C in an oil bath, residence time of 35 minutes under laminar flow conditions.

In general, the in situ preparation of active species takes place in more uncontrolled conditions compared to the use of an isolated or commercial sample. In the specific case of PdL$_n$ complexes, the addition of two equivalents of ligand L to the Pd salt precursor is reported to create unfavourable equilibria involving the more unstable low-coordinated Pd complexes which lead to the formation of particulate.[7] As shown in Table 3.6, however, only a moderate improvement was brought by the use of commercial Pd(PPh$_3$)$_4$, indicating that the in situ addition of ligands to Pd salts remains a viable method. When we compare the results of all ligands added in situ, it is not

surprising to observe that BINAP and PPh₃ are the best in stabilising the Pd^0 centre. Phosphines in fact, being good π-acceptors, are ideal ligands to stabilise late transition metals due to the strong two-ways bonding.[13] However, we would expect the BINAP ligand to perform better than triphenylphosphine, rather than the opposite, due to chelate effect. The reason why the use of $Pd(PPh_3)_4$ gives a better outcome is probably related to the mechanism of the Heck reaction, in which the elimination and addition of a monodentate ligand L plays a crucial role in the catalytic cycle (Figure 3.1). Therefore, opposite to the expectations, the presence of four independent ligands may be somewhat preferable to the presence of two chelated phosphines. In literature discussions regarding this issue, some authors argue that the use of chelating and bidentate phosphines can in fact present mechanistic complications. [2]

An alternative set of conditions for the Heck reaction was also explored. The ligand-free methodology employing the so-called Jeffery's conditions in Heck coupling[14] use a combination of a divalent palladium with a quaternary ammonium salt in the presence of an inorganic base. Jeffery *et al.* demonstrated that various tetraalkylammonium salts used as additives have an accelerating effect on the Heck reaction without the addition of ligands. We aimed to use a more active system in order to lower the loading of catalyst and therefore avoid the formation of particulate inside the microchannel. The arylation of methyl acrylate was performed in microchannel under Jeffery's conditions using tetraethylammonium chloride in the presence of $Pd(OAc)_2$ catalyst, potassium carbonate as a base, and carried out in a DMF: ethylene glycol solvent system. When 10 mol% loading of $Pd(OAc)_2$ was used, channel clogging occurred frequently, while smaller loading resulted in slightly improved yields compared to the flask.

Table 3.7. Heck coupling of iodobenzene with methyl acrylate using Jeffery's conditions.

Metal Catalyst	Catalyst load [mol%]	Flask Yield of 1[%]	PTFE Microflow Yield of 1[%]	Degree of clogging
Pd(OAc)₂	1	22	34	low
Pd(OAc)₂	5	29	52	low
Pd(OAc)₂	10	36	-	high

Reaction conditions – in microflow system: Pd(OAc)₂ (1, 5 or 10 mol%), Et₄NCl (1.0 mmol), iodobenzene (1.0 mmol), methyl acrylate (1.0 mmol), K₂CO₃ (1.0 mmol), in DMF: ethylene glycol (4:1), heating at 70°C in an oil bath, residence time of 50 minutes under laminar flow. *Reaction conditions* – in flask: Pd(OAc)₂ (X mol%), Et₄NCl (0.2 mmol), iodobenzene (0.2 mmol), methyl acrylate (0.2 mmol), K₂CO₃ (0.2 mmol), in DMF: ethylene glycol (4:1), heating at 70°C in an oil bath, residence time of 50 minutes under laminar flow.

3.1.2.2. Segmented flow

Segmented flow technique was applied to reactions previously carried out in laminar flow conditions in order to achieve further optimisation. We transformed laminar flow into segmented flow by introducing an immiscible inert liquid phase into the laminar flow as shown in Figure 3.7. We aimed to exploit the advantages of segmentation, *i.e.* the generation of internal circulation within segments leading to improved mixing compared to laminar diffusion. During this work, a paper was published by Ismagilov *et al.*[15] on the use of the same principles for various applications including organic synthesis. During our studies we came across limitations in applying the liquid-liquid

segmented flow technique specifically in the choice of the inert solvent, which needs to obey a number of criteria. Besides having to be immiscible with the reaction phase, the segmenter phase must not interfere with, or dissolve any of the reaction components, and have a boiling point compatible with the reaction conditions. In addition, in some cases where heating was applied, the inert phase homogenised with the reaction phase causing loss of segmentation, resulting in the formation of laminar flow. Even in such cases, segmentation can be applied anyway as a tool of pre-mixing reagents prior to heating. We also briefly considered the use of gas segmentation in our study, however the formation of gas-into-liquid segments presented intrinsic problems in the control the flow rate, which proved a difficult task to accomplish with the use of our apparatus. We therefore had to abandon the idea of using gaseous inert phase. Initially we conducted a comparison test between laminar and segmented flow applied to the Heck coupling of alkenes and aryl halides. The arylation of styrene and methyl acrylate with iodobenzene was performed using 10 mol% of $Pd(PPh_3)_4$ in DMF in the presence of triethylamine as a base. Segmentation was applied by introducing a hydrocarbon solvents (heptane, hexane, decane, or nonane) as the segmenter immiscible phase into the DMF reaction flow by using an additional inlet connected to the microflow system. However, some hydrocarbon solvents such as decane tended to homogenise with the DMF at high temperatures resulting in laminar flow. On the other hand perfluorocarbon solvents, such as perfluorodecalin, was found immiscible with DMF even at high temperatures (120 °C), hence it was used as the segmenting phase. However, some other perfluorocarbon solvents may also bear the disadvantage of homogenising with the reaction phase when high temperatures are applied. Due to their high cost, we could only use rather limited volumes of perfluorocarbon solvents, in absence of a recycling system.
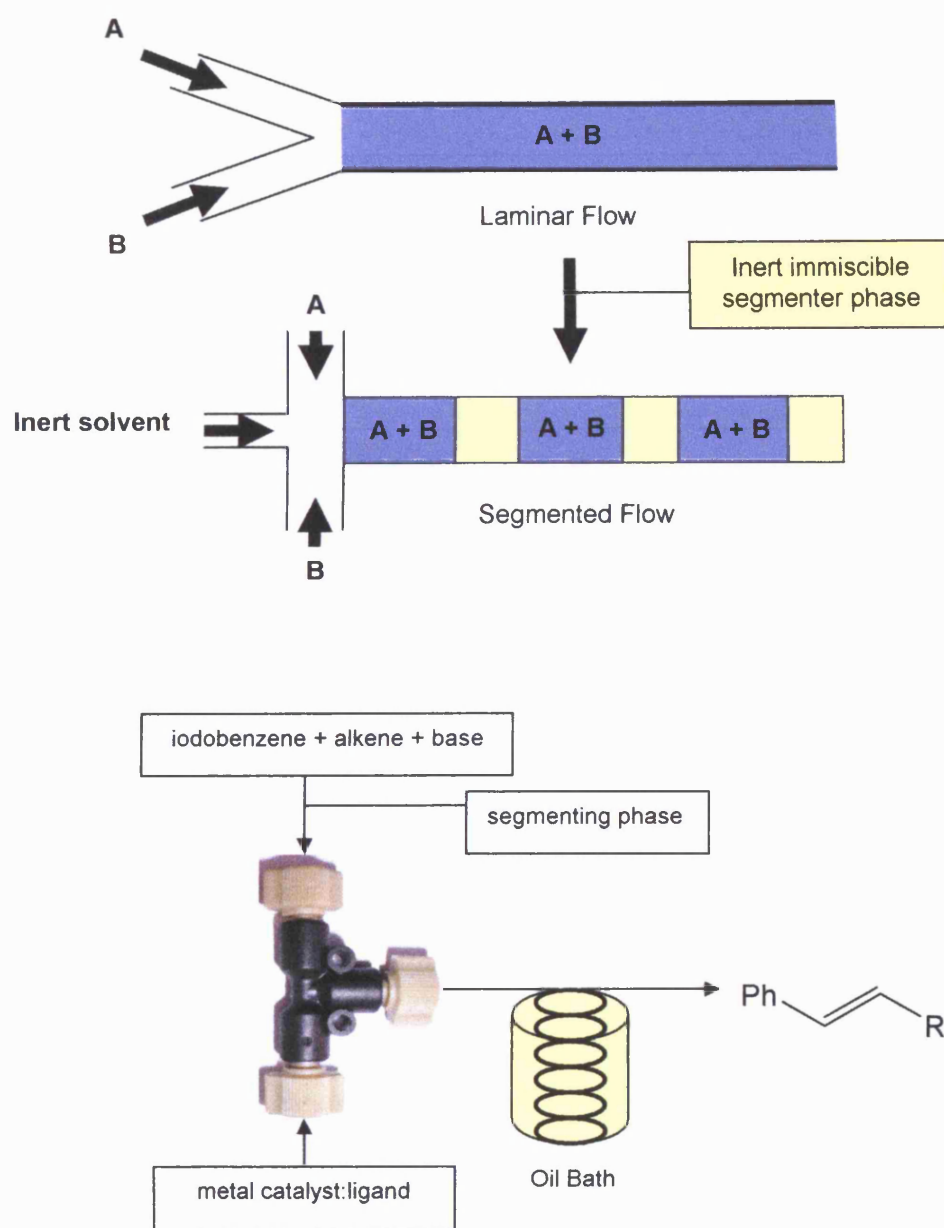
Figure 3.7. Reaction under laminar flow transformed into segmented flow by the introduction of an inert phase, either gas or immiscible liquid *(top)*. Typical segmented microflow system setup *(bottom)*.

As shown in Table 3.8, significant improvements in reaction yields for products methyl cinnamate 1 and stilbene 2 were obtained as a result of introducing segmentation, in agreement with our speculation and in accordance to Ismagilov's arguments[15] above, showing also that high conversions were achievable with relatively low loading of catalyst.

Table 3.8. Laminar *vs.* segmented flow applied to Heck coupling of iodobenzene with methyl acrylate to form methyl cinnamate (1) or styrene to form stilbene (2).

Alkene	*Residence Time*[a] approx. *(min)*	*Catalyst load* [mol%]	*Laminar flow* *Yield* [%]	*Segmented flow*[b] *Yield* [%]
methyl acrylate	35	5	36 (1)	65 (1)
methyl acrylate	35	10	53 (1)	76 (1)
styrene	45	5	38 (2)	57 (2)
styrene	45	10	43 (2)	59 (2)

Reaction conditions: Pd(PPh$_3$)$_4$ (5 or 10 mol%), iodobenzene (1.0 mmol), alkene (1.0 mmol), Et$_3$N (1.0 mmol), in DMF, heating at 70 °C in an oil bath. *a* Defined as the time that the reaction mixture spends in the flow channel (see Chapter 4, Eqs. 4.1a-c). *b* Segmentation created by introduction of decane as inert phase.

On the basis of the very encouraging results obtained in the first attempts to synthesize 1 and 2, the study was extended to a variety of Heck coupling substrates, leading to the use of substituted iodobenzene and bromobenzene with a variety of alkenes (Table 3.9). As expected, iodobenzene showed generally higher reactivity, whereas bromobenzene

often required longer residence times and higher temperatures; therefore we aimed to improve the reactivity of bromobenzene by ring functionalization. The presence of a nitro group in *para* position to the bromobenzene ring increased the reactivity due to the strong electron-withdrawing effect of the substituent, thus activating the C-Br bond. In general, a ring substitution creating an inductive or mesomeric effect that withdraws electron density from the carbon bonded to the halogen, has an accelerating effect.[2] In fact *p*-nitrobromobenzene showed similar product yields to iodobenzene under the same conditions. On the other hand, the presence of a methyl group in *para* position in a halobenzene forms less reactive substrates. The reactivity of styrene derivatives was increased with the presence of strong electron-withdrawing groups in *para* position, such in the case of *p*-fluorostyrene. On the other hand, *m*-nitrostyrene has shown the lowest reactivity in the set in the reaction with iodobenzene. Further optimisation studies on the coupling between iodobenzene and methyl acrylate showed that by increasing the concentration of iodobenzene inside the microchannel to 0.09M and increasing the temperature to 85 °C in the presence of 10 mol% of Pd(PPh$_3$)$_4$, the reaction rate was increased remarkably leading to a shorter residence time of approximately 1 minute to produce methylcinnamate **1** in 97% yield.

Next, we applied the segmented flow method to an additional type of Heck coupling of alkenes using arene-diazonium salts instead of aryl halides (Scheme 3.5).[16] Once the diazonium salt is formed *in situ* from an aminobenzene substrate under acidic conditions, rapid decomposition follows with rapid elimination of nitrogen gas. As a consequence, diazonium salts may generally give rapid and uncontrolled explosions, making their use generally hazardous in conventional flask especially on a large scale. One of the greatest advantages of microflow systems is that the generation of reactive

hazardous intermediates in a continuous flow does not represent a problem, due to the handling of small volumes at a time within a contained environment.
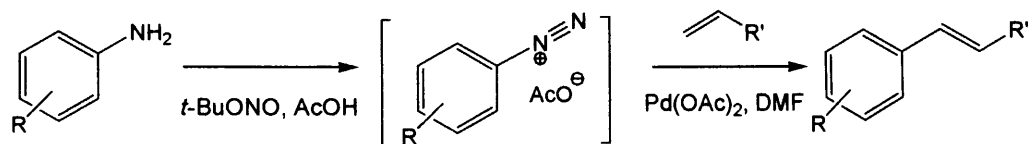
Scheme 3.5. Heck coupling of aniline with alkene under acidic conditions through a diazonium ion intermediate.

The microflow system setup for the Heck diazonium reaction was modified as shown in Figure 3.8, in order to allow the *in situ* diazotisation prior to the Pd catalysed coupling. We converted the aniline into a diazonium intermediate in the microflow system by pumping a mixture of *t*-butyl nitrite (*t*-BuONO) along with excess of acetic acid to aniline at temperatures below ambient (-20 to 0 °C). Once the diazonium is formed in the first section, which can be visually detected by a change in colour of the solution, catalyst Pd(OAc)₂ along with the alkene were introduced at the second section and the Heck reaction was left to take place at room temperature for a residence time of approx. 27 minutes. A variety of benzene-diazonium derivatives were reacted with several alkenes using 10 mol% of Pd(OAc)₂ successfully as shown in Table 3.10. Reasonable conversions were initially obtained when a diluted solution of *t*-BuONO and a standard solution of acetic acid in DMF were used. Hence, we aimed to accelerate the reaction and obtain better yields by increasing the number of equivalents of both *t*-BuONO and acetic acid, achieving the best conversions by using 4 equivalents of each reagent. An alternative successful methodology to generate diazonium consisted of preparing a different set of stock solutions, *i.e.* a solution of the aniline substrate mixed with an

excess of acetic acid (2 eq), and a solution of *t*BuONO (3eq) in DMF. The reactivity of the diazonium intermediate, largely influenced by the nature of the aniline substrate, has a noticeable effect on the reaction yields. The presence of electron-withdrawing substituents on the benzene ring, in fact, activates the diazonium intermediate whereas electron-donating substituents makes them more unreactive, as reflected in the very low yields given by substrates such as *p*-methoxyaniline, in contrast to the very good conversions achieved by using substrates such as *p*-nitroaniline. For comparison, we also performed a series of reactions using commercially available tetrafluoroborate-(*p*-nitrobenzenediazonium), to provide an alternative viable route with relatively high product yields as shown in Table 3.10. In general it is natural to expect improvements by the direct introduction of isolated intermediates, such as cleaner reactions and better yields; however, the fact that in our case such improvements were not that large means that the *in situ* production of active species in the microchannel works rather well.
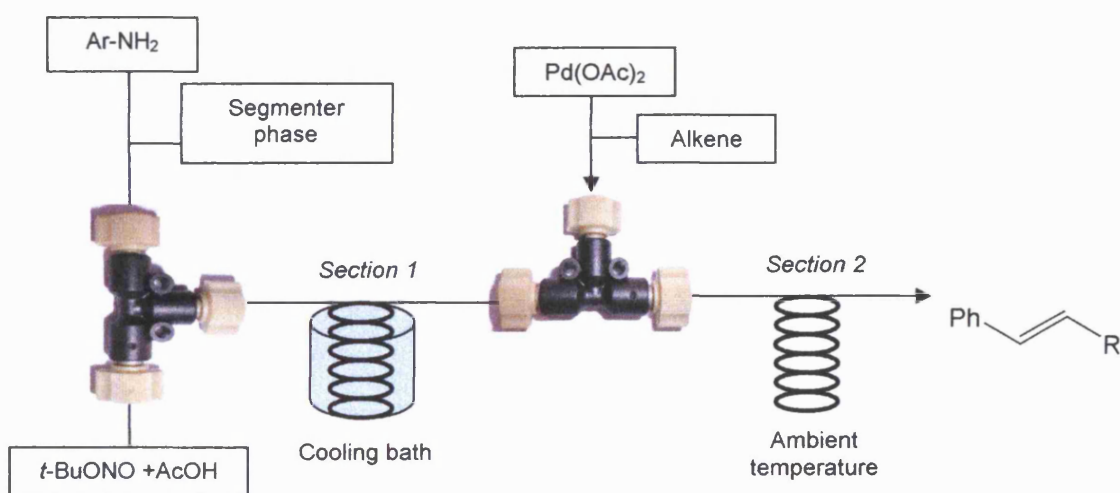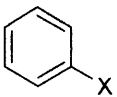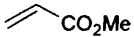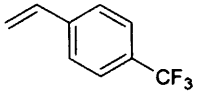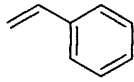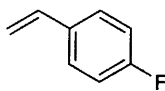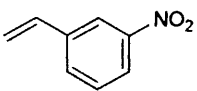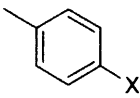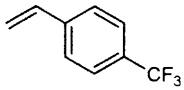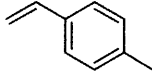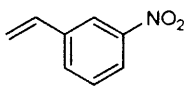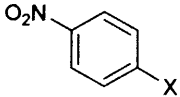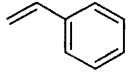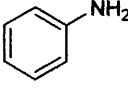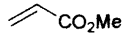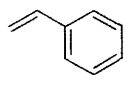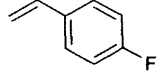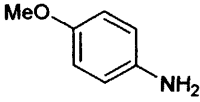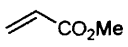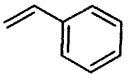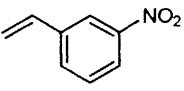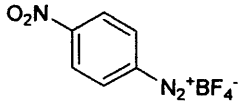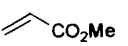
Figure 3.8. Microflow setup for Heck reaction *via* diazonium intermediate in the microflow consists of *section 1* used for diazotisation cooled to 0 °C and *section 2* used for Heck coupling carried out at room temperature.

Table 3.9. Heck coupling of aryl halides to give only *trans* isomer.

Substrates	Alkene	Yield [%]	Product (trans)
X = I /Br		[I /Br]	

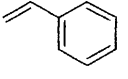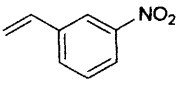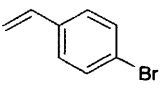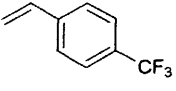| Substrates	Alkene	Yield [%]	Product (trans)
X = I ^{a} /Br ^{b}	CO$_2$Me alkene	68/51	**1**
	CF$_3$ styrene	63/38	**3**
	styrene	57/25	**2**
	F styrene	60/22	**4**
	NO$_2$ styrene	35/21	**5**
X = I ^{a} /Br ^{b} (p-methyl)	CF$_3$ styrene	49/32	**6**
	methyl styrene	47/29	**7**
	NO$_2$ styrene	44/19	**8**
X = Br ^{b} (p-nitro)	styrene	65	**9**

Reaction conditions: Pd(PPh$_3$)$_4$ (10 mol%), aryl halide (1.0 mmol), alkene (1.0 mmol), Et$_3$N (1.0 mmol), in DMF, residence time of 40 minutes. ^{a} ArI coupling heating at 70 °C. ^{b} ArBr coupling heating at 130 °C.

Table 3.10. Diazonium Heck coupling of aniline derivatives.

Substrates	Alkene	Yield [%]	Product (trans)
aniline (NH₂)	CO_2Me	54	1
	styrene	66	2
	4-F-styrene	72	4
4-MeO-aniline (NH_2)	CO_2Me	27	10
	styrene	33	11
	3-NO_2-styrene	18	12
4-O_2N-$N_2^+BF_4^-$	CO_2Me	64	13
	styrene	42	9
	3-NO_2-styrene	57	14
	4-Br-styrene	49	15
	4-CF_3-styrene	61	16

Reaction conditions: $Pd(OAc)_2$ (10 mol%), aryl halide (1.0 mmol), alkene (1.0 mmol), *t*-BuONO (4.0 mmol), AcOH (1.25 ml), in DMF, 0 °C to 25 °C, residence time of 27 minutes.

3.2. Multistep metal catalysed syntheses in microflow system

Carrying out consecutive multistep syntheses using microflow technique offers advantages over conventional methods. In addition to a better control over reaction parameters and fast optimisation, multistep microflow technique enables an improved and more controlled addition of reagents in a consecutive fashion which can be accomplished without delays. It is indeed the continuous nature of the system that allows efficient reaction optimisation: small aliquots of product can be collected as they are produced, and analysed in order to decide how to change reaction conditions and parameters without stopping the process. The efficiency and speed of optimisation could be further improved by introducing automation in addition to fast online analysis into the systems allowing the chemist to obtain faster feedback. There is a growing interest in the literature in carrying out consecutive multistep syntheses using microflow technique by exploiting the above mentioned advantages, such as in the notable works of Haswell, Watts and Ley.[17] The typical multistep microflow setup we used consists of two or more separate microflow sections connected to each other. In the two-step microflow setup, for example, the first reaction step takes place in *Section 1* where the reagents mix and react to form intermediate C as illustrated in Figure 3.9. Once the intermediate is formed, the second reaction step takes place after introducing the required reagents into *Section 2* to form product D. The obtained product D is then collected at the output of *Section 2*. A coiled PTFE microtubing setup is frequently used along with multi-way connectors enabling us to add or remove different sections, or introduce reagents as required, with good flexibility. In a multistep setup like the one shown in Figure 3.9, the flow rate f in a section is the ratio between section volume V and residence time t. V can be expressed for a circular channel as $\pi r^2 l$ where r is the channel radius and l is the section length, so the generic flow rate expression becomes f

$= \pi r^2 \cdot (l/t)$. The limitation with the multistep setup is that once the required residence time for *Section 1* has been set, the total flow rate in *Section 2* becomes fixed since it equals the sum of the flow rate of *Section1* plus the flow rate of *Condition 2*. As a consequence, the residence time of *Section 2* cannot be varied freely without changing the length of the section.
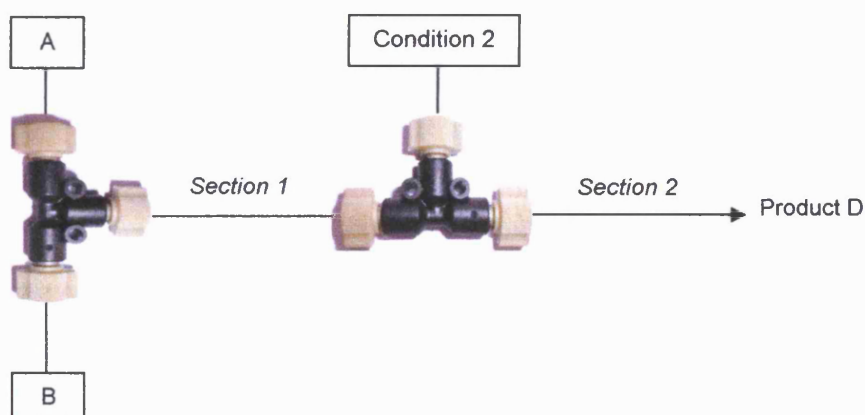

Figure 3.9. Multistep microflow setup consists of separate microchannel reaction sections.

3.2.1. Consecutive two-step Heck coupling

Our interest initially focused on carrying out a multistep microflow synthesis consisting of two consecutive Heck couplings on an aryl substrate containing two different reactive moieties. Such substrates are ideal precursors for a double alkenation where

76

each coupling can take place in two consecutive steps at different reaction conditions. For this we chose to use *p*-chloroaniline to couple with methyl acrylate using both the chloro and the amino group (Scheme 3.6). In the first step, the amino moiety is transformed into a diazonium intermediate under acidic conditions before reacting with methyl acrylate using Pd(OAc)$_2$, to obtain (*E*)-methyl 3-(4-chlorophenyl)acrylate **17**, followed by the coupling at the chloro moiety with another equivalent of methyl acrylate in the presence of Pd(PPh$_3$)$_4$.
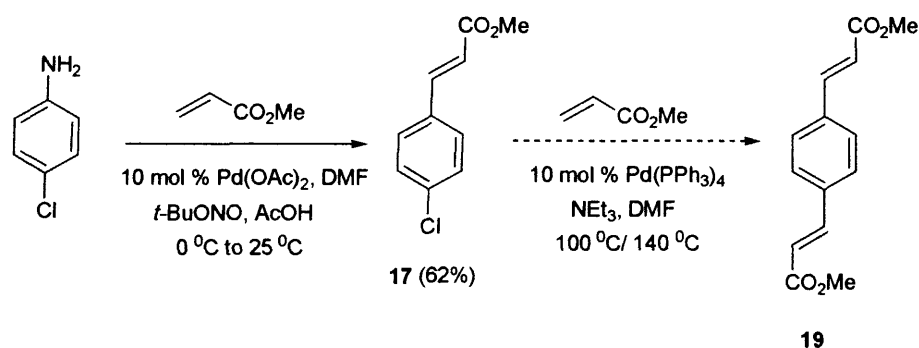
Scheme 3.6. Pd-catalysed double Heck coupling of *p*-chloroaniline with methyl acrylate: coupling of diazonium intermediate to obtain (*E*)-methyl 3-(4-chlorophenyl)-acrylate **17** followed by coupling at the chloro moiety to afford the bis -coupled product **19**.

The order in which the two consecutive steps are carried out is important; the diazonium coupling is conducted first since it requires lower temperatures compared to the coupling at the halide moiety. Separate standard solutions were prepared for each reagent involved in the first step as illustrated in Figure 3.10. Each solution was then loaded into syringes which were then connected to the microflow system through a designated inlet. The solutions were then delivered into the microchannel in a continuous segmented flow manner.
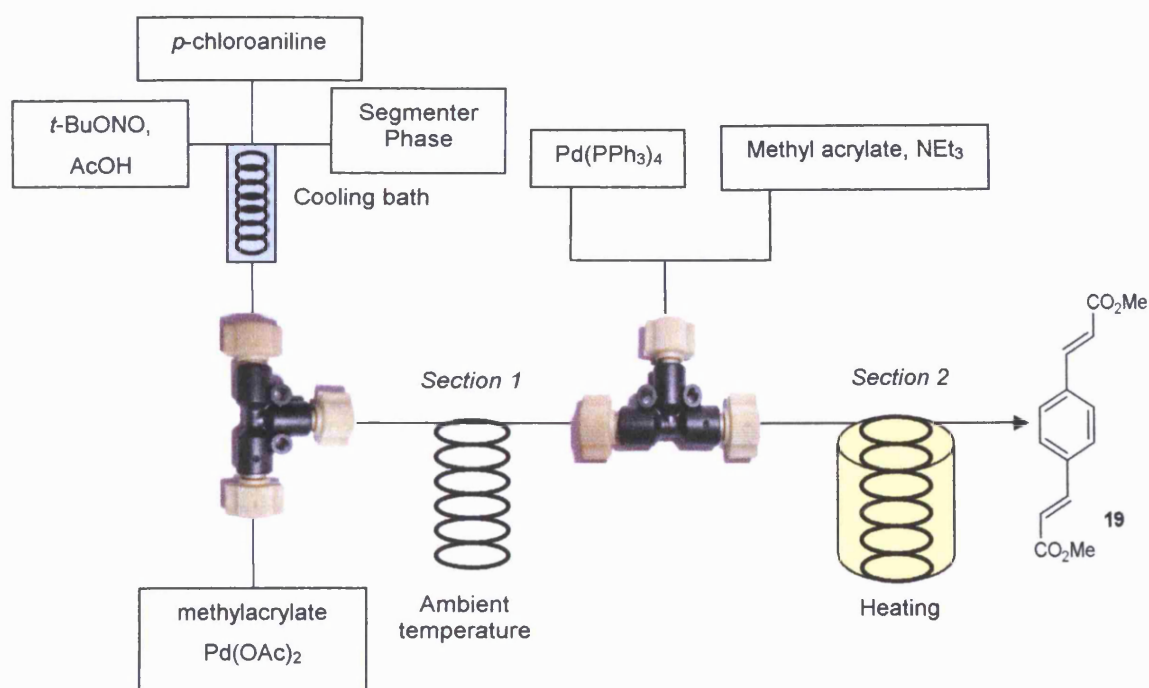
Figure 3.10. Two-step microflow setup for Pd-catalysed double Heck coupling of *p*-chloroaniline with methyl acrylate under segmented flow conditions.

The first step was optimised separately to obtain the best conversion of intermediate **17** (62% yield). The second coupling step was carried out in the multistep system at 100 °C, by introducing a flow of methyl acrylate along with triethylamine base and Pd(PPh$_3$)$_4$ into the flow of intermediate **17**. However, after several attempts to carry the second coupling of intermediate **17**, only large amounts of unreacted intermediate were obtained along with minor unknown impurities. The next sensible thing to do was to increase the temperature; nevertheless, increasing the temperature to 140 °C in the second step had no significant effect even at longer residence times, and only led to unknown impurities with intermediate **17** still being the major component. In order to

understand the cause of failure in the second step, the coupling of **17** was studied separately in microflow as a single step reaction, by using an isolated (*E*)-methyl 3-(4-chlorophenyl)-acrylate **17** as the starting compound. This precaution was taken to rule out the effects of the conditions of the first coupling on the second step. However, no sign of the expected product was observed in this case either, hence at this stage it was reasonable to speculate that the cause of the failure could be a result of the low reactivity of aryl chloro-substituent compared to other halogens. In order to test this hypothesis, we chose to use *p*-iodoaniline to carry out the double Heck coupling using analogous conditions (Scheme 3.7). The conditions of the first step were again optimised separately to obtain intermediate (*E*)-methyl 3-(4-iodophenyl) acrylate **18** in good yield (90%). When the multistep reaction was carried out, the second coupling step on the iodo moiety of intermediate **18** only produced a small amount of the di-coupled product **19** leading to the recovery of large amounts of intermediate **18** and *p*-iodoaniline. When the second coupling step of purified intermediate **18** was studied separately as a single step microflow reaction, no improvement in obtaining compound **19** was achieved after several attempts.
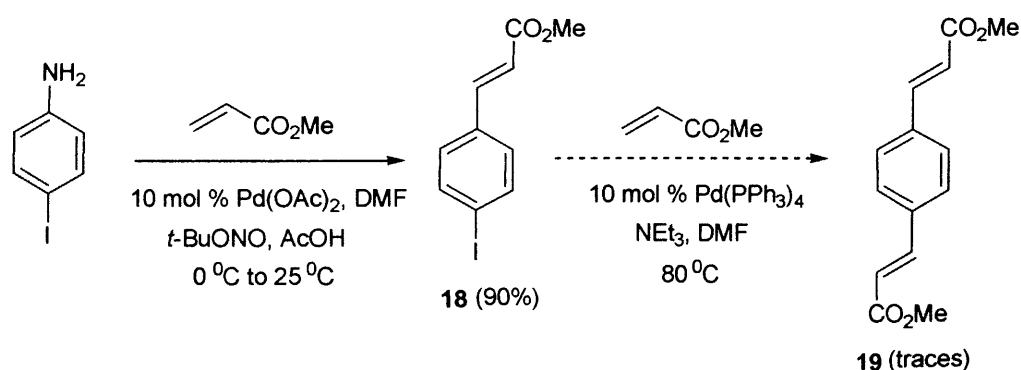

Scheme 3.7. Double Heck coupling of *p*-iodoaniline: coupling of diazonium intermediate to obtain (*E*)-methyl 3-(4-iodophenyl)-acrylate **18** followed by coupling at the iodine moiety.

In conclusion, these first efforts to carry out multistep reactions in microreactor systems were not successful compared to the single step Heck coupling examples shown previously. However, since there is evidence that compound 19 can be prepared under flask conditions, under ultrasonic irradiation at the ambient temperature (25 °C) to afford high yield of the corresponding product, therefore at this stage the results observed for the microflow system are not conclusive, and further reaction optimisation are necessary in order to successfully synthesise 19.[18] In fact, it is rather typical of all attempts of carrying out any organic processes microflow chemistry, to take into account in the optimisation process the number of added parameters compared to flask conditions before a full study is carried out.

3.2.2. Consecutive Heck coupling and ring closing metathesis in two-step microreactor

Our second example of a multistep reaction in microsystem involved the combination of ruthenium catalysed ring closing metathesis (RCM) followed by a Heck coupling (Scheme 3.8). Ring closing metathesis of t-butyl-2-(diallylamino)phenylcarbamate 25 to produce t-butyl-2-(2H-pyrrol-1(5H)-yl)-phenylcarbamate 26, was carried out using Grubbs' I or II catalysts[19] as the first step of the microflow synthesis, followed by Heck cyclisation to produce the tricyclic product. Structure of Grubbs' catalyst I and II are depicted below (Ph = phenyl, Cy = cyclohexyl). Toluene was chosen as solvent for both steps, due to its suitability with both reactions; the RCM step, in fact, requires the use of a solvent which is compatible with Grubbs' catalyst, while the Heck coupling needs to be carried in a relatively high boiling medium.
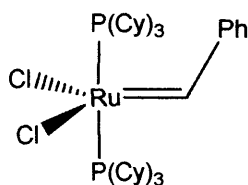
Grubbs catalyst I
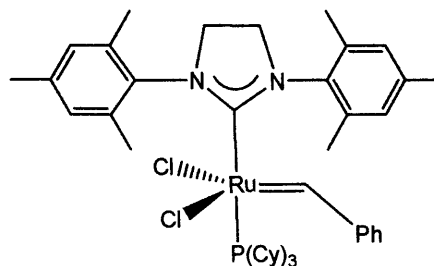
Grubbs catalyst II

However, there are very few solvents which are immiscible with toluene in order to create segmentation, such as water and ethylene glycol. Both solvents are incompatible with the reaction, because of the risk of catalyst deactivation. We chose perfluorocarbon solvents to create segmentation, due to their inertness as well as immiscibility with toluene. The RCM precursor, *t*-butyl-2-(diallylamino)phenylcarbamate **25**, was prepared in conventional flask by *N*-allylation of benzene-1,2-diamine with allyl bromide producing a mixture of five *N*-allylated derivatives (**20**, **21**, **22**, **23**, and **24**), where the desired *N*,*N*-diallyl-1,2-phenylenediamine **23** was the major product (Scheme 3.9). For an improved isolation of the desired intermediate **23**, we found that purification by MPLC chromatography gave better separation than conventional chromatography.
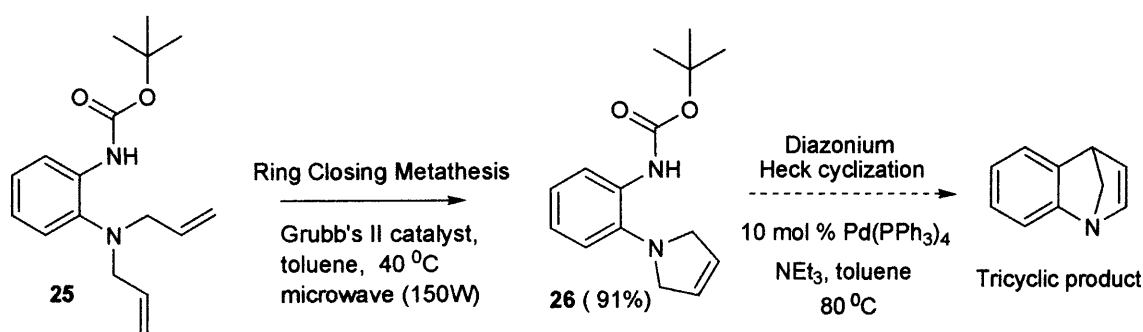
Scheme 3.8. Ring closing metathesis (RCM) of *t*-butyl-2-(diallylamino)phenylcarbamate **25** followed by Heck cyclisation of intermediate *t*-butyl 2-(2*H*-pyrrol-1(5*H*)-yl)-phenylcarbamate **26** to obtain the tricyclic substrate.
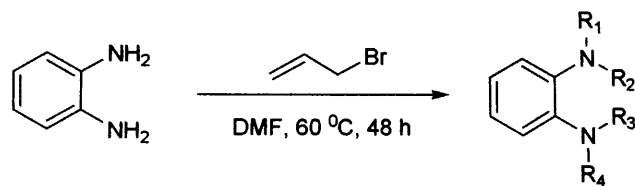
$R^1, R^2, R^3, R^4 = N, N, N', N'$-tetra-allyl   **20** (14-19% yield)

$R^1, R^2, R^3 = N, N, N'$-tri-allyl, $R^4 = H$ **21** (25-33% yield)

$R^1, R^4 = N, N'$-di-allyl, $R^2, R^3 = H$ **22** (10-15% yield)

$R^1, R^2 = N, N$-di-allyl, $R^3, R^4 = H$ **23** (39-55% yield)

$R^1 = N$-allyl, $R^2, R^3, R^4 = H$ **24** (2-7% yield)

Scheme 3.9. Preparation and isolation of precursor substrate N,N-diallyl-1,2-phenylenediamine **23** in conventional flask.

Prior to carrying out the RCM reaction, it was essential to protect the amino group on **23** to generate the carbamate derivative **25**, to avoid any deactivation of Grubbs' metathesis catalyst. The metathesis reaction was initially conducted on precursor **25** using 5 mol% of Grubbs' catalyst I [19] in a PTFE microtube at 40 °C, obtaining intermediate **26** in 63% yield, along with side product t-butyl-2-(1H-pyrrol-1-yl)-phenylcarbamate **27** in 32% yield. In order to improve the yield of intermediate **26**, we carried out a brief optimisation study of the metathesis reaction by investigating the effect of the four main factors affecting the reaction, *i.e.* choice of catalyst, loading of catalyst, heating method and temperature. The most significant results are summarised in Table 3.11. In general we observed that by changing the RCM catalyst type from Grubbs' I to Grubbs' II the yield of the desired intermediate **26** improved significantly while a general decrease on the side product **27** yield was attained.
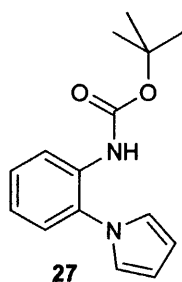

27

Table 3.11. Optimisation of RCM of *t*-butyl-2-(diallylamino)phenylcarbamate **25** in PTFE microtube

(first step in Scheme 3.8).

Catalyst	Catalyst load [mol%]	Heating method	Yield of 26[%]	Yield of 27[%]
Grubbs I	1	Oil bath	31	23
Grubbs I	5	Oil bath	63	32
Grubbs I	5	Microwave	73	21
Grubbs II	1	Oil bath	48	19
Grubbs II	5	Oil bath	87	16
Grubbs II	5	Microwave	91	4

Reaction conditions: Grubbs I or II catalyst (1 or 5 mol%), *t*-butyl-2-(diallylamino)phenylcarbamate **25** (0.4 mmol), in toluene, heating at 40°C using either microwave irradiation (150 W initial power) or oil bath heating, residence time of 10 minutes.

Further studies showed that catalyst loading higher than 5 mol% as well as increase in temperature led to an increase in the yield of side product **27** and a decrease in the yield of compound **26**. Overall, the best results were obtained by using microwave irradiation at 40 °C, in the presence of 5 mol% Grubbs' catalyst II, which gave compound **26** in yields up to 91% within 10 minutes of reaction time. In this particular example, we found that activating the metathesis reaction by microwave irradiation has more reproducible outcome than those previously seen for Heck examples (Section 3.1.1). After finding good metathesis conditions for precursor **25**, we aimed to accomplish the cyclisation of intermediate **26** with the removal of the carbamate protecting group in the Heck acidic conditions to restore the amino substituent, which then effectively converted into a diazonium moiety by using *t*-butyl nitrate and acetic acid. However,

instead of the desired tricyclic product, *t*-butyl-2-(1*H*-pyrrol-1-yl)-phenylcarbamate **27**

was obtained as the major product, along with small traces of the precursor **26**. The

oxidation of the pyrroline **26** to the pyrrole **27** was observed to occur slowly on the

isolated substrate exposed to the atmosphere, while it is accelerated in the presence of

Grubbs' or palladium catalysts (Scheme 3.10).[20]
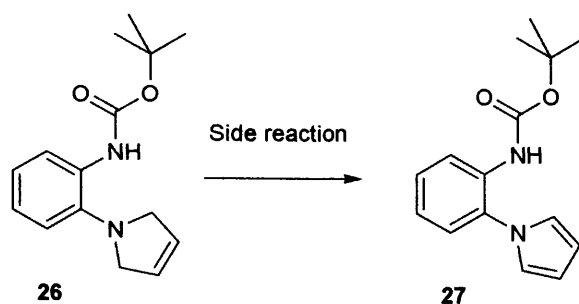
Scheme 3.10. Side reaction of intermediate *t*-butyl 2-(2*H*-pyrrol-1(5*H*)-yl)-phenylcarbamate **26** under

Heck reaction conditions to obtain *t*-butyl-2-(1*H*-pyrrol-1-yl)-phenylcarbamate **27**.

We also observed that the removal of the protecting group, necessary for the formation

of diazonium, did not take place. Acetic acid was probably not strong enough to ensure

the necessary restoration of the amino group. On the other hand, the use of stronger

acids was undesirable because stronger acidic conditions caused polymerisation of the

2,5-dihydropyrrole moiety. At this stage we decided to attempt the multistep synthesis

on another kind of substrate. A possible alternative solution was to use an iodo group in

place of the amino group, using 1-(2-iodophenyl)-2,5-dihydro-1*H*-pyrrole **30** in the

presence of a Pd^0 complex under basic conditions. Substrate **30** was prepared from the

metathesis of *N,N*-diallyl-2-iodobenzenamine **29** and isolated in 98% yield, with only

traces of the side product 1-(2-iodophenyl)-1*H*-pyrrole **31** (Scheme 3.11). Precursor **29**

was prepared in conventional flask by allylation of *o*-iodoaniline as shown in Scheme 3.12.
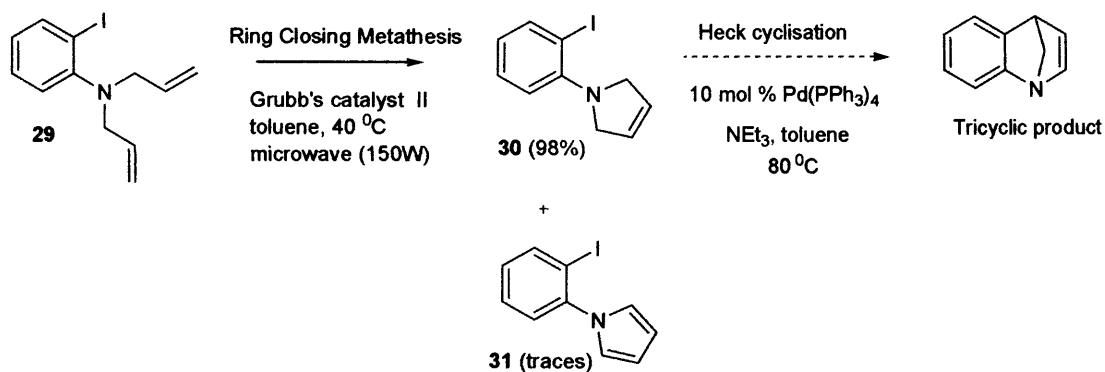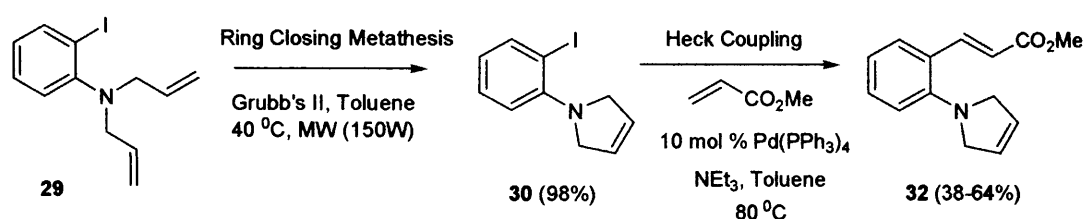

Scheme 3.11. Ring closing metathesis of 2-(diallylamino) iodobenzene **29** followed by Heck cyclisation of 1-(2-iodophenyl)-2,5-dihydro-1*H*-pyrrole **30** to obtain the tricyclic product.

By carrying out the cyclisation of **30** under Heck conditions using Pd(PPh₃)₄ in the presence of triethylamine, we were hoping to obtain the tricyclic product, however, we mainly observed 1-(2-iodophenyl)-1*H*-pyrrole **31** as the major product. Perhaps at this stage it is reasonable to speculate that formation of the desired tricyclic compound is somewhat intrinsically restricted by conformational requirements, thus the oxidation step is believed to take place instead.
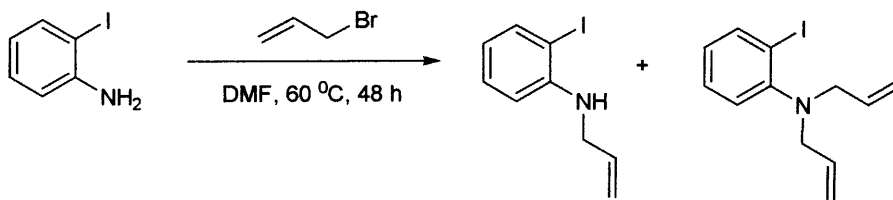
Scheme 3.12. Conventional preparation of *N,N*-diallyl-2-iodoaniline **29**.

Next, we decided to attempt Heck coupling instead of cyclisation, which should not

present any problems with conformational restraints. Heck coupling of **30** with methyl

acrylate was carried out after the metathesis of precursor **29** in the multistep system

(Scheme 3.13). After several attempts, (*E*)-Methyl 3-(2-(2*H*-pyrrol-1(5*H*)-yl) phenyl)

acrylate **32** was obtain in yields between 38% and 64%.

Scheme 3.13. Ring closing metathesis of 2-(diallylamino)iodobenzene **29** followed by Heck coupling of

1-(2-iodophenyl)-2,5-dihydro-pyrrole **30** with methyl acrylate affording (*E*)-methyl-3-(2-(2*H*-pyrrol-

1(5*H*)-yl)-phenyl)-acrylate **32**.

When Heck coupling was carried out using more hindered substrates such as styrene, *p*-

fluorostyrene, *p*-trifluoromethylstyrene and *m*-nitrostyrene, no coupling product was

observed. Another similar example of a consecutive RCM and Heck coupling reaction

was carried out in the same fashion as the previously mentioned example. The

metathesis precursor *N,N'*-diallylaniline **34** was prepared in 89% yield from aniline,

using the same conditions as seen before for the preparation of substrates **22** and **29**.

The RCM of *N,N'*-diallylaniline **34** was carried out in the presence of Grubbs' catalyst

II using the reaction setup shown in Figure 3.11 to afford intermediate 1-phenyl-2,5-

dihydro-1*H*-pyrrole **35** in 96% yield. Intermediate **35** was then promptly reacted with

iodobenzene to obtain 1,3-diphenyl-1*H*-pyrrole **37** in yields between 53% and 60% after several attempts (Scheme 3.14).
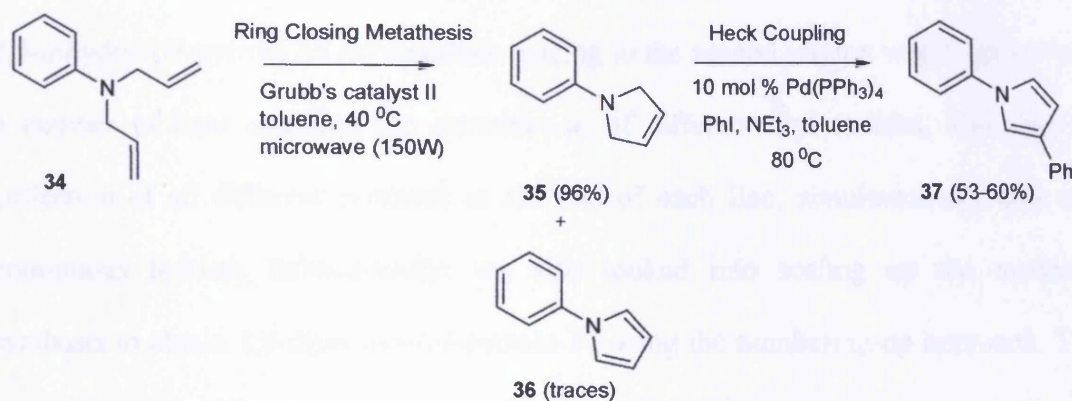
Scheme 3.14. Ring closing metathesis of *N,N'*-diallylaniline **34** followed by Heck coupling of 1-phenyl-2,5-dihydro-1*H*-pyrrole **35** with methyl acrylate, affording 1,3-diphenyl-1*H*-pyrrole **37**.
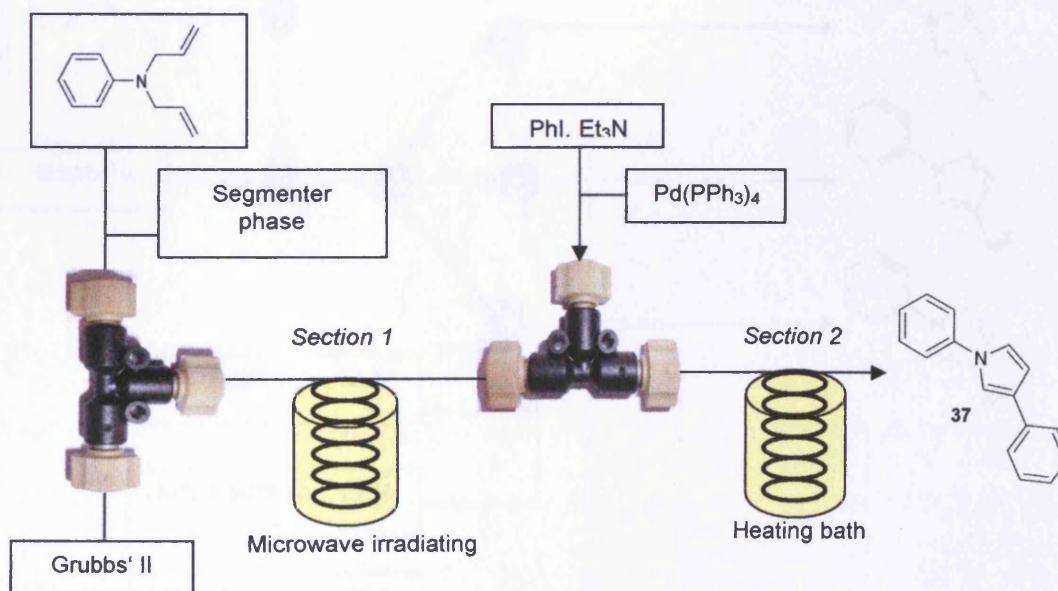

Figure 3.11. Two-step microreactor set up for RCM followed by Heck coupling under segmented flow conditions.

Finally, the success in obtaining product 1,3-diphenyl-1*H*-pyrrole **37** led to develop our study further, by attempting to build a small library of similar derivatives obtained by varying the ring substitution on the aryl iodide used in the second step. For this purpose we modified the microflow setup as illustrated in Figure 3.12. The outlet of 1-phenyl-2,5-dihydro-1*H*-pyrrole **35** intermediate leading to the second section was branched into a number of lines enabling the introduction of different aryl iodides, allowing the collection of all different products at the end of each line, simultaneously and in a continuous fashion. Subsequently, we also looked into scaling up the multistep synthesis to obtain 1,3-diphenyl-1*H*-pyrrole **37** using the numbering-up approach. This means increasing the number of flow channels (all holding the same volume) to carry out the reactions simultaneously in a parallel array of channels (Figure 3.13).
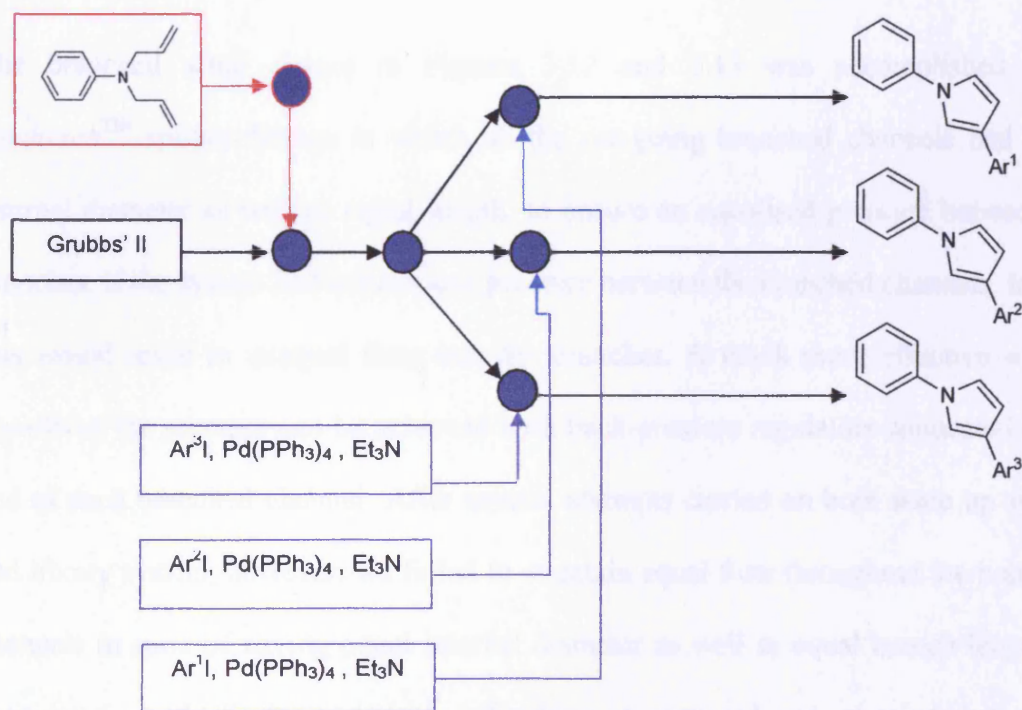

Figure 3.12. Small library of 1,3-diphenyl-1*H*-pyrrole derivatives generated by multistep synthesis.
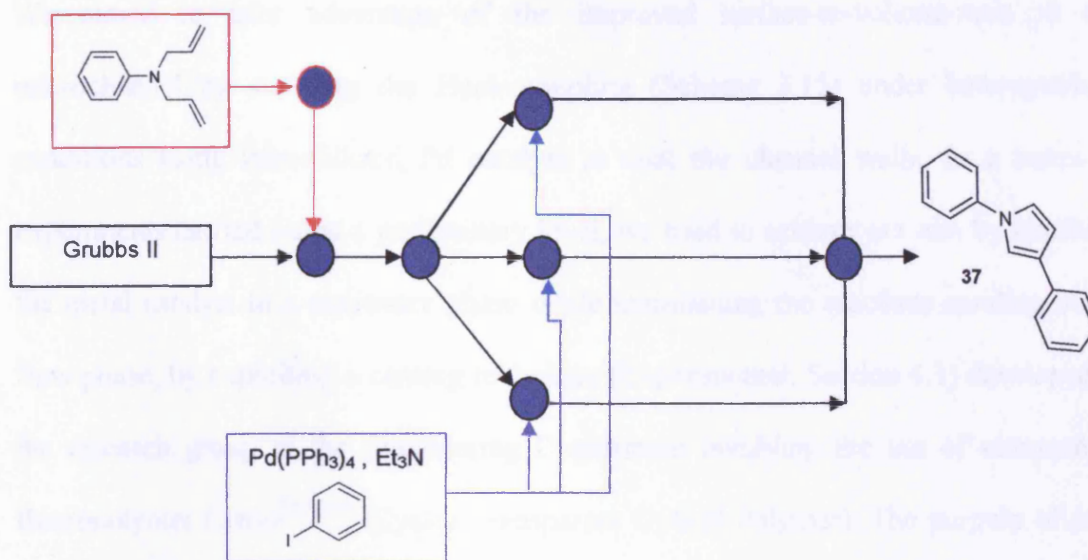
Figure 3.13. Scale up of 1,3-diphenyl-1*H*-pyrrole **37**.

The branched setup shown in Figures 3.12 and 3.13 was accomplished using *Upchurch*^TM splitter fittings in which all the out-going branched channels had equal internal diameter as well as equal length, to ensure an equalised pressure between the branches. If the system had unbalanced pressure between the branched channels, in fact, this would result in unequal flow into the branches. A much more effective way of equalising the pressure can be achieved with back-pressure regulators connected at the end of each branched channel. After several attempts carried on both scale up system and library system, however, we failed to maintain equal flow throughout the branched channels in spite of having equal internal diameter as well as equal branch length. In consideration of all the technical difficulties encountered, we concluded that the designed system is not entirely reliable at this stage and that more advanced level of engineering is required.

3.3. Heck coupling under heterogeneous catalytic conditions

We aimed to take advantage of the improved surface-to-volume-ratio in the microchannel by studying the Heck coupling (Scheme 3.15) under heterogeneous conditions using immobilized Pd catalyst to coat the channel walls. In a series of experiments carried out at a preliminary level, we tried to achieve our aim by attaching the metal catalyst to a stationary phase while maintaining the reactants residing in the flow phase, by exploiting a coating technique (Experimental, Section 4.1) developed in the research group in the Engineering Department involving the use of commercial fluoropolymer $Cytop^{TM}$ [21] (Cyclic Transparent Optical Polymer). The purpose of such coating was mainly to obtain smoother microchannel walls as well as to enhance their hydrophobicity. Using the same technique, we prepared a mixture of Pd/C (30 mol% relative to the amount of reagents) in $Cytop^{TM}$ solution with a volume corresponding at least to the entire volume of the channel, which then was used to coat the PTFE microtube surface.
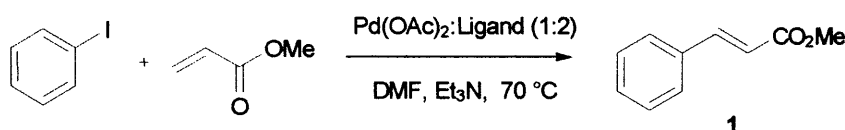
Scheme 3.15. Heck coupling using tris[4-(tridecafluorohexylphenyl]phosphine as the fluorinated phosphine ligand.

However, when the reaction mixture was delivered into the microchannel, the fluorinated catalytic surface layer was washed out instantly. We speculated that the difficulty of coating the PTFE channel surface could be due to its smoothness and

inertness, therefore our next approach involved the microfabrication of a PTFE disc device in which the surface of the channel was purposely roughened using a micromilling tool to ensure a better coating.
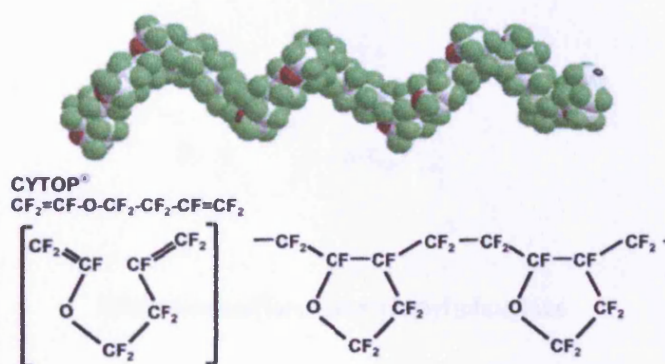

Figure 3.14. Structure of $Cytop^{TM}$. [21]

Although the roughness of the microchannel can in theory cause disturbances to the segmented flow, we were confident that the coating with the Pd/C-$Cytop^{TM}$ mixture would produce a smooth surface. However, as already explained in Section 2.3, the bonding of PTFE microdiscs was very hard to accomplish, while on the other hand PMMA could not be used due to its poor thermal resistance during the reaction. At the end a good compromise was obtained by avoiding bonding, and instead we held together a transparent PFA disc over an opaque PTFE disc very tightly in the microreactor housing. When the reaction mixture was flowed through the channel, we observed that some of the Pd/C catalyst passed into the reaction mixture as the reaction mixture flowed through. We initially thought that Pd/C did not possess any special affinity with the fluorinated phase probably due to lack of functionalities. We therefore employed a fluorinated Pd^0 complex by combining $Pd(OAc)_2$ with a fluorinated phosphine ligand tris[4-(tridecafluorohexylphenyl]phosphine to enhance the Pd

catalyst's affinity with the $Cytop^{TM}$ phase. Nonetheless, the same problem of catalyst diffusion into the reaction mixture was observed. At this point we decided not to develop the idea further, as creating affinity between catalyst and the inert fluorinated phase seems an intrinsically difficult task.
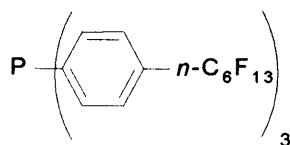
Tris[4-(tridecafluorohexylphenyl]phosphine

3.4. Summary and conclusions

By carrying out various examples of Heck reactions in microflow system, we observed better performances, both in biphasic and monophasic systems, compared to conventional flask. For Heck coupling under homogeneous single flow conditions, we were able to enhance performances, compared to the laminar flow, by the use of segmentation. In these cases segmentation was either maintained all along the reaction, or in some cases used as a tool for reagent pre-mixing before solvent homogenisation at high temperature. In many examples of Heck reactions, although the use of microwave irradiation was observed to give a general enhancement in the reaction performance, however, it proved to be not as reliable as one would hope in comparison to conventional heating, leading to many irreproducible results. By contrast, microwave irradiation proved to be a rather reliable tool to enhance the performances of ring-closing metathesis reactions. We looked at the improvement of reaction performance either by varying the substrate type, or by activating it *via* functionalization, with satisfactory results. Observations, however, suggest that in several cases further system

optimization may be brought in. We also showed that by varying parameters such as concentration, loading and type of catalyst, we were able not only to better handle the formation of Pd particulate within the channel, but also to increase the reaction rate. Although the advantage of the use of segmented flow technique to both monophasic and biphasic reaction systems is clear, however, the main limitation in the choice of solvent systems needs to be considered especially for the monophasic systems, in which segmentation is used to ensure better mixing. In fact, the appropriate choice of the segmentation solvent for the task required is made according to criteria of temperature-dependent immiscibility, non-interference with substrates and products, boiling point and low cost. Perhaps the best solution to overcome such limitation would be the use of gas segmentation, which however requires special techniques beyond the scope of this study.

We developed a microflow system to study multistep syntheses involving Pd-catalysed Heck reactions and Ru-catalysed ring-closing metathesis, successfully providing reagent and catalyst delivery in a consecutive fashion, achieving control over reaction parameters and accomplishing fast optimisation. The accomplishment of Heck multistep reaction in some cases was not as successful as in the single step coupling, calling for further reaction optimisation. Ring-closing metathesis, on the other hand, proved quite successful in the production of desired reagent intermediates. In the recent years we have witnessed the growing interest on integrating solid-supported reagents into flow chemistry. This is a very appealing prospect especially for the multistep flow reactions as a semi-purification tool between steps to improve the quality of each step. For example, the use of $Quadrapure^{TM}$ (Sigma-Aldrich) commercial metal scavengers, used to trap metal catalyst at the end of the reaction, could be an ideal approach for multistep metal-catalysed reactions in which different metal catalysts are used. On the other hand,

using a macro-porous or monolithic solid-supported metal catalyst would offer an advantage in terms of catalyst recycling. Although the building up of both library and scale up systems (Figures 3.12 and 3.13) is generally time-consuming and requires a number of connecting parts, however, once such systems have been set up, they are much more efficient than conventional flask methods. Nevertheless, the limited time on the project did not allow further improvements that we had in mind, namely the modification of the scale up and the library setup, needed in order to split the flow equally into the branched channels and be able to apply segmented flow technique for further reaction performance enhancement.

3.5. References

[1] F. Alonso, I. P. Beletskaya, M. Yus, *Tetrahedron* **2005**, *61*, 11771–11835.

[2] R. F. Heck, J. P. Nolley, *J. Org. Chem.* **1972**, *37*, 2320–2322; R. F. Heck, *Org. React.* **1982**, *27*, 345–390; I. P. Beletskaya, A. V. Cheprakov, *Chem. Rev.* **2000**, *100*, 3009–3066; J. P. Knowles, A. Withing, *Org. Biomol. Chem.* **2007**, *5*, 31–44.

[3] J. J. Masters, J. T. Link, L. B. Snyder, W. B. Young, S. J. Danishefsky, *Angew. Chem. Int. Ed. Engl.* **1995**, *34*, 1723–1726.

[4] C. Y. Hong, N. Kado, L. E. Overman, *J. Am. Chem. Soc.* **1993**, *115*, 11028–11029.

[5] B. M. Trost, J. Dumas, M. Villa, *J. Am. Chem. Soc.* **1992**, *114*, 9836–9845.

[6] K. Ohari, K. Kondo, M. Sodeoka, M. Shibasaki, *J. Am. Chem. Soc.* **1994**, *116*, 11737–11748.

[7] F. E. Ziegler, U. R. Chakraborty, R. B. Weisenfeld, *Tetrahedron* **1981**, *37*, 4035–4040.

[8] B. M. Bhanage, F.-G. Zhao, M. Shirai, M. Arai, *Tetrahedron. Lett.* **1998**, *39*, 9509–9512.

[9] W. A. Herrmann, C. W. Kohlpaintner, *Inorg. Synth.*, **1998**, *32*, 8–25.

[10] T. N. Glasnov, C. O. Kappe, *Macromol. Rapid Commun.* **2007**, 28, 395–410; S. Saaby, I. R. Baxendale, S. V. Ley, *Org. Biomol. Chem.* **2005**, *3*, 3365–3368; I. R. Baxendale, S. V. Ley,C. M. Griffths-Jones, G. K. Tranmer, *Chem. Eur. J.* **2006**, *12*, 4407–4416; E. Comer, M. G. Organ, *J. Am. Chem. Soc.* **2005**, *127*, 8160–8167; M. C. Bagley, R. L. Jenkins, M. C. Lubinu, C. Mason, R. Wood, *J. Org. Chem.* **2005**, *70*, 7003–7006; P. He, S. J. Haswell, P. D. I. Fletcher, *Lab Chip* **2004**, *4*, 38–41; P. He, S. J. Haswell, P. D. I. Fletcher, *Appl. Catal. A* **2004**, 274, 111–114, P. He, S. J. Haswell, P. D. I. Fletcher, *Sens. Actuators B* **2005**, *105*, 516 –520.

[11] Correspondence exchange with CEM technical representatives.

[12] X. Cui, Z. Li, C.-Z. Tao, Y. Xu, J. Li, L. Liu, Q.-X. Guo, *Org. Lett.* **2006**, *8*, 2467–2470.

[13] F. A. Cotton and G. Wilkinson, Advanced Inorganic Chemistry, 5th Ed., Wiley, **1988**.

[14] T. Jeffery, *Tetrahedron* **1996**, *52*, 10113–10130.

[15] D. L. Chen, L. Li, S. Reyes, D. N. Adamson, R. F. Ismagilov, *Langmuir* **2007**, *23*, 2255-2260; D. L. Chen, R. F. Ismagilov, *Curr. Opin. Chem. Biol.* **2006**, *10*, 226–231.

[16] A. Roglans, A. Pla-Quintana, M. Moreno-Mañas, *Chem. Rev.* **2006**, *106*, 4622–4643.

[17] P. Watts, C. Wiles, S. J. Haswell, E. Pombo-Villar, *Tetrahedron* **2002**, *58*, 5427–5439; I. R. Baxendale, J. Deeley, C. M. Griffiths-Jones, S. V. Ley, S. Saaby, G. K. Tranmer, *Chem. Commun.* **2006**, 2566–2568; T. Schwalbe, V. Autze, G. Wille, *Chimia* **2002**, *56*, 636–646; H. R. Sahoo, J. G. Kralj, K. F. Jensen, *Angew. Chem. Int. Ed.* **2007**, *46*, 5704–5708.

[18] Z. Zhang, Z. Zha, C. Gan, C. Pan, Y. Zhou, Z. Wang, M.-M. Zhou, *J. Org. Chem.* **2006**, *71*, 4339–4342.

[19] P. Schwab, R. H. Grubbs, J. W. Ziller, *J. Am. Chem. Soc.* **1996**, *118*, 100–110; S. J. Miller, H. E. Blackwell, R. H. Grubbs, *J. Am. Chem. Soc.* **1996**, *118*, 9606–9614; M. Scholl, S. Ding, C. Woo Lee, R. H. Grubbs, *Org. Lett.* **1999**, *1*, 953–956; N. Saito, Y. Sato, M. Mori, *Org. Lett.* **2002**, *4*, 803–805.

[20] J. E. Baeckvall, J. E. Nystroem, *Chem. Commun.* **1981**, 59–61.

[21] http://www.agc.co.jp/english/chemicals/shinsei/cytop/cytop.htm
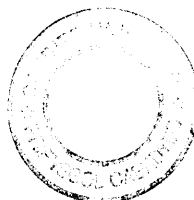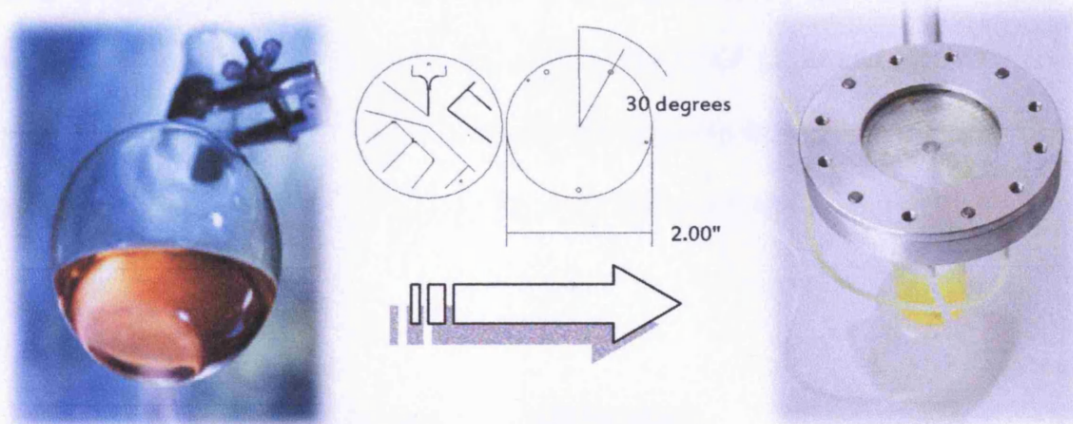
Chapter 4

Experimental and system setup

4.1. Microfabrication and microflow system setup

In this project we frequently used microflow systems made from a range of polymeric materials.[1] These are known to be compatible with a variety of reaction conditions and reagents and are economical in terms of material price and microfabrication cost. Microfabrication of polymer materials was carried out through mechanical milling technique on sheets of materials using *LPKF* milling machine (Figure 4.1).[2] A range of high precision engraving and drill tools supplied by *LPKF Laser* and *Electronics* were used to produce the inlet and outlet ports as well as microchannel in a uniform depth in a variety of sizes, typically in the range from 0.1 mm to 1.0 mm.
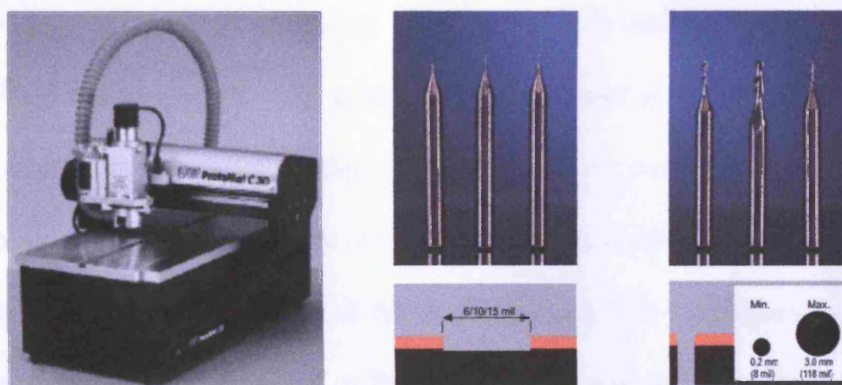

Figure 4.1. *Laser* and *Electronics LPKF* milling machine with *x*, *y*, *z* milling directions (left); typical *LPKF* engraving tools to form a square or rectangular shaped microchannels (middle); drilling tools to form inlet and outlet ports (right).

By using engraving milling tools, one is able to produce square or rectangular channel geometries. The size of the milling tool is selected according to the required width of the channel, while the depth can be controlled through the milling machine. On the

96

other hand, inlet and outlet ports were fabricated using a double edge cutter tool to make flat-bottomed circular ports with an internal diameter of 1.6 mm, the same diameter as the inlet tubes which connects the pump to the microflow device. Before carrying out the milling procedure, a pattern design of the microflow device was created by using *CorelDraw 10* software to implement the right measurements and size. The completed design is then imported into *CircuitCamp 3.2* software, where assignment of the milling and drilling tools to the specific job takes place followed by importing the information into *BoardMaster 3.0* software which controls the *LPKF* milling machine directly. Microfabrication consists of two main stages, namely the *micromilling*, to create an open microchannel in uniform depth, and the *bonding*, to create an enclosed microchannel.

The microfabricated microflow devices consisted of two sealed circular shape surface layers of 1½ " radius (Figure 4.2), a bottom surface layer containing the micromilled channel, arranged in a serpentine shape in order to fit in maximum length, and a top layer containing two inlets ports and one outlet port. Good performance in micromilling is generally related to the hardness of the material used. The two layers, which can be made either from the same material or from two different materials, were then sealed on top of each other, using different *bonding* techniques, mainly based either on *thermal* or *adhesive* methods, depending on the material used. Thermal bonding is based on pressing the two discs together while thermally reaching the polymer T_g (glass transition temperature), and is generally incompatible with the bonding of discs of two different materials. When that is the case, then adhesive bonding becomes the preferred technique, carried out by use of a layer of sealant between the two discs.
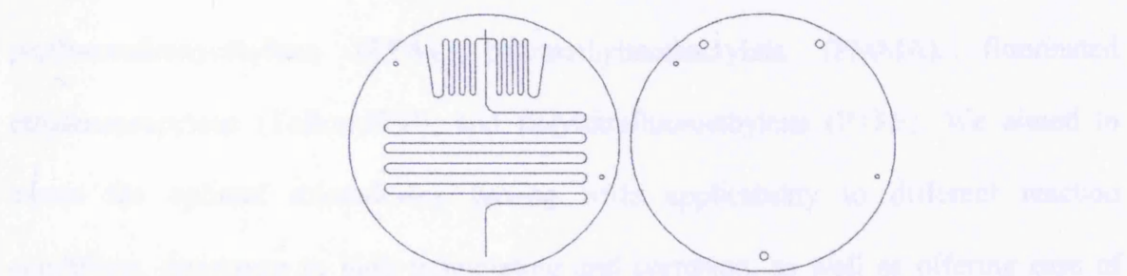
Step 1
Designing and microfabrication of two polymer
discs using LPKF milling

Inlet ports   Outlet port

Microchannel
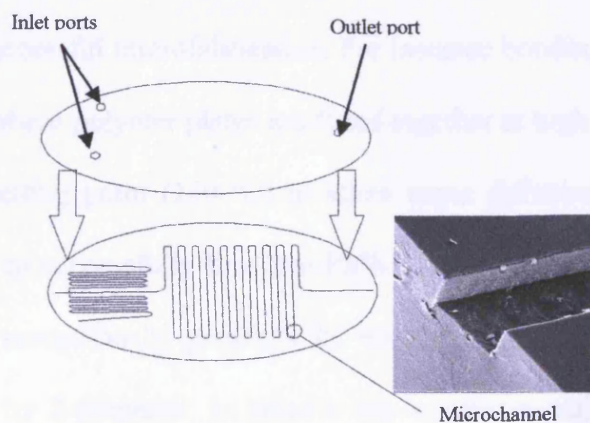
Step 2
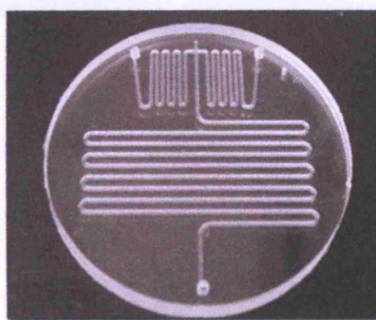Bonding both polymer discs

Figure 4.2. Microfabrication of polymeric microflow device.

We carried out our microfabrication using various polymeric materials, perfluoroalkoxyethylene (PFA), polymethylmethacrylate (PMMA), fluorinated ethylenepropylene (Teflon-FEP), and polytetrafluoroethylene (PTFE). We aimed to create the optimal microdevice having wide applicability to different reaction conditions, resistance to high temperature and corrosion, as well as offering ease of microfabrication. For that purpose we used polymer materials with a variety of physical properties. In general, polymers known for their chemical inertness and high thermal resistance (e.g. PTFE) are problematic in microfabrication, whereas less inert polymers make ideal candidates for successful microfabrication. For instance bonding for PMMA is best achieved thermally, where polymer plates are fused together at high temperature, usually 10 °C below the melting point (130 °C) to allow some diffusion of material between the plates. In order to successfully fuse two PMMA discs, the surface of each plate must be cleaned very scrupulously, generally by washing with organic solvents such as methanol followed by 2-propanol, to remove any contaminants, drying with nitrogen gas and then heating for 48 hours at 95 °C prior to fusion. Once the microdevice has been thermally bonded, sometimes we coat the microchannel in order to obtain a smoother wall surface and to give improved solvent resistance with a degree of hydrophobic nature. A technique applicable to polymer channels, already developed in the research group in the Engineering Department at Cardiff University, involved the use of commercial fluoropolymer $Cytop^{TM}$ [3] (Cyclic Transparent Optical Polymer), supplied by Asahi Glass. This is an amorphous, soluble fluoropolymer exhibiting the outstanding properties typical of highly fluorinated polymers, such as very low surface energies with respect to aqueous phases and maximum protection against degradation. The typical microdevice contained a T-shaped inlet junction with a dead-volume top-chamber, proved to be the best design to provide effective segmentation. Instead, for the

creation of parallel flow, a V-shaped mixing junction was used (Section 2.2), in which the best angle θ at the point where both phases meet (Figure 4.3) was between 60 and 90°, in order to obtain a stable flow.
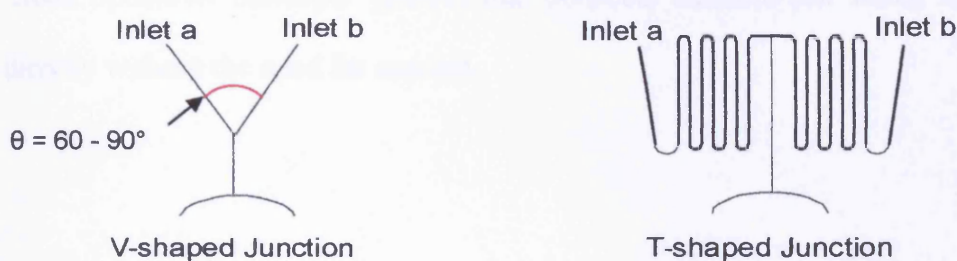

Figure 4.3. V-shaped and T-shaped inlet design.

Housing device

For efficient connection between the microflow device and the external elements such as pumps, manual or automated product collection, or online analysis instrument, we have designed and manufactured a microreactor housing (Figure 4.4), made of chemically resistant and thermally stable materials such as stainless steel (Figure 4.5) or polyetheretherketone (PEEK) (Figure 4.6). The housing was designed to embed in and hold firmly the microdevice while providing a tight-seal connection between the inlet ports and the pumps using capillary tubes, allowing the introduction of reagents over a range of flow rates and pressure, reliably and avoiding leakages. The microreactor housing contains a number of threaded holes specifically designed for the use of the finger-tight nut fittings from *Upchurch Scientific* (p-206), to allow a secure positioning of the capillary tubes (outside diameter 1/16 inches) (Figure 4.7). In addition, a rubber

seal was placed inside each screw, around the hole on the surface of the device. The design allows the connection of more than two inlets, hence more syringe pumps can be fitted in. Connection between capillary tubing and the reagent syringe was originally achieved using a silicone tube (length 30 mm) fitted between the needle and the capillary tube. We then later adopted the use of the safer M6 nut fittings-to-female luer-adapter from *Upchurch Scientific* (p-660) that connects standard nut fitting to the syringe directly without the need for needles.
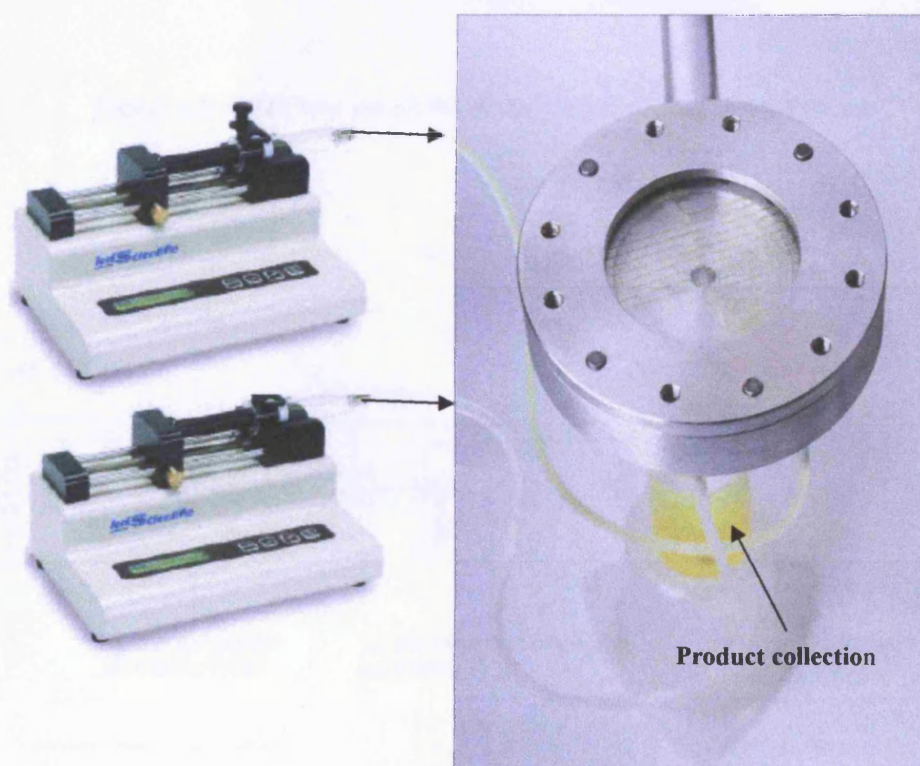

Figure 4.4. Microdevice experimental setup: syringe pump connected to microreactor stainless steel housing and sample outlet for collection of product.
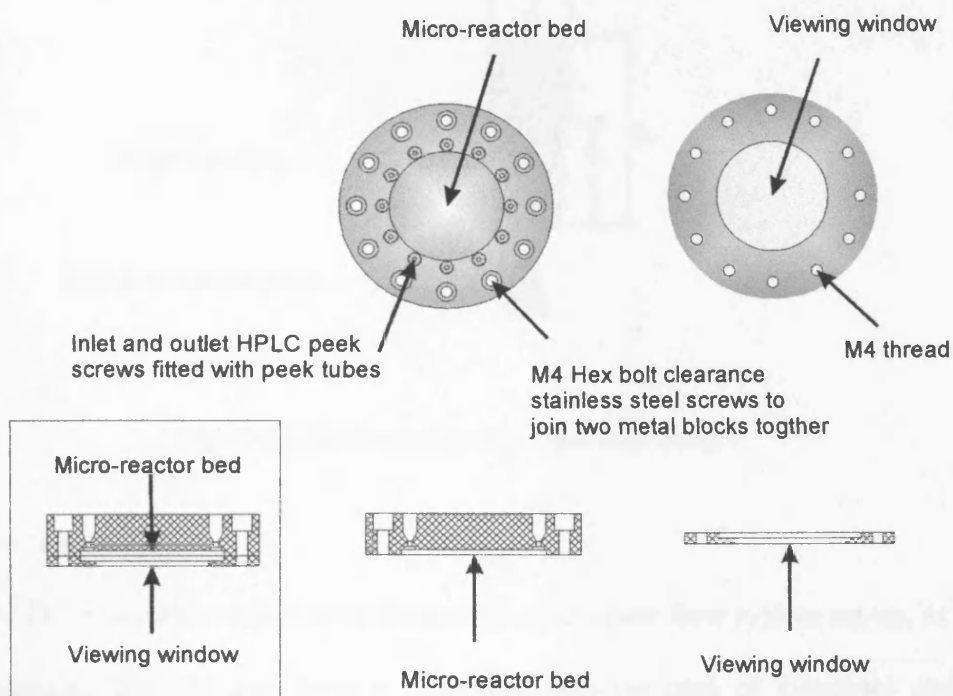
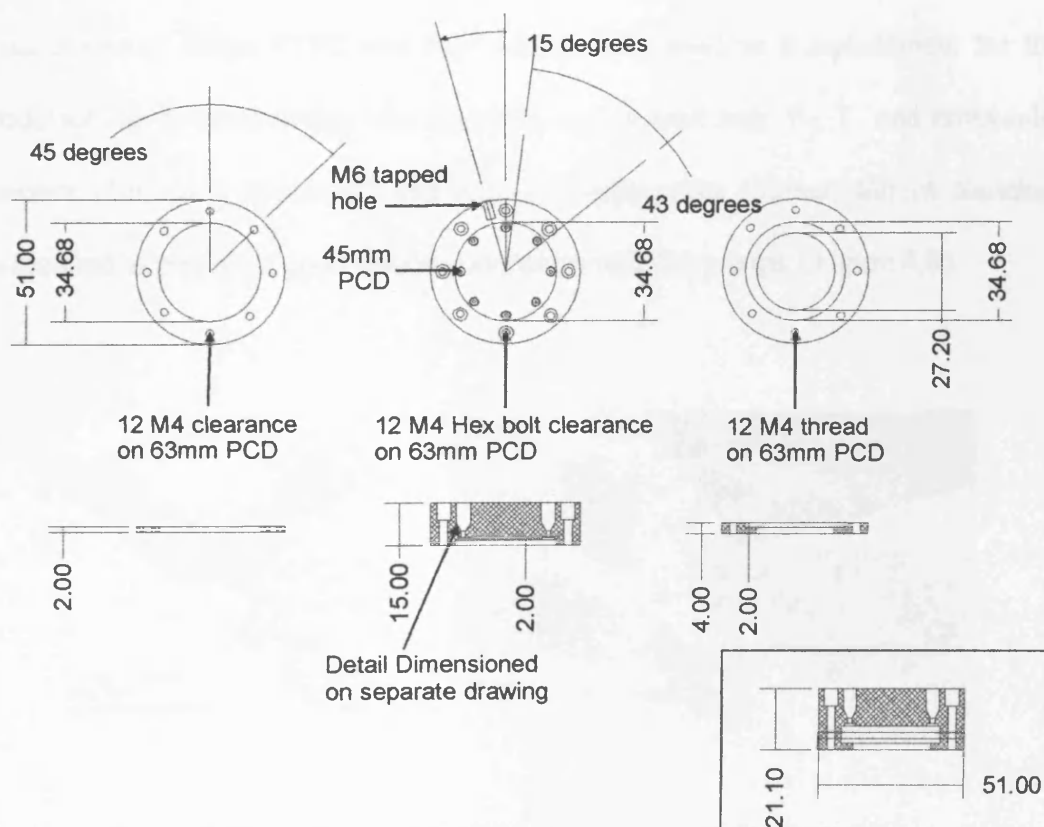Figure 4.5. *CorelDraw* design for the stainless steel microdevice housing.

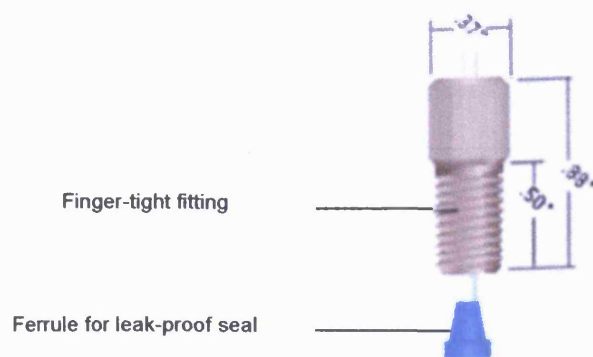Figure 4.6. *CorelDraw* design for the PEEK microdevice housing.

Figure 4.7. *Upchurch Scientific* finger-tight fitting.

Microflow tube setup

PTFE and FEP microflow tubes were frequently used in our flow system set-up, as they are economical, flexible, and have a good visibility (in case of clogging) and are resistant to a variety of chemical and physical conditions such as heating, cooling, microwave irradiation and sonication. PTFE and FEP tubing can be purchased in a variety of sizes, we tend to use the tubing with 1/16 inch outside diameter and vary the internal diameter. When PTFE and FEP tubing were used as a replacement for the microdevice, no housing design was required, and instead only Y-, T- and cross-inlet connectors (*Upchurch Scientific*) and *KEL-F* T-connectors (*Sigma–Aldrich Supelco*) were required to provide a good sealed connection with the pumps (Figure 4.8).
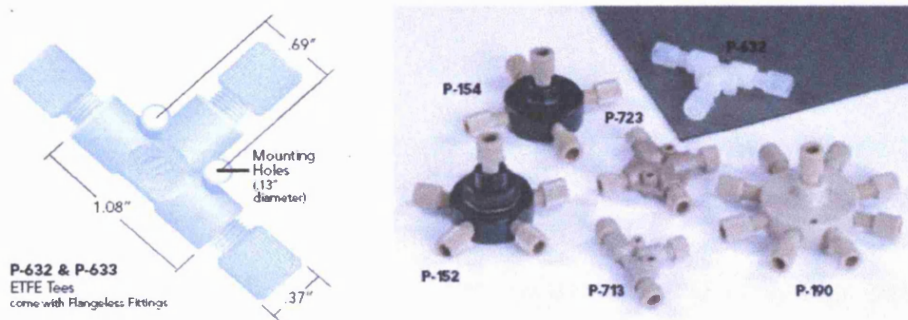

Figure 4.8. Flow splitter, cross, and T connectors from *Upchurch scientific*.

103

In the typical microflow setup the microflow was coiled around a glass or metal test tube to be immersed into a heating or cooling bath or inserted into a CEM microwave cavity (Figure 4.9).
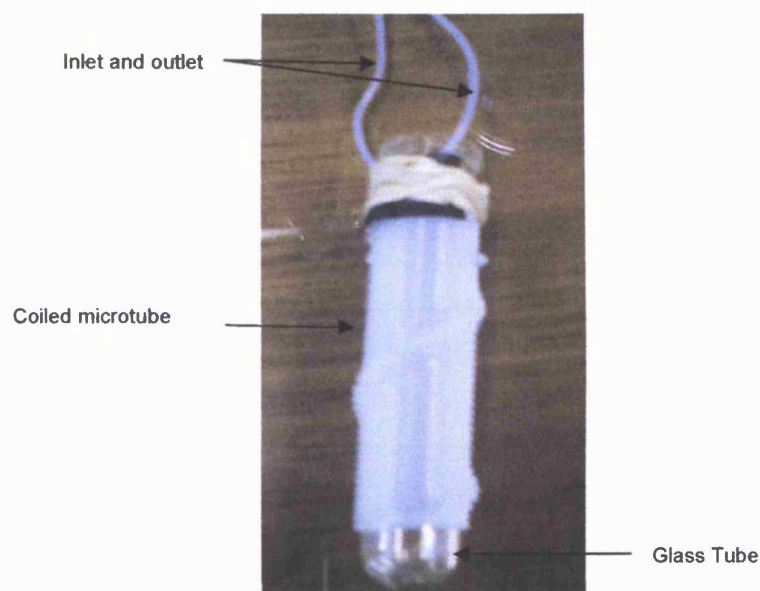

Inlet and outlet

Coiled microtube

Glass Tube

Figure 4.9. Coiled PTFE microflow on a standard test tube.

Reagent delivery

One of the most simple but crucial element of the use of microflow systems is the introduction of reagents into the microchannel, therefore the method of interfacing between the reagent reservoirs and microflow system represents a key challenge in the microsystem setup. We chose to deliver our reagents into the system *via* hydrodynamic pumping, which represents the most economical way, by using *KD Scientific* syringe pumps (models 100, 101, 200 and 250). This particular brand of syringe pumps has good accuracy of pulsed flow delivery, and it is simple to use. In addition, it can be either controlled manually or *via* automated system with use of software such as

104

Labview. The only few major drawback of syringe pumps is the limited volume (large scale up), unsuitable for high pressure systems and not allowing temperature control or stirring of the stock reagent. The theory behind regulating the delivery of reagents is quite straightforward (Equation 4.1a). The total flow rate f (ml·min^{-1}) in a microchannel system is expressed by the ratio between the section volume V (given by the channel cross section times the channel length) and the residence time t. The total flow rate can be also expressed as the sum of the flow rates (Equation 4.1b) of each reagent which in turn can be derived from their number of moles and concentration (Equation 4.1c) so that the total flow rate is easily expressed in function of individual reaction parameters we have full control of.

$$f = \frac{V}{t} \qquad \text{(Eq. 4.1a)}$$

$$f = (f_1 + f_2 + \ldots + f_n) \qquad \text{(Eq. 4.1b)}$$

$$f = \frac{(V_1 + V_2 + \ldots + V_n)}{t} = \frac{(n_1/c_1 + n_2/c_2 + \ldots + n_n/c_n)}{t} \qquad \text{(Eq. 4.1c)}$$

4.2. General experimental information

All commercially available substances were purchased from *Sigma-Aldrich*, *Merck*, *Lancaster*, *Strem* or *Acros organics*, and used without further purification, while anhydrous solvents were freshly distilled prior to use. Air sensitive reactions were prepared/carried out under an inert atmosphere of argon in oven-dried apparatus. Conventional heating was carried out using silicon oil bath placed on top of an *IKA*

hotplate, equipped with a temperature controller. Non-conventional heating was performed by microwave irradiation using *Discovery CEM* system at a frequency of 2450 MHz (0–300 W). Sonication was conducted using *Clifton Ultrasonic Bath* at frequencies between 30 and 40 kHz (80 W). Reaction monitoring was carried out by thin layer chromatography (TLC) using *Merck Kieselgel* silica gel 60 GF254 layers. Purification was carried out mainly using flash column chromatography or preparative thick layer chromatography using *Merck Kieselgel* 60 silica (230–400 mesh). Other methods included *Büchi* Medium-Performance Liquid Chromatography (MPLC) using Model 681 chromatography pump and *Büchi* UV/Vis filter photometer with an automated fraction collector. General operations of solvents evaporation were carried out at reduced pressure using *Büchi* rotary evaporator and diaphragm pumps. For thorough removal of solvent traces a high vacuum apparatus connected to a rotary oil pump was used. NMR spectroscopic analyses were carried out using Bruker 500 MHz, 400 MHz, or 250 MHz for ^{1}H NMR spectroscopy and Bruker 125 MHz, 100 MHz or 63 MHz for ^{13}C NMR spectroscopy. NMR spectra were recorded using 5 mm glass tubes and chloroform-*d* (CDCl$_3$) as deuterated solvent unless otherwise stated. All NMR measurements were carried out at 25 °C and the chemical shifts were reported in δ ppm values while the coupling constants were reported in Hz. The abbreviations are used to indicate the multiplicities are: s (singlet); d (doublet); t (triplet); q (quartet); m (multiplet); br (broad signal). The spectroscopic analysis of known compounds is in accord with the data reported in the literature. Analysis with Mass Spectroscopy was carried out using *Waters LCT Premier* XE-TOF (available detection methods EI, CI, ES, APCI). In all cases the mass fragments were reported in atomic mass units per elementary charge (m/z). High-resolution mass spectrometry was carried out at either Cardiff University or EPSRC NMSSC Swansea facilities. IR Spectroscopy was carried

out using *Perkin Elmer 1600* spectrometer (frequency values in cm^{-1}) in which samples were measured either neat or in CDCl$_3$ solution. Melting points were determined using electrothermal melting apparatus in open capillary tubes. The hydrolysis reaction transformation was monitored and analysed quantitatively using *Jasco* UV (V-570).

4.3. Microflow reactions general considerations

In a typical microflow experiment, the following steps are carried out:

(1) Preparation of stock solutions was carried out considering first the number of solutions to be used in the experiment, in order to deliver them individually into the microchannel using separate syringe pumps; however, when the number of reagents exceeded the number of pumps, one needed to consider carrying pre-mixing of reagents, provided they would not react before entering the system. The appropriate molar concentrations of reagents and catalysts were chosen accordingly to the stoichiometric ratio of the reaction and to the specific reagents solubilities, trying to compromise the practical advantage of preparing solutions of the same molarity with the requirement of having complete dissolution of substrates. When it was required to vary the loading of catalysts, either the concentration of catalyst in the stock solution will be increased accordingly by keeping the flow rate constant, or the catalyst-to-substrate flow rate ratio will be increased as necessary.

(2) Flow rates for each reagent are calculated according to the formula *flow rate = system volume / residence time* (Equations 4.1a-c), on a fixed volume (depending on spatial requirements and limitations), and with a pre-planned convenient residence time.

(3) Calculated flow rate values were then entered into the pumps settings to carry out the reaction. In the case where reaction optimisation is carried out, a set of residence

times are tested with a series of trial-and-error reaction runs, while monitoring using TLC, in order to determine the best conditions.

(4) The required collection time, *i.e.* the time needed to collect enough volume of product mixture to carry out an analysis, is then calculated according to the formula

total flow rate = required volume / collection time.

It is important to bear in mind that, when transforming the laminar flow into segmented by addition of a segmenter phase S to the two existing phases A and B, the collection time needs to be doubled compared to the simple case of case of the absence of segmenter. The total flow rate, in fact, will add the contribution of phase S (according to Equation 4.1b) in the segmented experiment. In order to carry out an accurate comparison of laminar *vs.* segmented, it is necessary to keep the same value of total flow rate in the two cases, as shown in the example below.

Experiment	Flow rate A	Flow rate B	Flow rate S	Total flow rate	Collection time	Collected volume
laminar	1 ml/min	1 ml/min	-	2 ml/min	1 min	2 ml of A+B
segmented	0.5 ml/min	0.5 ml/min	1 ml/min	2ml/min	2 min	2 ml of A+B plus 2 ml of S

The volume collected in the segmented experiment will be 50% composed of the segmenter phase S (considered that each A+B segment is equal in length to each S segment), it is therefore necessary to allow double the time of collection compared to the laminar experiment.

4.4. Experimental procedures

General procedure 1a for Biphasic hydrolysis under segmented flow of *p*-nitrophenyl acetate in PMMA microreactor at room temperature: In a typical hydrolysis experiment, the following stock solutions were prepared in individual volumetric flask: (A) 0.05M solution of *p*-nitrophenyl acetate (905.7 mg, 5.0 mmol) in toluene (100 ml); (B) 0.5M solution of sodium hydroxide (2.0 g, 50.0 mmol) in water (100 ml). Both solutions were then delivered into the PMMA microchannel (refer to Figures 4.10) using *KD Scientific* syringe pumps in a continuous segmented flow manner at various residence times (refer to chapter 2) using various flow rates calculated from Eq. 4.1a to 4.1c. The microchannel setup consisted of a PMMA microreactor fitted in a stainless steel housing (length 400 mm, with cross section areas ranging between 15,625 μm^2 and 144,500 μm^2 (refer to chapter 2). The reacted mixture was collected at the end of the channel into a pre-cooled small narrow vial. The collected reaction mixture was finally analysed quantitatively using UV spectrophotometry.
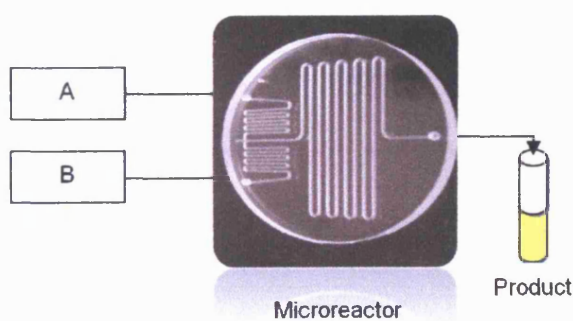

Figure 4.10. Polymer microreactor setup: length 400 mm, square or rectangular cross section shapes, with cross section areas ranging between 15,625 μm^2 and 144,500 μm^2.

General procedure 1b for Biphasic hydrolysis under segmented flow of *p*-nitrophenyl acetate in PTFE coiled microtube: In a typical hydrolysis experiment, the following stock solutions were prepared in individual volumetric flask: (A) 0.05M solution of *p*-nitrophenyl acetate (905.7 mg, 5.0 mmol) in toluene (100 ml); (B) 0.5M solution of sodium hydroxide (2.0 g, 50.0 mmol) in water (100 ml). Both solutions were then delivered into the PTFE microtube (refer to Figures 4.11) using *KD Scientific* syringe pumps in a continuous segmented flow manner at various residence times and temperatures (refer to chapter 2) using various flow rates calculated from Eq. 4.1a to 4.1c. The microchannel setup consisted of a PTFE coiled microtube fitted with upchurch T-Junctions (channel length 400 mm, internal diameter between 300 to 500 μm (refer to chapter 2). The reacted mixture was collected at the end of the channel into a pre-cooled small narrow vial. The collected reaction mixture was finally analysed quantitatively using UV spectrophotometry.
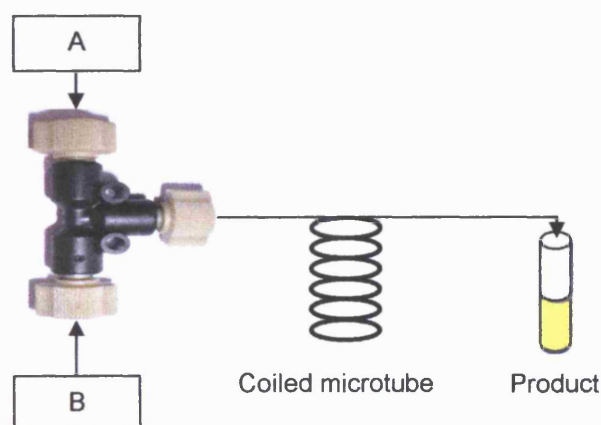

Figure 4.11. Polymer coiled microflow setup: length 400 mm, circular cross section shape, with internal diameters ranging between 500 μm and 300 μm.

General procedure 1c for Biphasic hydrolysis under parallel flow of *p*-nitrophenyl acetate in PMMA microreactor: In a typical hydrolysis experiment, the following stock solutions were prepared in individual volumetric flask: (A) 0.05M solution of *p*-nitrophenyl acetate (905.7 mg, 5.0 mmol) in 1:1 acetonitrile:toluene (100 ml); (B) 0.5M solution of sodium hydroxide (2.0 g, 50.0 mmol) in water (100 ml). Both solutions were then delivered into the PMMA microchannel (refer to Figures 4.10) using *KD Scientific* syringe pumps in a parallel flow manner at various residence times (refer to chapter 2) using various flow rates calculated from Eq. 4.1a to 4.1c. The microchannel setup consisted of a PMMA microreactor fitted in a V-inlet junction with a junction of 90^0 ((length 400 mm, cross section area 300 µm x 300 µm) (refer to chapter 2 and section 4.1). The reacted mixture was collected at the end of the channel into a pre-cooled small narrow vial. The collected reaction mixture was finally analysed quantitatively using UV spectrophotometry.
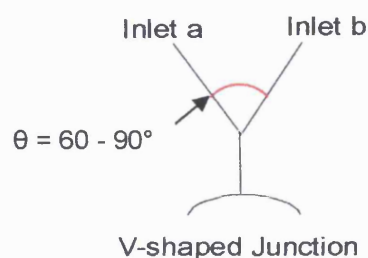
V-shaped inlet design for parallel flow microreactor.

General procedure 1d for Biphasic hydrolysis of *p*-nitrophenyl acetate in flask: In a typical hydrolysis experiment, the following solutions were prepared in individual volumetric flask as follow: (A) 0.05M solution of *p*-nitrophenyl acetate (905.7 mg, 5.0 mmol) in toluene (100 ml) or 1:1 acetonitrile:toluene (100 ml); (B) 0.5M solution of

sodium hydroxide (2.0 g, 50.0 mmol) in water (100 ml). Both solutions were then mixed in a round bottomed flask. The biphasic mixture was then stirred using a magnetic bar at moderated speed at the required temperature (refer to chapter 2). At the end of the reaction the organic layer was separated from the aqueous layer then analysed quantitatively using UV spectrophotometry.

General procedure 2 for Heck coupling under biphasic conditions in conventional flask (Table 4.1 and 4.2): A solution mixture of metal catalyst (0.002 mmol) along with TPPTS ligand (2.3 mg, 0.004 mmol) in ethylene glycol (5.0 ml) was prepared under inert conditions and heated at 60 °C. After 5 minutes of stirring, a solution mixture of iodobenzene (41.0 mg, 0.2 mmol) and alkene (0.2 mmol) in toluene (5.0 ml) was added followed by KOAc (19.6 mg, 0.2 mmol). The biphasic reaction mixture was then heated to the required temperature (70 °C or 140 °C) in oil bath while stirring. After continuing the reaction for an appropriate time, the toluene: ethylene glycol mixture was cooled then separated to extract the toluene crude mixture followed by concentration of the solvent volume under reduced pressure. Finally, the product was isolated by column chromatography on silica gel using an appropriate solvent system.

Table 4.1. Variation of metal catalyst in the flask Heck reaction at low and high temperature to form product (*E*)-methylcinnamate **1** or (*E*)-Stilbene **2**.

Metal Catalyst	Yield [%] 70 °C ^{a}	Yield [%] 140 °C ^{b}
PdCl$_2$	99 (**1**), 91 (**2**)	92 (**1**), 98 (**2**)
Pd(OAc)$_2$	98 (**1**), 99 (**2**)	94 (**1**), 89 (**2**)
Ni(OAc)$_2$	78 (**1**), 82 (**2**)	84 (**1**), 70 (**2**)
RuCl$_3$	62 (**1**), 51 (**2**)	66 (**1**), 71 (**2**)

Reaction conditions: Metal catalyst (1 mol%), TPPTS (2 mol%), iodobenzene (0.2 mmol), alkene (0.2 mmol), KOAc (0.2 mmol), in toluene (5.0 ml):ethylene glycol (10.0 ml). ^{a} Heating at 70 °C, reaction time (9-11 hours). ^{b} Heating at 140 °C, reaction time (4.5-7 hours).

General procedure 3 for Heck coupling under biphasic conditions in microflow (Tables 4.2 and 4.3): Stock solutions were prepared in individual Schlenk tubes under inert atmosphere. In a typical experiment, solutions would be prepared as follow (refer to Figure 4.12): (A) 0.04M solution of iodobenzene (204.0 mg, 1.0 mmol) and alkene (1.0 mmol) in toluene or *o*-xylene (25.0 ml); (B) 0.0005M solution of metal catalyst (PdCl$_2$ 1.8 mg, 0.01 mmol or Pd(OAc)$_2$ 2.2 mg, 0.01 mmol) with TPPTS ligand (11.4 mg, 0.02 mmol) in ethylene glycol (20.0 ml); and (C) 0.2M solution of KOAc (98.2 mg, 1.0 mmol) in ethylene glycol (5.0 ml). Each solution was loaded individually into a gas-tight glass syringe which was then connected onto the microflow system (PTFE) through a designated inlet using a T-inlet connector: length 2000 mm, internal diameter 500 μm, and system volume 392.5 μl. The solutions were then delivered into the microchannel in a continuous segmented flow manner using *KD Scientific* syringe pump

at the required residence times (Table 4.2 to 4.3) using various flow rates (calculated from Eq. 4.1a to 4.1c). The reactions were carried out while heating to the required temperature using either an oil bath or microwave irradiation for the appropriate residence time (Tables 4.2 and 4.3). After collecting the output from the reaction, the toluene: ethylene glycol (or *o*-xylene: ethylene glycol) mixture was separated to extract the toluene (or *o*-xylene) crude mixture followed by concentrating the solvent under reduced pressure. Finally, the product was isolated by column chromatography on silica gel using an appropriate solvent system.
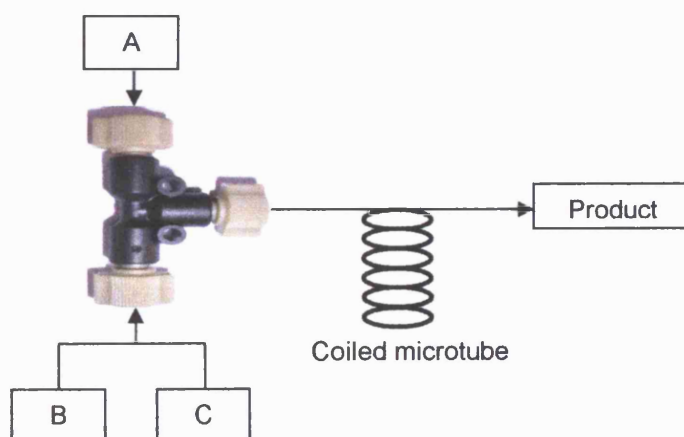
Figure 4.12. Microflow setup for biphasic conditions using coiled PTFE tubing immersed in a heating bath.: length 2000 mm, internal diameter 500 μm, and system volume 392.5 μl.

Table 4.2. Low temperature Heck Coupling: microflow *vs.* flask; and comparison low *vs.* high temperature in microchannel to form product (*E*)-methylcinnamate **1** or (*E*)-Stilbene **2**.

Metal Catalyst	Flask 70 °C ^{a} Yield [%]	PTFE Microflow 70 °C ^{a} Yield [%]	PTFE Microflow 140 °C ^{b} Yield [%]
PdCl$_2$	12 (1), 8 (2)	48 (1), 33 (2)	67 (1), 56 (2)
Pd(OAc)$_2$	10 (1), 11(2)	37 (1), 42 (2)	71 (1), 58 (2)

Reaction conditions: Metal catalyst (1 mol%), TPPTS (2 mol%), iodobenzene (1.0 mmol), alkene (1.0 mmol), KOAc (1.0 mmol), residence time of 55 minutes. ^{a} heating at 70°C in toluene: ethylene glycol (1:1). ^{b} heating at 140 °C in *o*-xylene: ethylene glycol (1:1).

Table 4.3. Microwave heating *vs.* oil bath heating of microflow system to form product (*E*)-methylcinnamate **1** or (*E*)-Stilbene **2**.

Metal Catalyst	Catalyst load [mol%]	Oil Bath Yield [%]	Microwave Yield [%]
PdCl$_2$	1	48 (1), 33 (2)	54 (1), 50 (2)
PdCl$_2$	10	51 (1), 55 (2)	67 (1), 59 (2)
Pd(OAc)$_2$	1	37 (1), 42 (2)	51 (1), 49 (2)
Pd(OAc)$_2$	10	49 (1), 56 (2)	69 (1), 70 (2)

Reaction conditions: Metal catalyst (1 or 10 mol%), TPPTS (2 or 20 mol%), iodobenzene (1.0 mmol), alkene (1.0 mmol), KOAc (1.0 mmol), in toluene: ethylene glycol (1:1), heating at 70°C using either microwave irradiation or oil bath heating, residence time of 55 minutes.

General procedure 4 for Heck coupling under homogeneous conditions in conventional flask (Table 4.4): A solution mixture of metal catalyst (0.02 mmol) and PPh₃ ligand (10.5 mg, 0.04 mmol) in DMF (5.0 ml) was prepared under inert conditions and heated at 60 °C. After 5 minutes of stirring, iodobenzene (41.0 mg, 0.2 mmol) and methyl acrylate (17.2 mg, 0.2 mmol) were added followed by Et₃N (20.2 mg, 0.2 mmol). The reaction mixture was then heated to the required temperature in oil bath while stirring. After continuing the reaction for 35 minutes, the DMF crude mixture was concentrated under reduced pressure. Finally, the product was isolated by column chromatography on silica gel using an appropriate solvent system.

General procedure 5 for monophasic Heck coupling under laminar flow conditions in microflow (Table 4.4 – 4.6 and 4.8): Stock solutions were prepared in individual Schlenk tubes under inert atmosphere. In a typical experiment, solutions would be prepared as follow (Figure 4.13): (A) 0.05M solution of iodobenzene (204.0 mg, 1.0 mmol) and alkene (1.0 mmol) and triethylamine (101.0 mg, 1.0 mmol) in DMF (20.0 ml); and (B) 0.002M solution of metal catalyst (0.01 mmol) with a choice of ligand (0.02 mmol) in DMF (5.0 ml). Each solution was loaded individually into a gas-tight glass syringe which was then connected onto the PTFE microflow system through a designated inlet using a T-connector length 2000 mm, internal diameter 500 μm, and system volume 392.5 μl. The solutions were then delivered into the microchannel in a laminar flow manner using *KD Scientific* syringe pump at the required residence times (refer to Table 4.4 - 4.6 and 4.8) using various flow rates (calculated from Eq. 4.1a to 4.1c). The reactions were carried out while heating to the required temperature using an oil bath for the appropriate residence time (Table 4.4 - 4.6 and 4.8). After collecting the output from the reaction, the DMF crude mixture was concentrated under reduced

pressure and all products were isolated by column chromatography on silica gel using an appropriate solvent system.

Table 4.4. Monophasic Heck coupling: flask *vs.* laminar flow.

Metal Catalyst	Flask Yield of 1 [%]	PTFE microflow Yield of 1 [%]
Pd(OAc)₂	26	53
RuCl₃	12	45
Ni(OAc)₂	20	34
Pt(COD)Cl₂	8	21
CoCl₂	17	28

Reaction conditions: In microflow system –metal catalyst (10 mol%), PPh₃ (20 mol%), iodobenzene (1.0 mmol), methyl acrylate (1.0 mmol), Et₃N (1.0 mmol), in DMF, heating at 70°C in an oil bath, residence time of 35 minutes under laminar flow. *Reaction conditions*: In flask – metal catalyst (10 mol%), PPh₃ (20 mol%), iodobenzene (0.2 mmol), methyl acrylate (0.2 mmol), Et₃N (0.2 mmol), in DMF, heating at 70°C in an oil bath, reaction time of 35 minutes.

Table 4.5. Variation of catalyst load in microchannel to form product (*E*)-methylcinnamate **1**.

Metal Catalyst	Catalyst load [mol %]	Yield of 1[%]
PdCl₂	1	19
PdCl₂	5	33
PdCl₂	10	47
Pd(OAc)₂	1	21
Pd(OAc)₂	5	22
Pd(OAc)₂	10	53

Reaction conditions: Metal catalyst: ligand (1:2), iodobenzene (1.0 mmol), methylacrylate (1.0 mmol), Et₃N (1.0 mmol), in DMF, heating at 70°C in an oil bath, residence time of 35 minutes under laminar flow conditions.

Figure 4.13. PTFE microtubing reaction set-up for laminar flow conditions: length 2000 mm, internal diameter 500 μm, and system volume 392.5 μl.

118

Table 4.6. Variation of ligand type in the microchannel Heck reaction to form product (*E*)-methylcinnamate **1**.

Metal Catalyst	Added Ligand	Degree of clogging	Yield of **1**[%]
Pd(OAc)₂	PPh₃	low	53
Pd(OAc)₂	*rac*-BINAP	low	39
Pd(OAc)₂	*N,N'*-bis-mesityl-imidazolium chloride	high	-
Pd(OAc)₂	*N,N*-dimethyl-*β*-alanine	high	-
Pd(PPh₃)₄	-	very low	62

Reaction conditions: Metal catalyst (10 mol%), ligand (20 mol%), iodobenzene (1.0 mmol), methyl acrylate (1.0 mmol), Et₃N (1.0 mmol), in DMF, heating at 70°C in an oil bath, residence time of 35 minutes under laminar flow conditions.

General procedure 6 for Heck coupling under Jeffery's conditions in conventional flask (Table 4.7): A mixture of K₂CO₃ (27.6 mg, 0.2 mmol) and Et₄NCl (33.0 mg, 0.2 mmol) in a mixture of DMF (4.0 ml):ethylene glycol (1.0 ml) was prepared and left to stir for 15 minutes. This was followed by addition of iodobenzene (41.0 mg, 0.2 mmol), methyl acrylate (17.2 mg, 0.2 mmol) and Pd(OAc)₂ (1 or 5 or 10 mol%: respectively 0.5 or 2.5 or 5.0 mg). The mixture was stirred while heating at 70 °C for 50 minutes. Following an aqueous wash the organic material was extracted with diethyl ether which was then evaporated under reduced pressure. Finally, the product was isolated by column chromatography on silica gel using an appropriate solvent system.

General procedure 7 for Heck coupling under Jeffery's laminar flow conditions in microflow (Table 4.7): Stock solutions were prepared in individual Schlenk tubes under inert atmosphere. In a typical experiment, solutions would be prepared as follow (refer to Figure 4.13): (A) 0.1M solution of iodobenzene (204.0 mg, 1.0 mmol) with methyl acrylate (86.1 mg, 1.0 mmol) in DMF (10.0 ml); and (B) 0.0006M solution of $Pd(OAc)_2$ (2.3 mg, 0.01 mmol), K_2CO_3 (98.2 mg, 1.0 mmol) and Et_4NCl (165.7 mg, 1.0 mmol) in DMF (10.0 ml):ethylene glycol (5.0 ml). Each solution was loaded individually into a gas-tight glass syringe which was then connected onto the microflow system (PTFE) through a designated inlet using a T-connector (Figure 4.13): length 2000 mm, internal diameter 500 μm, and system volume 392.5 μl. The solutions were then delivered into the microchannel using *KD Scientific* syringe pump at the required residence times (refer to Table 4.7) using various flow rates (calculated from Eq. 4.1a to 4.1c).The reactions were carried out while heating to the required temperature using an oil bath for the appropriate residence time (Table 4.7). After collecting the output from the reaction, the crude mixture was washed with water. The aqueous layer was extracted with diethyl ether, and then the combined organic extracts were concentrated under reduced pressure. Finally, the product was isolated by column chromatography on silica gel using an appropriate solvent system.

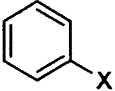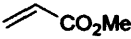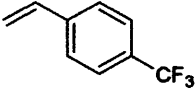**Table 4.7.** Heck coupling of iodobenzene using Jeffery's conditions to form product (E)-
methylcinnamate 1.

Metal Catalyst	Catalyst load [mol%]	Flask Yield of 1[%]	PTFE Microflow[a] Yield of 1[%]	Degree of clogging
Pd(OAc)₂	1	22	34	low
Pd(OAc)₂	5	29	52	low
Pd(OAc)₂	10	36	-	high

Reaction conditions – in microflow system: Pd(OAc)₂ (1, 5 or 10 mol%), Et₄NCl (1.0 mmol), iodobenzene (1.0 mmol), methyl acrylate (1.0 mmol), K₂CO₃ (1.0 mmol), in DMF: ethylene glycol (4:1), heating at 70°C in an oil bath, residence time of 50 minutes under laminar flow. *Reaction conditions* – in flask: Pd(OAc)₂ (X mol%), Et₄NCl (0.2 mmol), iodobenzene (0.2 mmol), methyl acrylate (0.2 mmol), K₂CO₃ (0.2 mmol), in DMF: ethylene glycol (4:1), heating at 70°C in an oil bath, residence time of 50 minutes.

General procedure 8 for monophasic Heck coupling under segmented flow conditions in microflow (Table 4.8 and 4.9): Stock solutions were prepared in individual Schlenk tubes under inert atmosphere. In a typical experiment, solutions would be prepared as follow (refer to Figure 4.14): (A) 0.2M solution of aryl halide (1.0 mmol) and alkene (1.0 mmol) and triethylamine (101.0 mg, 1.0 mmol) in DMF (5.0 ml); (B) 0.003M solution of Pd(PPh₃)₄ (57.8 mg, 0.05 mmol) in DMF (20.0 ml); and (C) pure hydrocarbon solvent (hexane, heptane, nonane or decane) used as a segmenting phase. Each solution was loaded individually into a gas-tight glass syringe which was then connected onto the microflow system (PTFE) through a designated inlet using a T-connector: length 2000 mm, internal diameter 500 μm, and system volume 392.5 μl.

The solutions were then delivered into the microchannel using *KD Scientific* syringe pump at the required residence times (refer to Table 4.8 and 4.9) using various flow rates (calculated from Eq. 4.1a to 4.1c).The reactions were carried out while heating to the required temperature using an oil bath for the appropriate residence time (Table 4.8 and 4.9). After collecting the output from the reaction, the volume of the DMF crude mixture in addition to the segmenter phase were concentrated under reduced pressure and finally the product was isolated by preparative TLC and column chromatography on silica gel using an appropriate solvent system.
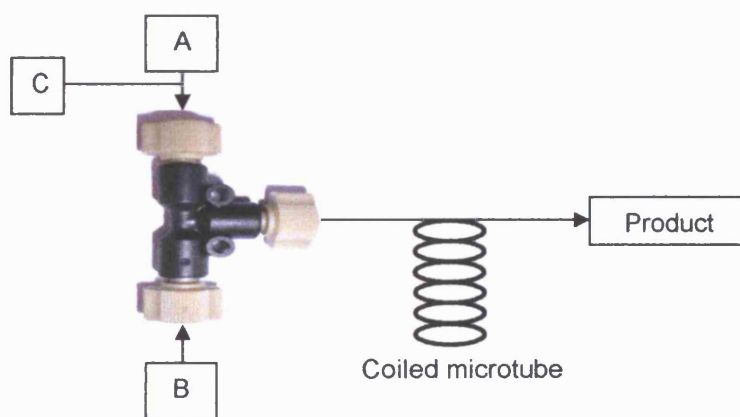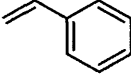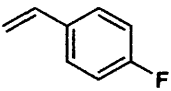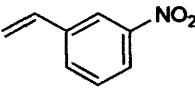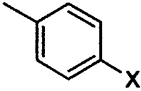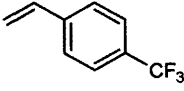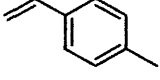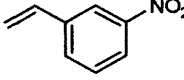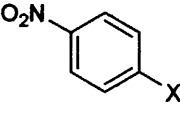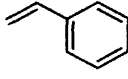

Figure 4.14. Reaction under laminar flow transformed into segmented flow by the introduction of an inert phase: system length 2000 mm, internal diameter 500 μm, system volume 392.5 μl.

Table 4.8. Laminar vs. segmented flow applied to Heck reaction of iodobenzene to form product (E)-methylcinnamate 1 or (E)-Stilbene 2.

Alkene	Res. Time approx. (min)	Catalyst load [mol%]	Laminar flow Yield [%]	Segmented flow Yield [%]
methyl acrylate	35	5	36 (1)	65 (1)
methyl acrylate	35	10	53 (1)	76 (1)
styrene	45	5	38 (2)	57 (2)
styrene	45	10	43 (2)	59 (2)

Reaction conditions: Pd(PPh₃)₄ (5 or 10 mol%), iodobenzene (1.0 mmol), alkene (1.0 mmol), Et₃N (1.0 mmol), in DMF, heating at 70 °C in an oil bath.
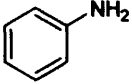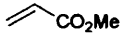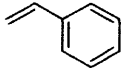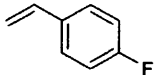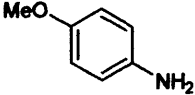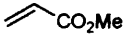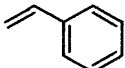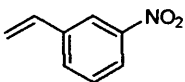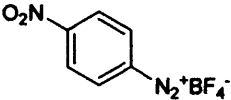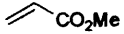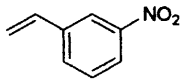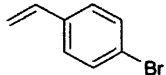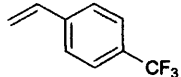
Table 4.9. Heck coupling of aryl halides to give only *trans* isomer.

Substrates	Alkene	Yield [%]	Product (trans)
X = I /Br		[I /Br]	

Substrates	Alkene	Yield [%]	Product (trans)
X = I ^{a} /Br ^{b}	$\diagup\diagup$CO$_2$Me	68/51	**1**
	(vinyl-C$_6$H$_4$-CF$_3$)	63/38	**3**
	(styrene)	57/25	**2**
	(vinyl-C$_6$H$_4$-F)	60/22	**4**
	(vinyl-C$_6$H$_4$-NO$_2$, meta)	35/21	**5**
X = I ^{a} /Br ^{b}	(vinyl-C$_6$H$_4$-CF$_3$)	49/32	**6**
	(vinyl-C$_6$H$_4$-CH$_3$)	47/29	**7**
	(vinyl-C$_6$H$_4$-NO$_2$, meta)	44/19	**8**
X = Br ^{b}	(styrene)	65	**9**

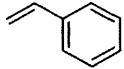*Reaction conditions*: Pd(PPh$_3$)$_4$ (10 mol%), aryl halide (1.0 mmol), alkene (1.0 mmol), Et$_3$N (1.0 mmol), in DMF, residence time of 40 minutes. ^{a} ArI coupling heating at 70 °C. ^{b} ArBr coupling heating at 130 °C.

General procedure 9 for Heck coupling *via* diazonium salt under homogeneous segmented flow conditions in microflow (Table 4.10): Stock solutions were prepared in individual Schlenk tubes under inert atmosphere. In a typical experiment, solutions would be prepared as follow: (A) 0.1M solution of aniline (93.2 mg, 1.0 mmol) in DMF (10.0 ml); (B) 0.005M solution of Pd(OAc)$_2$ (22.4 mg, 0.1 mmol) in DMF (20.0 ml); (C) 0.2M solution of olefin (1.0 mmol) in DMF (5.0 ml); (D) 0.8M solution of *t*-BuONO (4.0 mmol) and AcOH (1.25 ml) in DMF (5.0 ml); and (E) pure hydrocarbon solvent (hexane, heptane, nonane or decane) used as a segmenting phase. Each solution was loaded individually into a gas-tight glass syringe which was then connected onto the microflow system (PTFE) through a designated inlet using a T-connector (Figure 4.15): length 2920 mm (*section 1* 150 mm, residence time of 3.2 minutes) + (*section 2* - 2770 mm, residence time of 23.7 minutes), internal diameter 500 µm, and system volume 573 µl. The solutions were then delivered into the microchannel using *KD Scientific* syringe pump at the required residence times (refer to Table 4.10) using various flow rates (calculated from Eq. 4.1a to 4.1c). First the diazotisation of aniline was carried out in *section 1* at 0 °C by pumping solutions (A) along with solution (D) and (E), while in *section 2* solutions (B) and (C) were introduced then mixed with the diazotised flow from *section 1* at ambient temperature to carry out the Heck coupling. The reactions were carried out for the appropriate total residence time of approximately 27 minutes. After collecting the output of the reaction, the crude mixture was first washed with water followed by 5% aqueous bicarbonate solution. After drying the mixture with sodium sulphate the solvent was concentrated under reduced pressure. Finally, the product was isolated by preparative TLC and column chromatography on silica gel using an appropriate solvent system.

Table 4.10. Diazonium Heck coupling of aniline derivatives.

Substrates	Alkene	Yield [%]	Product (trans)
NH₂ (aniline)	CO₂Me	54	1
	styrene	66	2
	4-F-styrene	72	4
MeO–C₆H₄–NH₂	CO₂Me	27	10
	styrene	33	11
	NO₂-styrene	18	12
O₂N–C₆H₄–N₂⁺BF₄⁻	CO₂Me	64	13
	styrene	42	9
	NO₂-styrene	57	14
	Br-styrene	49	15
	CF₃-styrene	61	16

Reaction conditions (in microflow system): Pd(OAc)₂ (10 mol%), aryl halide (1.0 mmol), olefin (1.0 mmol), *t*-BuONO (4.0 mmol), AcOH (1.25 ml) in DMF, 0 °C to 25 °C, residence time of 27 minutes.
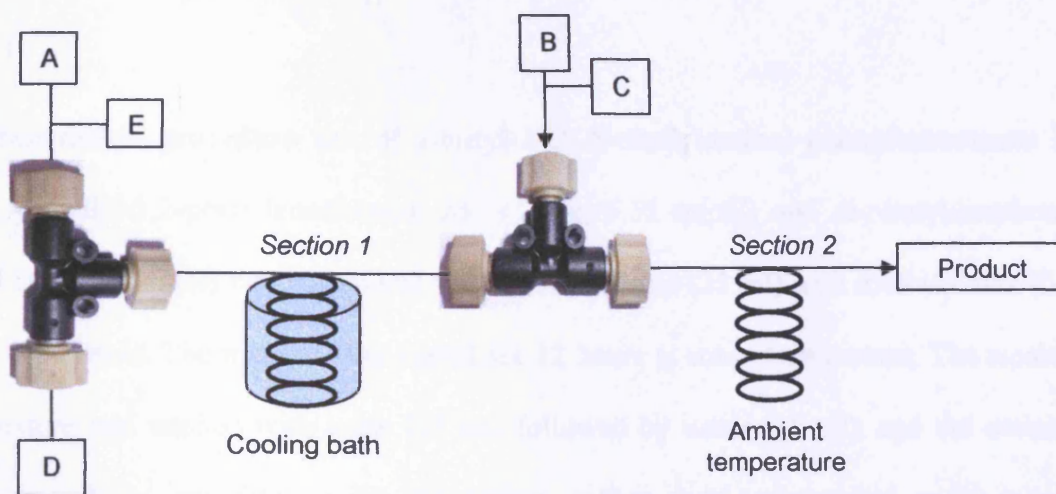
Figure 4.15. Reaction flow setup for Heck reaction *via* diazonium intermediate in the microflow consists of *section 1* used for diazotisation cooled to 0 °C and *section 2* used for Heck coupling carried out at room temperature; total length 2920 mm internal diameter 500 μm, and total system volume 573 μl.

General procedure 10 for Allylation of arylamines to produce *N,N*-diallyl-1,2-phenylenediamine 23, *N,N*-diallyl-2-iodobenzenamine 29, or *N,N'*-diallylaniline 34 in a conventional flask: To a solution of arylamine (1,2-phenylenediamine, 1.0 g, 9.2 mmol; *o*-iodoaniline, 1.0 g, 4.0 mmol; *or* aniline, 1.0 g, 10.7 mmol), allyl bromide (2.2 equivalents to the aniline) was added drop wise in dry DMF (10 – 15 ml) at 0 °C. The mixture was warmed to 60 °C and left to stir for 48 hours. The crude mixture was then treated with an aqueous solution of NaOH (10ml, 6.0M) then left to stir. After approx. 1 hour of stirring, the reaction mixture was extracted once with ethyl acetate (10ml) then dried over magnesium sulfate. The crude product was purified using medium pressure liquid chromatography (MPLC) to give the desired product, either *N,N*-diallyl-1,2-phenylenediamine **23** (0.9 g, 55% yield) as pale yellow oil, *N,N*-diallyl-2-iodobenzenamine **29** (0.93 g, 77% yield) as brown oil, or *N,N*-diallylaniline **34** (1.6 g, 89 %) as a colourless oil.

Preparation procedure for of *t*-butyl-2-(*N*,*N*-diallylamino)-phenylcarbamate 25:

N,*N*-Diallyl-1,2-phenylenediamine **23** (1.0 g, 5.32 mmol) and di-*t*-butyldicarbonate (1.39 g, 6.4 mmol) were dissolved in dichloromethane (25 ml) with triethylamine (0.80 g, 7.9 mmol). The mixture was stirred for 12 hours at room temperature. The resulting mixture was washed with brine (25 ml) followed by water (25 ml), and the extracted organic layer was dried using magnesium sulfate then concentrated under reduced pressure. The resulting crude mixture was purified using silica gel column chromatography (5% diethyl ether in hexane) to obtain a colourless oil.

General procedure 11 for ring closing metathesis (RCM) under segmented flow conditions in microflow (Table 4.11): Stock solutions were prepared in individual Schlenk tubes under inert atmosphere. In a typical experiment, solutions would be prepared as follows (refer to Figure 4.14): (A) 0.1M solution of *t*-butyl-2-(diallylamino)phenylcarbamate **24** (115.2 mg, 0.4 mmol) in toluene (4.0 ml): (B) 0.1M a solution of either Grubbs' catalyst I (16.5 mg, 0.02 mmol) or Grubbs' catalyst II (17.0 mg, 0.02 mmol) in toluene (0.2 ml); (C) pure perfluorocarbon solvent (perfluorodecalin or perfluorononane) used as a segmenting phase (5 ml). Each solution was loaded individually into a gas-tight glass syringe which was then connected onto the microflow system (PTFE) through a designated inlet using a T-connector: length 2000 mm, internal diameter 500 μm, and system volume 392.5 μl. The solutions were then delivered into the microchannel using *KD Scientific* syringe pump at the required residence times (refer to Table 4.11) using various flow rates (calculated from Eq. 4.1a to 4.1c). The reactions were carried out while heating to 40 °C using an oil bath or *CEM* microwave (150 W) for the appropriate residence time of 10 minutes (Table 4.11). After

collecting the output from the reaction, the cooled crude mixture was separated from the perfluorocarbon then evaporated under reduced pressure. The desired product 26 and 27 were then isolated by column chromatography on silica gel using an appropriate solvent system.

Table 4.11. Optimisation of RCM of *t*-butyl-2-(diallylamino)phenylcarbamate 25 in PTFE microflow .

Catalyst	Catalyst load [mol%]	Heating method	Yield of 26[%]	Yield of 27[%]
Grubbs I	1	Oil bath	31	23
Grubbs I	5	Oil bath	63	32
Grubbs I	5	Microwave	73	21
Grubbs II	1	Oil bath	48	19
Grubbs II	5	Oil bath	87	16
Grubbs II	5	Microwave	91	4

Reaction conditions:Grubbs I or II catalyst (1 or 5 mol%), *t*-butyl-2-(diallylamino)phenylcarbamate 25 (0.4 mmol), in toluene (4.2 ml) heating at 40 °C using either microwave irradiation (150 W) or oil bath heating under segmented flow conditions using perfluorocarbon, at residence time approx. 10 minutes.

General procedure 12 for multi-step synthesis *via* ring closing metathesis (RCM) followed by Heck coupling under segmented flow conditions in microflow: Stock solutions were prepared in individual Schlenk tubes under inert atmosphere. In a typical experiment, solutions would be prepared as follows: (A) 0.1M solution of diallylamino derivative (either 29 - 199.6 mg, 0.4 mmol; or 34 - 69.2 mg, 0.4 mmol) in toluene (4.0

129

ml): (B) 0.1M a solution of Grubbs' catalyst II (16.9 mg, 0.02 mmol) in toluene (0.2

ml); (C) either pure perfluorononane or perfluorodecalin solvent used as the segmenting

phase; (D) 0.004M solution of $Pd(PPh_3)_4$ (46.2 mg, 0.04 mmol) in toluene (10.0 ml); (E)

0.4M alkene or aryl halide (0.4 mmol), and triethylamine (40.4 mg, 0.4 mmol) in toluene

(1.0 ml). Each solution was loaded individually into a gas-tight glass syringe which was

then connected onto the multistep microflow system (PTFE) through a designated inlet

using a number of T-connectors (Figure 4.16): length 43700 mm (*section 1* 2000 mm,

residence time of 10.0 minutes) + (*section 2* − 41700 mm, residence time of 60

minutes), internal diameter 500 μm, and system volume 8576 μl. The solutions were

then delivered into the microchannel using *KD Scientific* syringe pump at the required

residence times using various flow rates (calculated from Eq. 4.1a to 4.1c). First the

RCM of diallylamino moiety was carried out at 40 °C by pumping solutions (A) along

with solution (B) and (C) into the *section 1* (Figure 4.16) placed in the *CEM* microwave

cavity. While in *section 2* solutions (D) and (E) were introduced then mixed with the

cyclised substrate flow from *section 1* at 80 °C using an oil bath to carry out the Heck

coupling. The reactions were carried out for the appropriate total residence time of

approximately 70 minutes. After collecting the output from the reaction, the cooled

toluene crude mixture was separated manually from the segmented phase evaporated

under reduced pressure. The purification was carried out using column chromatography
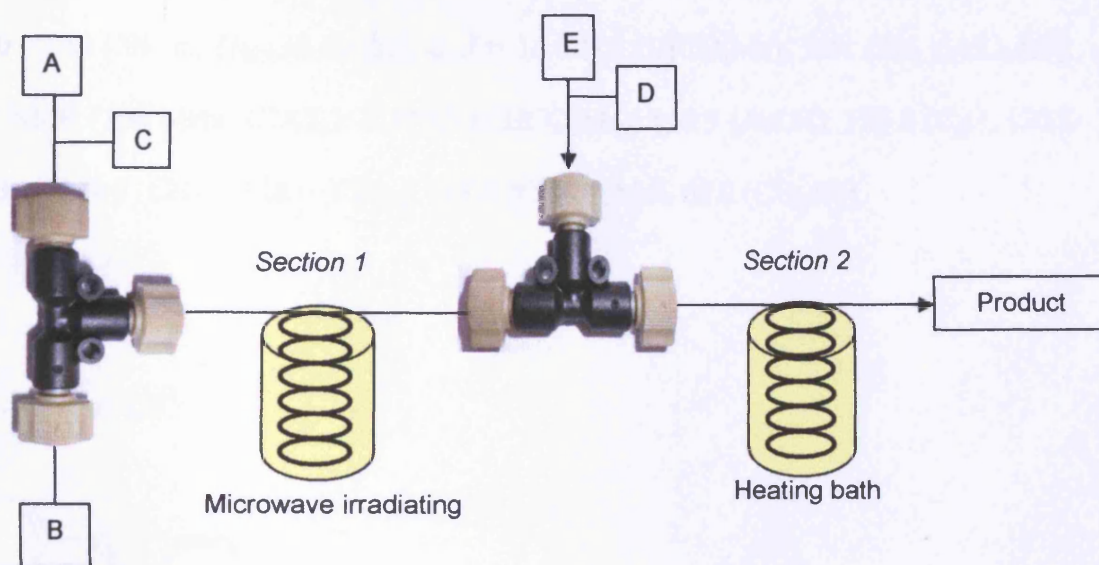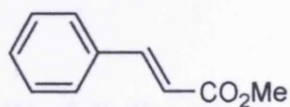
using an appropriate solvent system.

Figure 4.16. Two-step microreactor set up for RCM followed by Heck coupling under segmented flow conditions.
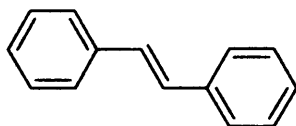
4.5. Experimental analysis

(E)-Methyl cinnamate (1)[4]

Synthesis carried out according to General Procedure 2 to 9 obtained in range of 10% to 99% yield as oil after purification by column chromatography on silica gel using 2% of diethyl ether in hexane.

^{1}H NMR (500 MHz, CDCl$_3$): δ 7.74 (1H, d, J = 16.0 Hz, ArCH), 7.57 (2H, m, H_{Ar}), 7.40 –7.49 (3H, m, H_{Ar}), 6.49 (1H, d, J = 16.0 Hz, CHCO$_2$Me), 3.84 (3H, s, CO$_2$$Me$); ^{13}C NMR (100 MHz, CDCl$_3$): δ 173.5 (CHCO$_2$Me), 144.5 (ArCH), 134.5 (C_{Ar}), 130.5 (CH_{Ar}), 129.0 (CH_{Ar}), 128.0 (CH_{Ar}), 117.5 (CHCO$_2$Me), 52.0 (CO$_2$$Me$).

(E)-Stilbene (2)[5]

Synthesis carried out according to General Procedure 2, 3, 5, 8 and 9 obtained in range of 8% to 99% yield as solid after purification by column chromatography on silica gel using hexane. Mp 122–125 °C (lit. mp 124–127°C); ^{1}H NMR (500 MHz, CDCl$_3$): δ 7.57 (4H, d, J = 7.4 Hz, H_{Ar}), 7.39 (4H, m, H_{Ar}), 7.29 (2H, t, J = 7.3 Hz, H_{Ar}), 7.19 (2H, s, ArCH); ^{13}C NMR (100 MHz, CDCl$_3$): δ 137.5 (C_{Ar}), 129.1 (CH_{Ar}), 128.9 (ArCH), 127.6 (CH_{Ar}), 126.5 (CH_{Ar}).
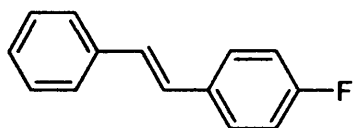
(E)-(4-Trifluoromethyl)-stilbene (3)[6]
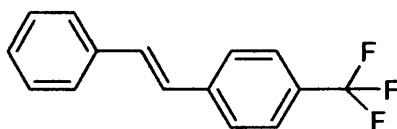
Synthesis carried out according to General Procedure 8 obtained in 38% to 63% yield as a solid after purification by column chromatography on silica gel using 10% diethyl ether in hexane. Mp 127-129 °C (lit. mp 132-134 °C); ^{1}H NMR (500 MHz, CDCl$_3$): δ

7.55 (4H, s, H_{Ar}), 7.49 (2H, d, J = 7.4 Hz, H_{Ar}), 7.32 (2H, t, J = 7.5 Hz , H_{Ar}), 7.23 (1H,

t, J = 7.2 Hz, H_{Ar}), 7.12 (1H, d, J = 16.0 Hz, ArCH), 7.06 (1H, d, J = 16.8 Hz, ArCH);

^{13}C NMR (100 MHz, CDCl$_3$): δ 141.0 (C_{Ar}), 139.5 (C_{Ar}), 136.5 (C_{Ar}), 131.2 (CH_{Ar}),

129.4 (CH_{Ar}), 129.1 (CH_{Ar}), 127.1 (CH_{Ar}), 126.8 (ArCH), 126.6 (ArCH), 125.7 (CH_{Ar}),

123.1 (ArCF$_3$).

(E)-(4-Fluoro)-stilbene (4)[7]

Synthesis carried out according to General Procedure 8 and 9 obtained in 22% to 72%

yield as solid after purification by column chromatography on silica gel using 10%

diethyl ether in hexane. Mp 118-120 °C (lit. mp 122 °C); ^{1}H NMR (500 MHz, CDCl$_3$):
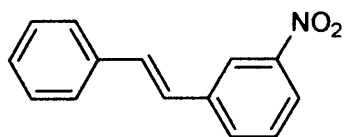
δ 7.45-7.52 (4H, m, H_{Ar}), 7.29 (2H, m, H_{Ar}), 7.25 (1H, t, J = 7.0 Hz, H_{Ar}), 7.04-6.97

(3H, m, H_{Ar} and ArCH), 6.89 (1H, d, J = 16.0 Hz, ArCH); ^{13}C NMR (100 MHz,

CDCl$_3$):δ 163.5 (CF), 137.1 (C_{Ar}), 137.2 (C_{Ar}), 128.7 (CH_{Ar}), 128.5 (CH_{Ar}), 128.0

(CH_{Ar}), 127.9 (ArCH), 127.7 (ArCH), 127.3 (CH_{Ar}), 126.5 (CH_{Ar}), 115.6 and 115.4

(CH_{Ar}).

(E)-(3-Nitro)-stilbene (5) [8]

Synthesis carried out according to General Procedure 8 obtained in 21% to 35% yield as solid after purification by column chromatography on silica gel using 15% diethyl ether in hexane. Mp 98–101 °C (lit. mp 105–106 °C); ^{1}H NMR (500 MHz, CDCl$_3$): δ 8.30 (1H, s, H_{Ar}), 8.00 (1H, d, J = 7.3 Hz, H_{Ar}), 7.72 (1H, d, J = 7.9 Hz, H_{Ar}), 7.50-7.40 (3H, m, H_{Ar}), 7.35 (2H, m, H_{Ar}), 7.29 (1H, m, Hz, H_{Ar}), 7.26 (1H, d, J = 16.1 Hz, Ar*CH*), 7.15 (1H, d, J = 16.3 Hz, Ar*CH*); ^{13}C NMR (100 MHz, CDCl$_3$): δ 148.7 (*C*NO$_2$), 139.2 (*C*$_{Ar}$), 136.3 (*C*$_{Ar}$), 132.2 (*C*H$_{Ar}$), 131.8 (*C*H$_{Ar}$), 129.6 (*C*H$_{Ar}$), 128.9 (*C*H$_{Ar}$), 128.5 (*C*H$_{Ar}$), 126.9 (Ar*C*H), 126.1 (Ar*C*H), 122.1 (*C*H$_{Ar}$), 120.9 (*C*H$_{Ar}$).
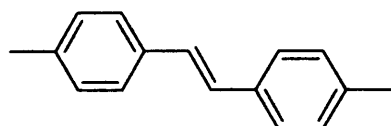
(E)-4-methyl-(4′-trifluoromethyl)stilbene (6) [6]
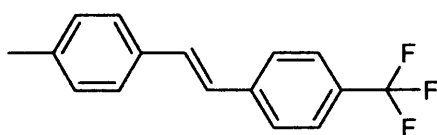
Synthesis carried out according to General Procedure 8 obtained in 32% to 49% yield as solid after purification by column chromatography on silica gel using 10% diethyl ether in hexane. Mp 182–184 °C (lit. mp 187–189 °C); ^{1}H NMR (500 MHz, CDCl$_3$): δ 7.49-7.59 (4H, s, H_{Ar}), 7.38 (2H, d, J = 8.0 Hz, H_{Ar}), 7.11 (2H, d, J = 7.5 Hz, H_{Ar}), 7.09 (1H, d, J = 16.5 Hz, Ar*CH*), 7.01 (1H, d, J = 16.3 Hz, Ar*CH*), 2.3 (3H, s, Ar*Me*); ^{13}C NMR

(100 MHz, CDCl$_3$): δ 140.9 (C_{Ar}), 138.3 (C_{Ar}), 133.8 (C_{Ar}), 131.1 (CCF$_3$), 129.5 (CH_{Ar}),

126.7 (ArCH), 126.4 (ArCH), 126.1 (CH_{Ar}), 125.6 (CH_{Ar}), 125.5 (CH_{Ar}), 121.0 (CF$_3$),

21.3 (Me).

(*E*)-(4,4'-Dimethyl)-stilbene (7)[6]

Synthesis carried out according to General Procedure 8 obtained in 29% to 47% yield as

solid after purification by column chromatography on silica gel using hexane. Mp

179–180 °C (lit. mp 180 °C); ^{1}H NMR (500 MHz, CDCl$_3$): δ 7.35 (4H, d, J = 7.9 Hz,

H_{Ar}), 7.09 (4H, d, J = 8.0 Hz, H_{Ar}), 6.8 (2H, s, ArCH), 2.35 (6H, s, ArMe); ^{13}C NMR

(100 MHz, CDCl$_3$): δ 137.5 (C_{Ar}), 135.0 (C_{Ar}), 129.4 (CH_{Ar}), 127.6 (ArCH), 126.3
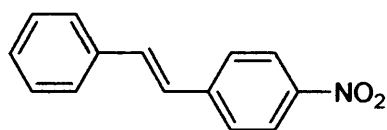
(CH_{Ar}), 20.3 (Me).

(E)-(3-Nitro)-(4'-methyl)-stilbene (8) [9]
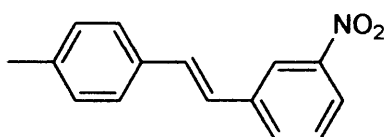
Synthesis carried out according to General Procedure 8 obtained in 19% to 44% yield as

oil after purification by column chromatography on silica gel using 15% diethyl ether in

hexane.^{1}H NMR (500 MHz, CDCl$_3$): δ 8.29 (1H, s, H_{Ar}), 8.10 (1H, d, J = 7.7 Hz, H_{Ar}),

7.71 (1H, d, J = 7.9 Hz, HAr), 7.46 (1H, m, H_{Ar}), 7.38 (2H, d, J = 7.9 Hz, H_{Ar}), 7.18 (1H, d, J = 16.0 Hz, ArCH), 7.15 (1H, d, J = 7.5 Hz, H_{Ar}), 7.03 (1H, d, J = 16.3 Hz, ArCH), 2.38 (3H, s, ArMe); ^{13}C NMR (100 MHz, CDCl$_3$): δ 147.0 (C_{Ar}), 139.4 (C_{Ar}), 138.6 (C_{Ar}), 133.5 (C_{Ar}), 132.1 (CH_{Ar}), 131.7 (CH_{Ar}), 129.6 (CH_{Ar}), 129.5 (CH_{Ar}), 126.8 (ArCH), 125.1 (ArCH), 121.8 (CH_{Ar}), 120.8 (CH_{Ar}), 21.3 (Me).

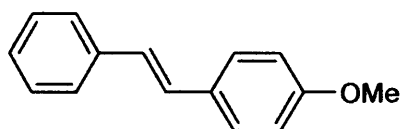## (E)-(4-Nitro)-stilbene (9)[8]

Synthesis carried out according to General Procedure 8 and 9 obtained in 42% to 65% yield as solid after purification by column chromatography on silica gel using 15% diethyl ether in hexane. Mp 151–154 °C (lit. mp 156–157 °C); ^{1}H NMR (500 MHz, CDCl$_3$): δ 8.15 (2H, d, J = 8.6 Hz, H_{Ar}), 7.55 (2H, m, H_{Ar}), 7.49 (2H, d, J = 7.4 Hz, H_{Ar}), 7.35 (2H, t, J = 8.0 Hz, H_{Ar}), 7.28 (1H, t, J = 7.0 Hz, H_{Ar}), 7.22 (1H, d, J = 16.9 Hz, ArCH), 7.09 (1H, d, J = 17.0 Hz, ArCH); ^{13}C NMR (100 MHz, CDCl$_3$): 146.1 (CNO$_2$), 136.3 (C_{Ar}), 131.5 (C_{Ar}), 128.9 (CH_{Ar}), 128.8 (CH_{Ar}), 128.0 (CH_{Ar}), 127.0 (ArCH), 126.8 (ArCH), 126.3 (CH_{Ar}), 124.8 (CH_{Ar}).

(E)-Methyl-(4-methoxyphenyl)-acrylate (10)[9]

MeO
CO₂Me
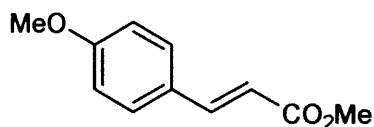
Synthesis carried out according to General Procedure 9 obtained in 27% yield as oil after purification by column chromatography on silica gel using 10% diethyl ether in hexane. ^{1}H NMR (500 MHz, CDCl₃): δ 7.59 (1H, d, J = 15.9 Hz, ArCH), 7.45 (2H, d, J = 6.8 Hz, H_{Ar}), 6.85 (2H, d, J = 6.8 Hz, H_{Ar}), 6.28 (1H, d, J = 16.1 Hz, CHCO₂Me), 3.79 (3H, s, ArOMe), 3.72 (3H, s, CO₂Me); ^{13}C NMR (100 MHz, CDCl₃): δ 167.8 (CO₂Me), 161.4 (C_{Ar}OMe), 144.5 (ArCH), 129.7 (CH$_{Ar}$), 127.1 (C_{Ar}), 115.2 (CHCO₂Me), 114.3 (CH$_{Ar}$), 55.4 (ArOMe), 51.6 (CO₂Me).
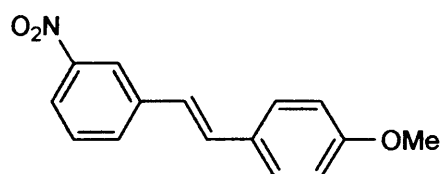
(E)-4-Methoxystilbene (11):[9]

OMe

Synthesis carried out according to General Procedure 9 obtained in 33% yield as solid after purification by column chromatography on silica gel using 10% diethyl ether in hexane. Mp 134–135 °C (lit. mp 136 °C); ^{1}H NMR (500 MHz, CDCl₃): δ 7.45 (2H, d, J = 7.9 Hz, H_{Ar}), 7.40 (2H, d, J = 7.4 Hz, H_{Ar}), 7.29 (2H, t, J = 7.9 Hz, H_{Ar}), 7.18 (1H, t, J = 8.0 Hz, H_{Ar}), 7.02 (1H, d, J = 16.0 Hz, ArCH), 6.90 (1H, d, J = 15.9 Hz, ArCH), 6.85 (2H, d, J = 8.2 Hz, H_{Ar}), 3.75 (3H, s, ArOMe); ^{13}C NMR (100 MHz, CDCl₃): δ 159.0

(C_{Ar}OMe), 131.0 (C_{Ar}), 130.5 (C_{Ar}), 128.7 (CH_{Ar}), 128.2 (CH_{Ar}), 127.7 (ArCH), 127.2 (ArCH), 126.6 (CH_{Ar}), 126.2 (CH_{Ar}), 114.1 (CH_{Ar}), 55.0 (OMe).

(E)-1-(4-Methoxystyryl)-3-nitrobenzene (12)[10]

Synthesis carried out according to General Procedure 9 obtained in 18% yield as oil after purification by column chromatography on silica gel using 15% diethyl ether in hexane. ^{1}H NMR (500 MHz, CDCl$_3$): δ 8.29 (1H, s, H_{Ar}), 8.01 (1H, d, J = 7.9 Hz, H_{Ar}), 7.70 (1H, d, J = 8.0 Hz, H_{Ar}), 7.49–7.39 (3H, m, H_{Ar}), 7.14 (1H, d, J = 16.8 Hz, ArCH), 6.93 (1H, d, J = 16.0 Hz, ArCH), 6.88 (2H, d, J = 7.9 Hz, H_{Ar}), 3.79 (3H, s, ArOMe); ^{13}C NMR (100 MHz, CDCl$_3$): δ 160.0 (C_{Ar}OMe), 146.6 (C_{Ar}NO$_2$), 139.0 (C_{Ar}), 132.0 (CH_{Ar}), 131.3 (CH_{Ar}), 129.5 (ArCH), 129.1 (ArCH), 129.0 (C_{Ar}), 128.2 (CH_{Ar}), 123.9 (CH_{Ar}), 121.6 (CH_{Ar}), 120.6 (CH_{Ar}), 114.3 (CH_{Ar}), 55.7 (OMe).
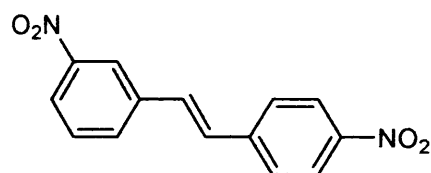
(E)-Methyl-(4-nitrophenyl)-acrylate (13)[11]
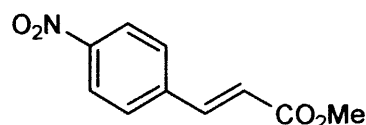
Synthesis carried out according to General Procedure 9 obtained in 64% yield as waxy solid after purification by column chromatography on silica gel using 15% diethyl ether in hexane. ^{1}H NMR (500 MHz, CDCl$_3$): δ 8.20 (2H, d, J = 7.9 Hz, H_{Ar}), 7.67 (1H, d, J =

16.0 Hz, ArC*H*), 7.59 (2H, d, *J* = 6.8 Hz, H_{Ar}), 6.49 (1H, d, *J* = 15.9 Hz, C*H*CO$_2$Me), 3.76 (3H, s, CO$_2$*Me*); ^{13}C NMR (100 MHz, CDCl$_3$): δ 160.0 (*C*O$_2$Me), 149.0 (*C*$_{Ar}$NO$_2$), 141.9 (Ar*C*H), 128.7 (*C*H$_{Ar}$), 124.2 (*C*H$_{Ar}$), 122.1 (*C*H$_{Ar}$), 110.0 (*C*HCO$_2$Me), 52.1 (CO$_2$*Me*).
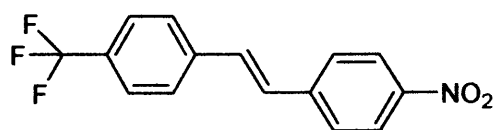
(E)-3,4′-Dinitrostilbene (14) [12]

Synthesis carried out according to General Procedure 9 obtained in 57% yield as oil after purification by column chromatography on silica gel using 15% diethyl ether in hexane. ^{1}H NMR (500 MHz, CDCl$_3$): δ 8.36 (1H, s, H_{Ar}), 8.21 (2H, d, *J* = 7.9 Hz, H_{Ar}), 8.12 (1H, d, *J* = 8.0 Hz, H_{Ar}), 7.79 (1H, d, *J* = 8.0 Hz, H_{Ar}), 7.64 (2H, d, *J* = 8.0 Hz, H_{Ar}), 7.55 (1H, t, *J* = 8.0 Hz, H_{Ar}), 7.2 (2H, d, *J* = 16 Hz, ArC*H*); ^{13}C NMR (100 MHz, CDCl$_3$): δ 152.0 (*C*$_{Ar}$NO$_2$), 147.5 (*C*$_{Ar}$NO$_2$), 142.8 (*C*$_{Ar}$), 137.9 (*C*$_{Ar}$), 132.7 (*C*H$_{Ar}$), 130.5 (*C*H$_{Ar}$), 129.8 (Ar*C*H), 129.3 (Ar*C*H), 127.3 (*C*H$_{Ar}$), 124.3 (*C*H$_{Ar}$), 123.1 (*C*H$_{Ar}$), 121.4 (*C*H$_{Ar}$).
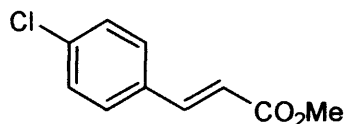
(E)- 4-Nitro-(4′-bromo)-stilbene (15)[13]
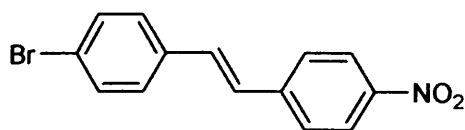
Synthesis carried out according to General Procedure 9 obtained in 49% yield as sticky solid after purification by column chromatography on silica gel using 10% diethyl ether in hexane. ^{1}H NMR (500 MHz, CDCl$_3$): δ 8.17 (2H, d, J = 7.0 Hz, H_{Ar}), 7.59 (2H, d, J = 8.7 Hz, H_{Ar}), 7.48 (2H, d, J = 7.4 Hz, H_{Ar}), 7.35 (2H, d, J = 7.2 Hz, H_{Ar}), 7.13 (1H, d, J = 15.7 Hz, ArCH), 7.09 (1H, d, J = 16.2 Hz, ArCH); ^{13}C NMR (100 MHz, CDCl$_3$): δ 143.4 (C_{Ar}NO$_2$), 140.5 (C_{Ar}), 135.1 (C_{Ar}), 132.1 (CH$_{Ar}$), 131.9 (CH$_{Ar}$), 128.4 (ArCH), 126.9 (ArCH), 126.8 (CH$_{Ar}$), 124.2 (CH$_{Ar}$), 123.0 (C_{Ar}Br).

(E)-4-Trifluoromethyl-(4′-nitro)-stilbene (16) [14]

Synthesis carried out according to General Procedure 9 obtained in 61% yield as solid after purification by column chromatography on silica gel using 10% diethyl ether in hexane. Mp 168–170 °C (lit. mp 171–172 °C); ^{1}H NMR (500 MHz, CDCl$_3$): δ 8.19 (2H, d, J = 9.0 Hz, H_{Ar}), 7.55–7.64 (6H, m, H_{Ar}), 7.22 (1H, d, J = 16.0 Hz, ArCH), 7.18 (1H, d, J = 15.9 Hz, ArCH).

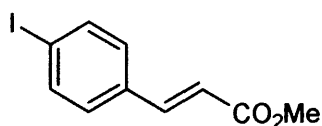**(*E*)-Methyl 3-(4-chlorophenyl)-acrylate (17):** [11]

Synthesis carried out according to General Procedure 9 obtained in 62% yield as solid after purification by column chromatography on silica gel using 5% diethyl ether in hexane. ^{1}H NMR (500 MHz, CDCl$_3$): δ 7.59 (1H, d, J = 16.0 Hz, ArCH), 7.39 (2H, d, J = 8.4 Hz, H_{Ar}), 7.30 (2H, d, J = 6.4 Hz, H_{Ar}), 6.35 (1H, d, J = 16.2 Hz, CHCO$_2$Me), 3.78 (3H, s, CO$_2$*Me*); ^{13}C NMR (100 MHz, CDCl$_3$): δ 171.1 (*C*O$_2$Me), 143.4 (Ar*C*H), 133.1 (C_{Ar}), 133.0 (C_{Ar}), 129.2 (CH$_{Ar}$), 129.1 (CH$_{Ar}$), 118.4 (*C*HCO$_2$Me), 51.8 (CO$_2$*Me*).

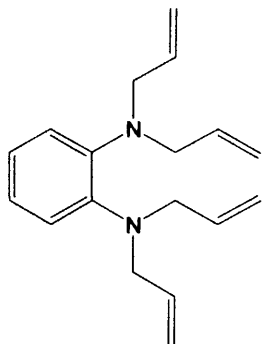**(*E*)-Methyl 3-(4-iodophenyl)-acrylate (18)** [15]

Synthesis carried out according to General Procedure 9 obtained in 90% yield as solid after purification by column chromatography on silica gel using 7% diethyl ether in hexane. ^{1}H NMR (500 MHz, CDCl$_3$): δ 7.68 (2H, d, J = 8.5 Hz, H_{Ar}), 7.55 (1H, d, J = 16.3 Hz, ArCH), 7.19 (2H, d, J = 9.0 Hz, H_{Ar}), 6.37 (1H, d, J = 15.8 Hz, CHCO$_2$Me), 3.75 (3H, s, CO$_2$*Me*); ^{13}C NMR (100 MHz, CDCl$_3$): δ 167.0 (*C*O$_2$Me), 143.0 (Ar*C*H), 138.0 (CH$_{Ar}$), 136.5 (C_{Ar}), 129.9 (CH$_{Ar}$), 118.9 (*C*HCO$_2$Me), 101.0 (C_{Ar}I), 51.5 (CO$_2$*Me*).

N,*N*,*N'*,*N'*-Tetrallyl-1,2-phenylenediamine (20)[16]

Synthesis carried out according to General Procedure 10 obtained in a range of 14% to 19% yield as oil after purification by medium performance liquid chromatography on silica gel using 2% diethyl ether in hexane. ^{1}H NMR (500 MHz, CDCl$_3$): δ 6.75–6.9 (4H, m, *H*$_{Ar}$), 5.60–6.80 (4H, m, NCH$_2$C*H*CH$_2$), 4.90–5.11 (8H, m, NCH$_2$CHC*H*$_2$), 3.72 (8H, m, NC*H*$_2$CHCH$_2$); ^{13}C NMR (100 MHz, CDCl$_3$): δ 143.5 (*C*$_{Ar}$), 135.5 (NCH$_2$*C*HCH$_2$), 121.9 (*C*H$_{Ar}$), 121.5 (*C*H$_{Ar}$), 117.0 (NCH$_2$CH*C*H$_2$), 53.1 (N*C*H$_2$CHCH$_2$).
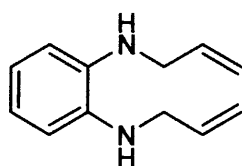
N,*N*,*N'*-Triallyl-1,2-phenylenediamine (21)[16]
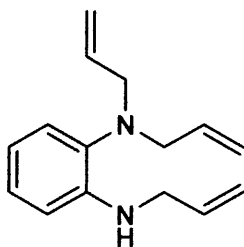
Synthesis carried out according to General Procedure 10 obtained in a range of 25% to 33% yield as oil after purification by medium performance liquid chromatography on silica gel using 2% diethyl ether in hexane. ^{1}H NMR (500 MHz, CDCl$_3$): δ 6.60–6.42

(2H, m, H_{Ar}), 6.29–6.08 (2H, m, H_{Ar}), 5.55–5.42 (1H, m, NHCH₂C*H*CH₂), 5.35–5.22

(2H, m, N[CH₂C*H*CH₂]₂), 4.72–4.55 (6H, m, NCH₂CHC*H₂*), 4.48 (1H, br, N*H*),

3.38–3.24 (2H, m, NHC*H₂*CHCH₂), 3.11–2.99 (4H, m, N[C*H₂*CHCH₂]₂); ¹³C NMR

(100 MHz, CDCl₃): δ 144.1 (C_{Ar}), 136.8 (C_{Ar}), 135.8 (NHCH₂*C*HCH₂), 135.3

(N[CH₂*C*HCH₂]₂), 125.1 (CH$_{Ar}$), 122.3 (CH$_{Ar}$), 117.0 (N[CH₂CHC*H₂*]₂), 116.2 (CH$_{Ar}$),

115.5 (NHCH₂CHC*H₂*), 110.2 (CH$_{Ar}$), 55.3 (N[*C*H₂CHCH₂]₂), 46.3 (NH*C*H₂CHCH₂).

_N,N′_-Diallyl-1,2-phenylenediamine (22) [16]

Synthesis carried out according to General Procedure 10 obtained in a range of 10% to

15% yield as oil after purification by medium performance liquid chromatography on

silica gel using 2% diethyl ether in hexane. ¹H NMR (500 MHz, CDCl₃): δ 6.78–6.68
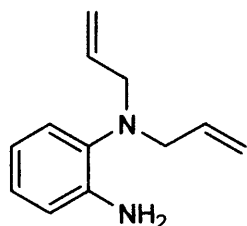
(2H, m, H_{Ar}), 6.64–6.55 (2H, m, H_{Ar}), 5.98–5.85 (2H, m, NHCH₂C*H*CH₂), 5.19 (2H, d,

J_{trans} = 17.3 Hz, NHCH₂CHCH*H_{trans}*), 5.07 (2H, d, J_{cis} = 10.2 Hz, NHCH₂CHCH*H_{cis}*),

3.67 (4H, d, J = 5.0 Hz, NHC*H₂*CHCH₂), 3.25 (2H, br, N*H*); ¹³C NMR (100 MHz,

CDCl₃): δ 137.1 (C_{Ar}), 135.8 (NHCH₂*C*HCH₂), 119.2 (CH$_{Ar}$), 116.3 (NHCH₂CHC*H₂*),

112.2 (CH$_{Ar}$), 47.1 (NH*C*H₂CHCH₂).
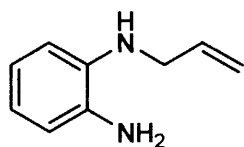
N,N-Diallyl-1,2-phenylenediamine (23)[16]

Synthesis carried out according to General Procedure 10 obtained in a range of 39% to 55% yield as oil after purification by medium performance liquid chromatography on silica gel using 2% diethyl ether in hexane. ^{1}H NMR (500 MHz, CDCl$_3$): δ 7.02 (1H, dd, J = 1.4, 8.0 Hz, H_{Ar}), 6.94 (1H, td, J = 1.5, 8.0 Hz, H_{Ar}), 6.75 (2H, m, H_{Ar}), 5.90–5.75 (2H, m, NCH$_2$CHCH$_2$), 5.20 (2H, d, J_{trans} = 17.0, Hz, NCH$_2$CHCHH_{trans}), 5.17 (2H, d, J_{cis} = 12.0 Hz, NCH$_2$CHCHH_{cis}), 4.08 (2H, br, NH_2), 3.58 (4H, d, J = 6.0 Hz, NCH_2CHCH$_2$); ^{13}C NMR (100 MHz, CDCl$_3$): δ 142.6 (C_{Ar}NAllyl$_2$), 137.2 (C_{Ar}NH$_2$), 135.2 (NCH$_2$CHCH$_2$), 124.7 (CH$_{Ar}$), 122.7 (CH$_{Ar}$), 117.9 (CH$_{Ar}$), 117.2 (NCH$_2$CHCH$_2$), 115.2 (CH$_{Ar}$), 55.3 (NCH$_2$CHCH$_2$).

N-Allyl-1,2-phenylenediamine (24)[16]

Synthesis carried out according to General Procedure 10 obtained in a range of 2% to 7% as oil after purification by medium performance liquid chromatography on silica gel using 2% diethyl ether in hexane. ^{1}H NMR (500 MHz, CDCl$_3$): δ 6.90–6.71 (4H, m, H_{Ar}), 5.45 (1H, m, NCH$_2$CHCH$_2$), 5.15 (1H, d, J_{trans} = 16.5 Hz, CH$_2$CHCHH_{trans}), 5.09 (1H, d, J_{cis} = 11.0 Hz, CH$_2$CHCHH_{cis}), 3.77 (2H, d, J = 6.1 Hz, NCH_2CHCH$_2$), 3.45

(2H, s, NH_2); ^{13}C NMR (100 MHz, CDCl$_3$): δ 141.9 (C_{Ar}NHAllyl), 137.2 (C_{Ar}NH$_2$),

130.0 (NCH$_2$$CHCH_2$), 125.5 ($CH_{Ar}$), 124.9 ($CH_{Ar}$), 119.5 ($CH_{Ar}$), 116.5

(NCH$_2$CHCH$_2$), 112.0 (CH$_{Ar}$), 51.5 (NCH$_2$CHCH$_2$).

tert-Butyl-2-(diallylamino)-phenylcarbamate (25)

Synthesis carried out according to preparation of **25** obtained in 86% yield as oil after

purification by column chromatography on silica gel using 5% diethyl ether in

hexane. ^{1}H NMR (500 MHz, CDCl$_3$): δ 7.71 (1H, br, H_{Ar}), 7.13–7.08 (2H, m, H_{Ar}), 6.95

(1H, m, H_{Ar}), 5.85–5.72 (2H, m, NCH$_2$CHCH$_2$), 5.10 (2H, d, J_{trans} = 17.2 Hz,

NCH$_2$CHCHH_{trans}), 5.05 (2H, d, J_{cis} = 10.0 Hz, NCH$_2$CHCHH_{cis}), 3.5 (4H, d, J = 6.0

Hz, NCH_2CHCH$_2$), 1.54 (9H, s, OCMe_3); ^{13}C NMR (100 MHz, CDCl$_3$): δ 153.0

(NCO$_2$CMe$_3$), 147.0 (C_{Ar}NAllyl$_2$), 135.2 (C_{Ar}NHCO$_2$CMe$_3$), 134.4 (NCH$_2$$CHCH_2$),
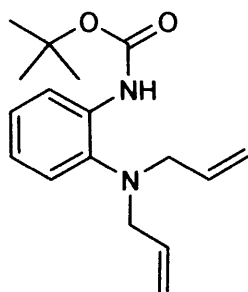
125.4 (CH$_{Ar}$), 122.9 (CH$_{Ar}$), 121.8 (CH$_{Ar}$), 118.0 (CH$_{Ar}$), 117.8 (NCH$_2$CHCH$_2$), 80.1

(OCMe$_3$), 56.7 (NCH$_2$CHCH$_2$), 28.4 (OCMe_3); MS (APCI) m/z (%): 289(15) [M+H$^+$],

HRMS for [M+H$^+$] for [C$_{17}$H$_{24}$N$_2$O$_2$+H]$^+$: calc. 289.1916, found 289.1922; IR: v (cm^{-1}):

3367.1, 3077.8 (CH=CH$_2$), 2979.5 (CH$_2$), 1809.9, 1727.9 (NCO$_2$$t$Bu), 1643.0

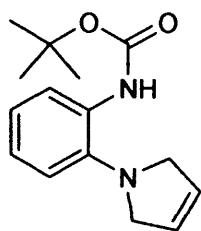(CH=CH$_2$), 1590.9, 1515.8, 1448.3, 1218.8, 1157.1, 1070.3, 922.7.

tert-Butyl 2-(2_H_-pyrrol-1(5_H_)-yl)-phenylcarbamate (26)

Synthesis carried out according to General Procedure 11 obtained in 91% yield as oil after purification by column chromatography on silica gel using 20% diethyl ether in petroleum ether. ^{1}H NMR (500 MHz, CDCl$_3$): δ 7.41 (1H, br, H_{Ar}), 7.09 (1H, dd, J = 1.2, 7.6 Hz, H_{Ar}), 6.97 (1H, td, J = 2.1, 7.9 Hz, H_{Ar}), 6.90 (1H, td, J = 2.4, 8.3 Hz, H_{Ar}), 5.82 (2H, s, NCH$_2$CH), 3.92 (4H, s, NCH_2CH), 1.43 (9H, s, OCMe_3) ; ^{13}C NMR (100 MHz, CDCl$_3$): δ 153.5 (NCO$_2$CMe$_3$), 140.9 (C_{Ar}NC$_4$H$_6$), 134.0 (C_{Ar}NCO$_2$CMe$_3$), 126.9 (NCH$_2$$C$H), 124.1 ($CH_{Ar}$), 123.4 ($CH_{Ar}$), 121.3 ($CH_{Ar}$), 119.9 ($CH_{Ar}$), 80.1 ($CMe_3$), 59.7 (N$CH_2$CH), 28.4 ($CMe_3$); MS (ES) _m/z_ (%): 261(4) [M+H$^+$], HRMS for [M+H$^+$] for [C$_{15}$H$_{20}$N$_2$O$_2$+H]$^+$: calc. 261.1603, found 261.1594; IR: ν (cm^{-1}): 3362.3, 2976.6, 2866.7 (NCH$_2$), 1728.9 (NCO$_2$_t_Bu), 1593.9, 1516.7, 1158.0, 832.1, 747.3 (_cis_-CH=CH).
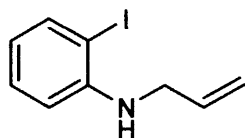
tert-Butyl-2-(1_H_-pyrrol-1-yl)-phenylcarbamate (27)
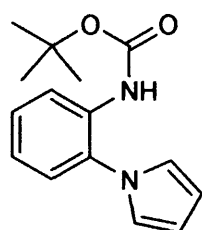
Synthesis carried out according to General Procedure 11 obtained in 32% yield as oil after purification by column chromatography on silica gel using 20% diethyl ether in

petroleum ether. ^{1}H NMR (500 MHz, CDCl$_3$): δ 8.12 (1H, dd, J = 1.2, 7.6 Hz, H_{Ar}), 7.28

(1H, td, J = 1.2, 7.6 Hz, H_{Ar}), 7.12 (1H, dd, J = 1.6, 7.6 Hz, H_{Ar}), 6.90 (1H, td, J = 1.6,

7.6 Hz, H_{Ar}), 6.71 (2H, t, J = 2.0 Hz, NCHCH), 6.32 (2H, t, J = 2.0 Hz, NCHCH), 1.41

(9H, s, OCMe_3) ; ^{13}C NMR (100 MHz, CDCl$_3$): δ 152.6 (NCO$_2$CMe$_3$), 134.1

(C_{Ar}NC$_4$H$_4$), 129.9(C_{Ar}NCO$_2$CMe$_3$), 128.6 (CH_{Ar}), 126.9 (CH_{Ar}), 122.8 (CH_{Ar}), 122.0

(NCHCH), 119.8 (CH_{Ar}), 110.2 (NCHCH), 80.9 (CMe$_3$), 28.3 (CMe_3); MS (EI) m/z

(%): 258(10) [M$^+$], HRMS for [M$^+$] for [C$_{15}$H$_{18}$N$_2$O$_2$]$^+$: calc. 258.1368, found 258.1374;

IR: v (cm^{-1}): 3413.4, 3053.7, 2985.3, 2305.5, 1726.9 (NCO$_2t$Bu), 1595.8, 1523.5,

1483.0, 1450.2, 1265.1 (NCH=CH), 1158.0, 895.8, 739.5 (NCH=CH).

N-Allyl-2-iodobenzenamine (28)[17]

Synthesis carried out according to General Procedure 10 obtained in 31% yield as oil

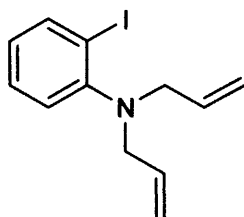after purification by column chromatography on silica gel using 10% diethyl ether in

hexane. ^{1}H NMR (500 MHz, CDCl$_3$): δ ^{1}H NMR (500 MHz, CDCl$_3$): δ 7.82 (1H, d, J =

8.1 Hz, H_{Ar}), 7.10 (1H, t, J = 9.0 Hz, H_{Ar}), 6.98 (1H, d, J = 7.1 Hz, H_{Ar}), 6.79 (1H, t, J =

7.4 Hz, H_{Ar}), 5.8–5.9 (1H, m, NCH$_2$CHCH$_2$), 5.25 (1H, d, J_{trans} = 17.2 Hz,

NCH$_2$CHCHH_{trans}), 5.10 (1H, d, J_{cis} = 11.1 Hz, NCH$_2$CHCHH_{cis}), 3.65 (2H, d, J = 4.4

Hz, NCH_2CHCH$_2$); ^{13}C NMR (100 MHz, CDCl$_3$): δ 152.0 (C_{Ar}N), 137.5 (CH_{Ar}), 135.2

(NCH$_2$$CHCH_2$), 128.0 ($CH_{Ar}$), 124.9 ($CH_{Ar}$), 123.7 ($CH_{Ar}$), 116.3 (NCH$_2CHCH_2$), 99.1

(C_{Ar}I), 53.0 (NCH$_2$CHCH$_2$).

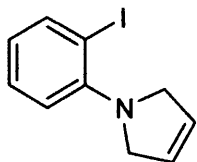**N,N-Diallyl-2-iodobenzenamine (29)** [18]

Synthesis carried out according to General Procedure 10 obtained in 77% yield as oil after purification by column chromatography on silica gel using 10% diethyl ether in hexane. ^{1}H NMR (500 MHz, CDCl$_3$): δ 7.90 (1H, dd, J = 2.0, 8.0 Hz, H_{Ar}), 7.30 (1H, td, J = 2.0, 8.0 Hz, H_{Ar}), 7.05 (1H, dd, J = 2.0, 8.0 Hz, H_{Ar}), 6.82 (1H, td, J = 2.0, 8.0 Hz, H_{Ar}), 5.90–5.80 (2H, m, NCH$_2$CHCH$_2$), 5.20 (2H, d, J_{trans} = 17.2 Hz, NCH$_2$CHCHH_{trans}), 5.13 (2H, d, J_{cis} = 10.0 Hz, NCH$_2$CHCHH_{cis}), 3.65 (4H, d, J = 6.0 Hz, NCH_2CHCH$_2$); ^{13}C NMR (100 MHz, CDCl$_3$): δ 151.8 (C_{Ar}N), 139.9 (CH_{Ar}), 134.8 (NCH$_2$CHCH$_2$), 128.4 (CH_{Ar}), 125.6 (CH_{Ar}), 124.2 (CH_{Ar}), 117.7 (NCH$_2$CHCH$_2$), 100.4 (C_{Ar}I), 56.1 (NCH$_2$CHCH$_2$).

1-(2-Iodophenyl)-2,5-dihydro-1H-pyrrole (30) [18]

Synthesis carried out according to General Procedure 11 obtained in 98% yield as oil after purification column chromatography on silica gel using 5% ethyl acetate in hexane. ^{1}H NMR (500 MHz, CDCl$_3$): δ 7.79 (1H, dd, J = 2.0, 8.0 Hz, H_{Ar}), 7.18 (1H, td, J = 1.2, 8.2 Hz, H_{Ar}), 6.90 (1H, dd, J = 1.5, 8.2 Hz, H_{Ar}), 6.59 (1H, td, J = 1.1, 8.0 Hz, H_{Ar}), 5.85 (2H, s, NCH$_2$CH), 4.20 (4H, s, NCH_2CH); ^{13}C NMR (100 MHz, CDCl$_3$): δ

152.0 (C_{Ar}N), 141.3 (*CH*$_{Ar}$), 128.9 (*CH*$_{Ar}$), 126.6 (NCH$_2$*CH*), 123.2 (*CH*$_{Ar}$), 120.0 (*CH*$_{Ar}$), 90.8 (C_{Ar}I), 58.36 (N*CH*$_2$CH).

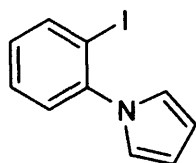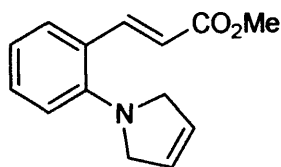## 1-(2-Iodophenyl)-1*H*-pyrrole (31)[19]

Synthesis carried out according to General Procedure 11 obtained as sticky oil after purification by column chromatography on silica gel using 5% ethyl acetate in hexane. ^{1}H NMR (500 MHz, CDCl$_3$): δ 7.96 (1H, dd, J = 1.2, 7.6 Hz, H_{Ar}), 7.38 (1H, td, J = 1.2, 7.6 Hz, H_{Ar}), 7.28 (1H, dd, J = 1.6, 7.6 Hz, H_{Ar}), 7.11 (1H, td, J = 1.6, 7.6 Hz, H_{Ar}), 6.77 (2H, t, J = 2.0 Hz, NC*H*CH), 6.30 (2H, t, J = 2.0 Hz NCHC*H*); ^{13}C NMR (100 MHz, CDCl$_3$): δ 146.0 (C_{Ar}N), 139.0 (*CH*$_{Ar}$), 131.0 (*CH*$_{Ar}$), 129.5 (*CH*$_{Ar}$), 128.5 (*CH*$_{Ar}$), 120.8 (N*CH*CH), 108.0 (NCH*CH*), 95.0 (C_{Ar}I).

(*E*)-Methyl 3-(2-(2*H*-pyrrol-1(5*H*)-yl)phenyl)acrylate (32)
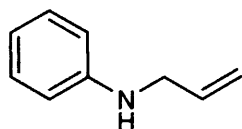

Synthesis carried out according to General Procedure 12 obtained in 64% yield as oil after purification by column chromatography on silica gel using 15% diethyl ether in petroleum ether. ^{1}H NMR (500 MHz, CDCl$_3$): δ 8.10 (1H, d, J = 15.7 Hz, ArC*H*), 7.29 (1H, dd, J = 1.2, 7.6 Hz, H_{Ar}), 7.19 (1H, td, J = 2.1, 7.9 Hz, H_{Ar}), 6.85–6.72 (2H, m,

H_{Ar}), 6.15 (1H, d, J = 16.1 Hz, CHCO$_2$Me), 5.80 (2H, s, NCH$_2$CH), 4.15 (4H, s,

NCH_2CH), 3.69 (3H, s, CO$_2$$Me$); ^{13}C NMR (100 MHz, CDCl$_3$): δ 167.0 (CO$_2$Me),

161.2 (C_{Ar}N), 140.5 (ArCH), 130.7 (CH$_{Ar}$), 129.6 (CH$_{Ar}$), 127.7 (CH$_{Ar}$), 126.2

(NCH$_2$$C$H), 122.8 ($CH_{Ar}$), 117.0 ($CHCO_2$Me), 109.9 ($CH_{Ar}$), 58.8 (N$CH_2$CH), 51.6

(CO$_2$$Me$); MS (ES) m/z (%): 230 (100) [M+H$^+$], 231 (15), HRMS for [M+H$^+$] for

[C$_{14}$H$_{15}$NO$_2$+H]$^+$: calc. 230.1181, found 230.1185; IR: v (cm^{-1}): 2978.5, 1963.2, 1726.9

(CH=CH-CO), 1444.4, 1382.7, 1350.9, 1296.9, 1130.1, 1076.1, 1043.3, 934.3 (*trans*-

CH=CH), 845.6, 794.5 (*cis*-CH=CH).

N-Allyl-aniline (33) [20]

Synthesis carried out according to General Procedure 10 obtained in 8% yield as oil

after purification by column chromatography on silica gel using 10% diethyl ether in

petroleum ether. ^{1}H NMR (500 MHz, CDCl$_3$): δ 7.12–7.14 (2H, t, J = 7.7 Hz, H_{Ar}), 6.71

(1H, t, J = 8.1 Hz, H_{Ar}), 6.48 (2H, d, J = 7.8 Hz, H_{Ar}), 5.77 (1H, m, CH$_2$CHCH$_2$), 5.18

(1H, d, J_{trans} = 16.0 Hz, NCH$_2$CHCHH_{trans}), 5.03 (1H, d, J_{cis} = 11.1 Hz,

NCH$_2$CHCHH_{cis}), 3.64 (2H, d, J = 5.0 Hz, NCH_2CHCH$_2$), 3.56 (1H, br, NH); ^{13}C NMR

(100 MHz, CDCl$_3$): δ 146.9 (C_{Ar}N), 135.0 (NCH$_2$$CHCH_2$), 128.5 ($CH_{Ar}$), 116.9 ($CH_{Ar}$),

115.5 (NCH$_2$CHCH$_2$), 113.0 (CH$_{Ar}$), 44.5 (NCH$_2$CHCH$_2$).
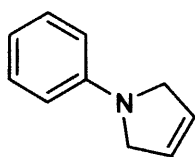
N,N-Diallyl-aniline (34)[20]
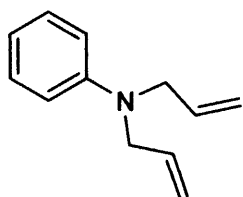
Synthesis carried out according to General Procedure 10 obtained oil in 89% yield as oil after purification by column chromatography on silica gel using 10% diethyl ether in petroleum ether. ^{1}H NMR (500 MHz, CDCl$_3$): δ 7.30–7.20 (2H, m, H_{Ar}), 6.78–6.69 (3H, m, H_{Ar}), 5.89 (2H, m, NCH$_2$CHCH$_2$), 5.22 (2H, d, J_{trans} = 16.3 Hz, NCH$_2$CHCHH_{trans}), 5.14 (2H, d, J_{cis} = 10.0 Hz, CH$_2$CHCHH_{cis}), 3.98 (4H, d, J = 4.9 Hz, NCH_2CHCH$_2$); ^{13}C NMR (100 MHz, CDCl$_3$): δ 148.7 (C_{Ar}N), 134.1 (NCH$_2$CHCH$_2$), 129.1 (CH$_{Ar}$), 116.3 (NCH$_2$CHCH$_2$), 116.0 (CH$_{Ar}$), 112.4 (CH$_{Ar}$), 52.5 (NCH$_2$CHCH$_2$).
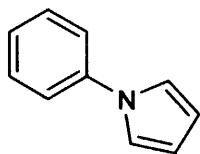
1-Phenyl-2,5-dihydro-1H-pyrrole (35)[21]

Synthesis carried out according to General Procedure 11 obtained in 96% yield as oil after purification by column chromatography on silica gel using 10% diethyl ether in petroleum ether.. ^{1}H NMR (500 MHz, CDCl$_3$): δ 7.20 (2H, t, J = 8.0 Hz, H_{Ar}), 6.6 (1H, t, J = 7.8 Hz, H_{Ar}), 6.45 (2H, d, J = 7.3 Hz, H_{Ar}), 5.86 (2H, s, NCH$_2$CH), 4.00 (4H, s, NCH_2CH); ^{13}C NMR (100 MHz, CDCl$_3$): δ 147.1 (C_{Ar}N), 129.4 (CH$_{Ar}$), 126.4 (NCH$_2$CH), 115.6 (CH$_{Ar}$), 111.2 (CH$_{Ar}$), 54.5 (NCH$_2$CH).

1-Phenyl-1*H*-pyrrole (36) [22]

Synthesis carried out according to General Procedure 11 obtained in traces as solid after purification by column chromatography on silica gel using 10% diethyl ether in petroleum ether. ^{1}H NMR (500 MHz, CDCl$_3$): δ 7.48–7.56 (4H, m, H_{Ar}), 7.31-7.35 (1H, m, H_{Ar}), 7.21 (2H, t, J = 2.0 Hz, NC*H*CH), 6.50 (2H, t, J = 2.0 Hz, NCHC*H*); ^{13}C NMR (100 MHz, CDCl$_3$): δ 139.7 (C_{Ar}N), 129.5 (CH$_{Ar}$), 126.0 (NCHCH), 121.3 (CH$_{Ar}$), 118.1 (CH$_{Ar}$), 111.6 (NCHCH).
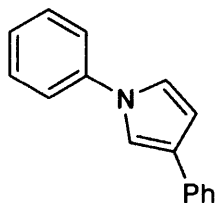
1,3-Diphenyl-1*H*-pyrrole (37) [23]

Synthesis carried out according to General Procedure 12 obtained in 60% yield as sticky oil after purification by column chromatography on silica gel using 10% diethyl ether in petroleum ether.. ^{1}H NMR (500 MHz, CDCl$_3$): mp 119–121 °C (lit. mp 118-119 °C); δ NMR (500 MHz, CDCl$_3$): δ 7.61 (2H, d, J = 8.1 Hz, H_{Ar}), 7.49–7.19 (5H, m, H_{Ar}), 7.34 (2H, t, J = 7.6 Hz, H_{Ar},), 7.25 (1H, t, J = 7.9 H_{Ar}), 7.15 (1H, dd, J = 1.1, 2.8 Hz, NC*H*CPh), 6.85 (1H, dd, J = 1.6, 4.1 Hz, NC*H*CH), 6.39 (1H, dd, J = 2.8, 4.1 Hz, NCHC*H*); ^{13}C NMR (100 MHz, CDCl$_3$): δ 146.5 (C_{Ar}N), 138.5 (C_{Ar}CCH), 138.0 (CH$_{Ar}$), 129.6 ($C_{Ar}C$CH), 128.9 (CH$_{Ar}$), 128.8 (CH$_{Ar}$), 127.2 (CH$_{Ar}$), 126.6 (CH$_{Ar}$), 126.2 (CH$_{Ar}$), 122.3 (NCHCH), 111.2 (NCHCPh), 100.0 (NCHCH).

4.6. References

[1] http://en.wikipedia.org/wiki/Teflon; http://en.wikipedia.org/wiki/Acrylic_glass

[2] http://www.lpkf.com.

[3] http://www.agc.co.jp/english/chemicals/shinsei/cytop/cytop.htm.

[4] P. Zhou, Y. Li, P. Sun, J. Zhou, J. Bao, *Chem. Commun.* **2007**, 1418–1420.

[5] W. S. Wadsworth, W. D. Emmons, *J. Am. Chem. Soc.***1961**, *83*, 1733 – 1738; J. X. Wang, K. Wang, L. Zhao, H. Li, Y. Fu, Y. Hu, *Adv. Synth. Catal,* **2006**, *348*, 1262–1270.

[6] B. Mu, T. Li, W. Xu, G. Zeng, P. Liu, Y. Wu, *Tetrahedron,* **2007**, *63*, 11475–11488; Philip Warner, R. Sutherland, *J. Org. Chem.* **1992**, *57*, 6294–6300.

[7] R. G. Pews, N. D. Ojha, *J. Am. Chem. Soc.* **1969**, *91*, 5769–5773; L. Djakovitch, H. Heise, K. Kohler, *J. Organomet. Chem.* **1999**, *584*, 16–26.

[8] M. Cai, Y. Huang, H. Zhao, C. Song, *J. Organomet. Chem.* **2003**, *682*, 20–25.

[9] G. A. Grasa, R. Singh, E. D. Stevens, S. P. Nolan, *J. Organomet. Chem.* **2003**, *687*, 269–279.

[10] G. M. Anstead, J. A. Katzenellenbogen, *J. Phys. Chem.* **1988**, *92*, 6249–6258.

[11] Z. Zhang, Z. Wang, *J. Org. Chem.* **2006**, *71*, 7485–7487.

[12] C. Ling, M. Minato, P. M. Lahti, H. V. Willigen, *J. Am. Chem. Soc.* **1992**, *114*, 9959–9969.

[13] B. M. Choudary, M. L. Kantam, N. M. Reddy, N. M. Gupta, *Catal. Lett.* **2002**, *82*, 79–83.

[14] P. E. Hanna, R. E. Gammans, R. D. Sehon, M. K. Lee, *J. Med. Chem.* **1980**, *23*, 1038–1044.

[15] H. Brunner, N. L. Cousturier de Courcy, J. P. Genêt, *Tetr. Lett.* **1999**, *40*, 4815–4818.

[16] B. Ding, Z. Teng, R. Keese, *J. Org. Chem.* **2002**, *67*, 8906–8910.

[17] J. A. Nieman, M. D. Ennis, *J. Org. Chem.* **2001**, *66*, 2175–2177.

[18] P. Evans, R. Grigg, M. Monteith, *Tetr. Lett.* **1999**, *40*, 5247–5250.

[19] M. A. Campo, R. C. Larock, *J. Org. Chem.* **2002**, *67*, 5616–5620.

[20] V. Pace, F. Martínez, M. Fernández, J. V. Sinisterra, A. R. Alcántara, *Org. Lett.* **2007**, *9*, 2661–2664.

[21] J. M. Bobbitt, L.H. Amundsen, R. I. Steiner, *J. Org. Chem.,* **1960**, *25*, 2230–2231.

[22] L. Zhu, L. Cheng, Y. Zhang, R. Xie, J. You, *J. Org. Chem.* **2007**, *72*, 2737–2743.

[23] S. Kagabu, H. Tsuji, I. Kawai, H. Ozeki, *Bull. Chem. Soc. Jpn.* **1995**, *68*, 341–349.

Overview, conclusions and future directions

In this work we aimed to investigate the application of microflow system to a selected set of organic transformations of particular relevance using a practical and economical system setup in order to develop a basic methodology for synthetic chemists. Accordingly, we adhered in this thesis to a terminology typical of laboratory based experimental chemistry. We started off our project in the first of two experimental chapters (Chapter 2) with the study of a biphasic hydrolysis reaction, observing remarkable improvements in reaction conversions by use of microflow techniques compared to flask methods. The study of the hydrolysis reaction also provided the opportunity to optimise further the microflow techniques, allowing to investigate varieties of microflow patterns, heating techniques, channel materials and geometries, and activation methods. In particular, remarkable results were observed with the employment of segmented flow pattern, microwave heating technique, activation by sonication and use of phase transfer catalysts. In order to extend the scope of this type of study it would be beneficial to look into different hydrolysis methods such as acidic hydrolysis and enzymatic hydrolysis, and to go deeper in the study of the kinetics of these processes. In the second experimental chapter (Chapter 3) we used the microflow technique to enhance the performance of important transition metal-catalysed organic transformations such as Heck coupling and ring-closing metathesis. This study represented a very challenging ground presenting a high number of variables both in the chemistry and in the engineering part of the work. Such challenges included ensuring the suitability of the organic transformation for the microflow study; the compatibility of the channel material with reactants, solvents and catalysts employed; the non-trivial effort of connecting all channel parts correctly; and the pumping of reagents and catalysts in the channel in the right sequence and with the right pressure. Clearly the aim of a microflow study is not limited to taking the

reaction to completion like in the flask reaction, but it is extended to avoid a certain number of issues, such as the occurrence of precipitation in the microchannel leading to clogging, the occurrence of bubbling and generation of gas causing disturbance inside the microchannel, or the degradation of reactants in the stock solution reservoirs. Overall the use of microflow technique, applied to such a large number of reactions of various types and carried out with many chemical and engineering variables, allowed us to observe overall reaction performances enhancement compared to conventional flask chemistry, on the whole rather agreeably, reproducibly, and displaying very regular trends. The encouraging results obtained in the course of our studies and reported in this thesis are of course far from being conclusive. Our applications of microflow techniques to chemical transformations are only at an early stage of becoming a fully established discipline. In spite of the clear advantages brought by the microflow techniques, however, the more we get acquainted with the techniques the more we become aware of certain issues that need to be addressed. One of the problems has to do with the unavailability on the market of fully efficient flow systems specific for a synthetic use, as most commercially available parts (pumps, flow cells, connectors) are made for other purposes, mainly analytical. Therefore such parts do not hold harsh conditions for very long, thus requiring frequent replacement. Furthermore, there is clearly a gap still existing between the chemists who need to use these systems and the science of engineering and chemical engineering. Such gap can be bridged by creating tighter collaborations between the two disciplines. Since the microflow route is supposed to provide speed, a great benefit would also come from integrating the flow system with robotised elements, to enable faster introduction of reactants, faster liquid fraction collection and, most of all, on-line analysis.